# Real-Time Anticipatory Suspension Control for Single Event Disturbances

**Master's Thesis No. 620/16**

Author: Christopher Kappes, B.Sc. | XX XX XXX (TUD) | XX XX XX XXX (VT)

Major: Master of Science in Mechanical and Process Engineering

TECHNISCHE
UNIVERSITÄT
DARMSTADT


Christopher Kappes

Matrikelnummer TUD: XX XX XXX
Major TUD: Master of Science in Mechanical and Process Engineering

Student ID VT: XX XX XX XXX
Major VT: Master of Science in Mechanical Engineering

Master's Thesis No. 620/16
Topic: Real-Time Anticipatory Suspension Control for Single Event Disturbances
Thema: Antizipierende Echtzeit Fahrwerksregelung bei Einzel-Störereignissen

Submission Date: 2017-05-04

Technische Universität Darmstadt
Fachbereich Maschinenbau
Fachgebiet Fahrzeugtechnik
Prof. Dr. rer. nat. Hermann Winner
Otto-Berndt-Straße 2
64287 Darmstadt
Germany

Virginia Polytechnic Institute and State University
Department of Mechanical Engineering
Performance Engineering Research Lab
Prof. Dr. Steve C. Southward
1145 Perry Street
Blacksburg VA 24061
United States of America

## Thesis Statement

Thesis Statement pursuant to § 22 paragraph 7 of APB TU Darmstadt

I herewith formally declare that I have written the submitted thesis independently. I did not use any outside support except for the quoted literature and other sources mentioned in the paper. I clearly marked and separately listed all of the literature and all of the other sources which I employed when producing this academic work, either literally or in content.

This thesis has not been handed in or published before in the same or similar form. In the submitted thesis the written copies and the electronic version are identical in content.

Date: 2017-05-04 Signature:

TECHNISCHE UNIVERSITÄT DARMSTADT

# Master thesis No. 620/16 in Mechanical and Process Engineering (30 CP)

of Mr. Christopher Kappes

| | |
|---|---|
| Start: | 01.07.2016 |
| Interims presentation | 22.09.2016 |
| End: | 30.06.2017 |

**Topic:** **Real-Time Anticipatory Suspension Control for Single Event Disturbances**

***Thema:*** ***Antizipierende Echtzeit Fahrwerksregelung bei Einzel-Störereignissen***

Research and development efforts for controlling the primary suspensions on ground vehicles have largely focused on either improving ride or improving handling. The handling category can be further segmented into sub-categories such as traction control, vehicle stability control, anti-lock braking, and rollover mitigation, etc. It is well known that ride and handling objectives cannot be satisfied simultaneously.

A third relatively recent category has been introduced which aims to improve vehicle response to single event disturbances such as potholes, bumps, humps, and road breakaway. We are interested in finding real-time solutions for controllable suspensions that enable the vehicle to mitigate short duration events with a balance between ride and handling. Unfortunately, the traditional primary suspension control methods for ride and handling do not adequately address this category.

To support this need, researchers in the Performance Engineering Research Lab at Virginia Tech have developed offline solutions, unique to this particular class of problems, which have been used to predict the ideal control force profile required to achieve the control objective, whether that be ride, handling, or a dynamically weighted combination. These tools have demonstrated the capability to predict key design parameters such as peak instantaneous force and maximum actuation bandwidth as a function of vehicle speed and the geometric characteristics of the single event excitation.

In an effort to maximize the value-added of a real-time anticipatory suspension control system for mitigating single event excitations, researchers at Virginia Tech have evaluated the use of pneumatic actuation systems. This research effort has resulted in a set of design tools as well as a positive indication that pneumatic actuators can be used to achieve the requirements for a range of vehicles and single event excitations.

**Research Objectives:**

This research effort will focus on the design and validation of a real-time anticipatory suspension control law that is capable of mitigating the effects of single event disturbances. Leveraging results from the previous research effort, the initial phase of this research will focus on the control law development, and therefore, will assume unlimited actuation.

Fachgebiet Fahrzeugtechnik

FZD

Prof. Dr. rer. nat. Hermann Winner

Otto-Berndt-Straße 2
64287 Darmstadt

Tel. +49 6151 16 – 24200
Fax +49 6151 16 – 24205
winner@fzd.tu-darmstadt.de
www.fahrzeugtechnik-darmstadt.de

Date
10.04.2017

After a working real-time anticipatory control law has been validated, a realistic actuator model will be incorporated into the closed-loop system. This addition may require modification to the control law.

Development of the real-time anticipatory control law will leverage the initial research effort, which resulted in a set of tools for determining the ideal control force profiles. This set of tools was based on an anti-causal adaptive filter implementation that is engineered for this specific problem. Even though the adaptive filter performed extremely well, only a causal control law can be implemented in practice. Causal implementations of the adaptive filter will be investigated that include a combination of fast adaptation with gain-scheduled filters using the database of solutions from the previous research effort.

The specific design tasks for this research effort will be:

- Evaluate the database of ideal force profiles to determine whether a mathematical correspondence exists for a given profile at different vehicle speeds
- Evaluate the database of ideal force profiles to determine whether a mathematical correspondence exists between given profiles at a constant vehicle speed
- Implement a open-loop non-adaptive gain-scheduled control law based on the database profiles and evaluate the mitigation performance
- Implement a closed-loop adaptive control law and evaluate the mitigation performance and maximum convergence rate of the adaptation process
- Merge the closed-loop adaptive and open-loop gain-scheduled control laws and evaluate the mitigation performance and maximum convergence rate of the adaptation process
- Incorporate a realistic pneumatic actuator model into the closed-loop simulation and implement any required modifications to the control law

The Master thesis remains property of the institutes. It is pointed to the notes of the Institute of Automotive Engineering and of the Performance Engineering Research Lab.

Prof. Dr. rer. nat. Hermann Winner

Prof. Dr. Steve C. Southward

# Abstract

Most commercial vehicles currently on the market are still equipped with a passive suspension system, while some luxury brands may already use an adaptive suspension. Active suspension systems on the other hand are rarely found, however, they offer great opportunities to close the gap of the well-known trade-off between ride comfort and handling. Besides that, they can also be used to mitigate single event disturbances, an objective of the USA army as announced in a solicitation which initiated and motivated this research. In addition to that, several studies were found stating the impact and danger of potholes and their impact on the vehicle and passenger.

Reviewing the literature, several control strategies for controlling active suspension systems were found. However, most of these approaches used feedback control and did not try to mitigate single event disturbances. Since literature also suggested making use of look ahead preview, research at the Performance Engineering Research Lab at Virginia Tech was started in 2015 combining look ahead preview and an adaptive system to generate optimal force profiles. This introductory research succeeded and proved the used approach to be very promising. However, the used adaptive system was not designed to operate in real-time and did not show any correlation between different road profiles.

Therefore, the main objective of this research project is to evaluate and analyze each of the adaptive systems by searching for correlations in their solutions. The results then should be used in order to design a control law which emulates the adaptive system and can be used in a real-time environment.

First, an overall research methodology was derived. According to this a software application was developed which extracts ideal force profiles from single event disturbance signals in order to mitigate their impact to the vehicle. The application uses a quarter car model with a partially loaded active suspension system, a set of predefined road profiles, a road profile preprocessor, and an adaptive algorithm. The preprocessing includes geometric filtering using a Tandem-Cam Model and the adaptive processor used an iterative version of the Filtered-X Last-Mean-Square algorithm.

During evaluation and analysis of several generated data sets, high correlations in the generated and adjusted adaptive systems were discovered. From these an empirical and theoretical universal filter model was derived, which was then used to design an open-loop control law named Optimal Force Control.

The original control law and an adjusted version designed for a real-time environment were tested for all predefined road profiles over all considered vehicle velocities and prove to perform much better than the offline solution using the adaptive system.

In summary, a control law named Optimal Force Control was designed which can be used and implemented in a vehicle to extract an analytical and ideal force profile given a road profile input. Implementing an active suspension system with tracking controller, this approach can be used in order to mitigate single event disturbance signals by reducing the vertical vehicle acceleration.

## Acknowledgements

First, I would like to thank my two academic advisors Prof. Dr. Steve C. Southward from Virginia Tech and Prof. Dr. rer. nat. Hermann Winner from Technische Universität Darmstadt for their support and for giving me the opportunity to work on this research project. Second, I would like to thank Prof. Dr. Jan H. Bøhn from Virginia Tech and Prof. Dr.-Ing. Manfred J. Hampe from Technische Universität Darmstadt for their consistent work and effort in order to make this Dual Degree Master Program at Technische Universität Darmstadt and Virginia Tech possible. I enjoyed the experience of being a student and learn at both universities, which made me grow personally and academically.

I also would like to thank Mrs. Kerstin Gutierrez, Mrs. Gabriele von Laufenberg, and Mr. Nils Magiera from Technische Universität Darmstadt and Mrs. Cathy Hill from Virginia Tech for their support and help with all administrative activities concerning the Dual Degree Master Program as well as this Master's Thesis.

My special thanks and recognition also goes to my two good friends Sebastian Gonsior from Johann Wolfgang Goethe-Universität Frankfurt am Main and Jackson Klein from Virginia Tech for their feedback and comments as the second readers of this Master's Thesis.

# Table of Contents

# Formula Symbols and Indices

Latin Letters:

| Symbol | Unit | Description |
|---|---|---|
| $a$ | $\frac{m}{s^2}$ | acceleration |
| $a$ | m | contact length |
| $a$ | variable | placeholder variable |
| $a$ | 1 | shape parameter |
| $b$ | variable | placeholder variable |
| $b$ | 1 | shape parameter |
| $c$ | variable | placeholder variable |
| $c$ | 1 | shape parameter |
| $d$ | Ns/m | damping coefficient |
| $d$ | $\frac{m}{s^2}$ | desired signal |
| $D$ | 1 | delay element |
| $e$ | $\frac{m}{s^2}$ | error signal |
| $f$ | 1 | function |
| $F$ | N | force |
| $F$ | Hz | sample frequency |
| $FG$ | N | force generator |
| $FGC$ | 1 | force generator controller |
| $h$ | m | height |
| $k$ | N/m | spring stiffness |
| $l$ | m | length |
| $m$ | kg | mass |
| $MSE$ | $\frac{m^2}{s^4}$ | mean-square-error |
| $nloops$ | 1 | number of iteration iFX-LMS algorithm |
| $p$ | 1 | ellipse length parameter |
| $P$ | variable | plant |
| $r$ | m | radius |
| $TF$ | variable | transfer-function |
| $u$ | variable | control signal |
| $w$ | m | effective height |
| $w$ | 1 | weight |
| $W$ | 1 | weight vector |
| $x$ | variable | placeholder variable |
| $x$ | m | travel distance |
| $X$ | m | global travel distance |
| $y$ | variable | placeholder variable |
| $y$ | m | vertical displacement |
| $z$ | variable | placeholder variable |
| $z$ | m | vertical displacement |
| $z^{-1}$ | 1/z | unit delay |

Greek Letters:

| Symbol | Unit | Description |
|---|---|---|
| $\mu$ | 1 | step size LMS algorithm |
| $\nabla$ | variable | gradient |

Indices:

| Symbol | Description |
|---|---|
| *a* | effective acceleration sprung mass |
| *ae* | half ellipse height a |
| *b* | basic function |
| *be* | half ellipse height b |
| *ce* | ellipse exponent |
| $d_s$ | shock absorber sprung mass |
| $d_t$ | shock absorber tire |
| *e* | elliptical cam |
| *eo* | effective rolling |
| *f* | offset |
| *F* | force |
| *gf* | geometric filtered |
| *k* | at time k |
| $k_s$ | spring of sprung mass |
| $k_t$ | spring of tire |
| *o* | unloaded |
| *r* | road |
| *s* | sample |
| *s* | suspension |
| *s* | sprung mass |
| *sh* | shift length |
| *step* | step |
| *t* | tire |
| *u* | unsprung mass |
| *z* | vertical road displacement |

## List of Abbreviations

| | |
|---|---|
| AASHTO | American Association of State Highway and Transportation Officials |
| ADP | Advanced Design Project |
| A.k.a. | Also known as |
| CA | Road Profile Curb A |
| CB | Road Profile Curb B |
| CC | Road Profile Curb C |
| CD | Road Profile Curb D |
| CE | Road Profile Curb E |
| Cf. | Confer |
| CF | Road Profile Curb F |
| CG | Road Profile Curb G |
| Corr. | Correlation |
| E | Evaluation |
| EUFW | Empirical Universal Filter Model for $W$ |
| FG | Force Generator |
| FGC | Force Generator Controller |
| FIR | Finite-Impulse-Response |
| FZD | Fahrzeugtechnik Darmstadt |
| HS | Road Profile Seminole Profile Hump |
| HW | Road Profile Watts Profile Hump |
| iFX-LMS | Iterative Filtered-X Least-Mean-Square Algorithm |
| JLTV | Joint Light Tactical Vehicle |
| LMS | Least-Mean-Square |
| LTI | Linear Time Invariant |
| MISO | Multiple Input Single Output |
| MRAP | Mine Resistant Ambush Protected Vehicle |
| No. | Number |
| Ot. | Own Translation |
| P | Plant |

| | |
|---|---|
| P | Profile |
| PERL | Performance Engineering Research Lab |
| P1 | Road Profile Pothole 1 |
| P2 | Road Profile Pothole 2 |
| P3 | Road Profile Pothole 3 |
| RDECOM | Research, Development, and Engineering Command |
| SBIR | Small Business Innovation Research |
| SS | State-Space System |
| TF | Transfer-Function |
| TUD | Technische Universität Darmstadt |
| TUFW | Theoretical Universal Filter Model for $W$ |
| URA | Road Profile Uneven Road A |
| URB | Road Profile Uneven Road B |
| URC | Road Profile Uneven Road C |
| V | Velocity |
| VT | Virginia Polytechnic Institute and State University, also known as Virginia Tech |

## List of Figures

## List of Tables

# 1 Introduction

The research project presented in this Master's Thesis aims to develop a real-time anticipatory suspension controller for an active suspension system mitigating single event disturbances by using a Least-Mean-Square (LMS) algorithm based on a quarter car model. It is a joint research project between the Institute of Automotive Engineering (FZD) at Technische Universität Darmstadt (TUD) and the Performance Engineering Research Lab (PERL) at Virginia Polytechnic Institute and State University (VT), also known as Virginia Tech. The research project is advised by Prof. Dr. Steve C. Southward (VT) and by Prof. Dr. rer. nat. Hermann Winner (TUD).

The overall research project was initiated and motivated by a solicitation from the US Department of Defense.[1] This Master's Thesis continues and builds on outcomes from previous research done at PERL VT.[2]

This first chapter states the motivation behind the overall research project[3], followed by a description of the state of the art[4], introduces previous work done at PERL VT[2], and closes by outlining the research objectives of this Master's Thesis research project[5].

## 1.1 Motivation

The initiator and basis of the overall research project, which began at PERL VT in 2015, was a solicitation by the US Army RDECOM. The solicitation "High Capability Off-Road Active Suspension System"[6] was released in November of 2013 under the Army SBIR Program.[7]

In this solicitation the Army is addressing two of their largest mobility issues, "soft soil (mud and sand) mobility"[6] and "vehicle rollovers caused by road breakaways"[6], for "Mine Resistant Ambush Protected Vehicles"[8] (MRAP) and "Joint Light Tactical Vehicles"[9] (JLTV). Therefore, the Army is looking for innovative and new ways to use advanced (active) suspension systems to allow their vehicles to walk themselves out of immobilized conditions and reduce the risk of vehicle rollovers caused by road breakaways.[10]

---

1 See US Army Research, Development, and Engineering Command (RDECOM): ARMY 14.1 Small Business Innovation Research (SBIR) Proposal Submission Instructions, 2013, pp. 94-95.

2 See chapter 1.3 Previous Work.

3 See chapter 1.1 Motivation.

4 See chapter 1.2 State of the Art.

5 See chapter 1.4 Research Objectives.

6 US Army Research, Development, and Engineering Command (RDECOM): ARMY 14.1 Small Business Innovation Research (SBIR) Proposal Submission Instructions, 2013, p. 94.

7 Cf. SBIR STTR: High Capability Off-Road Active Suspension System, 2013, pp. 1-2.

8 Military.com: Cougar 6x6 MRAP, 2017.

9 Military.com: Joint Light Tactical Vehicle (JLTV), 2017.

10 Cf. US Army Research, Development, and Engineering Command (RDECOM): ARMY 14.1 Small Business Innovation Research (SBIR) Proposal Submission Instructions, 2013, pp. 94-95.

In order to solve these two issues, the Army asks for a detailed system design which

- is applicable for 10 – 37 t wheeled MRAPs and JLTVs,
- detects situations in which a vehicle is stuck or in danger of rolling over,
- controls and takes advantage of the entire travel range of a vehicle's suspension,
- uses an active suspension system,
- maximizes soft soil mobility by generating alternating side axle loads to walk a vehicle out of stuck situations, and
- mitigates road breakaway rollovers appropriately by responding to unexpected events up to a speed of 65 mph.[11]

According to the Army, significant work has been done in the past to improve ride and handling control using advanced suspension systems. Unfortunately, none of these works have developed control algorithms to either improve soft soil mobility or mitigate vehicle rollovers, both of which are of special importance to the Army.[11]

While the solicitation background for the Army was to improve their armed forces' performance in rough terrain[11], research at Virginia Tech aims to take this approach and relate it to civil road traffic. The main focus of VT PERL's research is on mitigating single event disturbances, which is the upper category of road breakaways and includes all kinds of short duration road disturbances such as curbs, humps, potholes, etc. Improving soft soil mobility is not part of the overall research project, since it is not as important for the civilian road traffic as it is to the Army.

Potholes and their impact on vehicles are good examples of single event disturbances. It is well known that potholes are most likely to cause an uncomfortable shock through the vehicle which can result in discomfort, stress, and, in an extreme scenario, medical injuries for the occupants of the vehicle. Beside these facts, potholes can also cause serious damage to the vehicle and may cause crashes. A study from the American Automobile Association, published in February of 2016 by the Automobile Club Southern California, reveals potholes cause damage worth three billion dollar in the Unites States of America each year.[12] Even though a publication from the Society of Automotive Engineers in 1996 states that the impact of potholes only causes vertical and longitudinal forces to the vehicle but no significant sides forces to veer the vehicle from its intended course[13], several studies claim potholes at least contribute to crash frequency and severity. According to *The Times of India*, nearly eleven thousand people were killed in 2015 due to crashes caused by potholes, speed breakers, and

[11] Cf. US Army Research, Development, and Engineering Command (RDECOM): ARMY 14.1 Small Business Innovation Research (SBIR) Proposal Submission Instructions, 2013, pp. 94-95.

[12] Cf. Automobile Club Southern California: Pothole Damage Costs Drivers $3 Billion Annually Nationwide, 2016.

[13] Cf. Rudny, D. F., and Sallmann, D. W.f: Analysis of Accidents Involving Alleged Road Surface Defects (i.e., Shoulder Drop-offs, Loose Gravel, Bumps and Potholes), 1996, pp. 10-13.

roads under construction.[14] Another statistic gives the percentage of accidents which occur where various road conditions, such as surface defects and poor road conditions, contributed to crash frequency or severity in the United States of America in the year of 2006.[15] The statistic is presented in Table 1-1, but should be treated with caution since surface defects and poor road conditions are only two out of the 22 considered factors.[16]

Table 1-1: Traffic Crash Incidents in the USA from 2006[17]

| | no. of crashes | % | no. of non-fatally injured people | % | no. of people killed | % |
|---|---|---|---|---|---|---|
| all crashes | 17.0 M | 100 | 5.7 M | 100 | 42.6 k | 100 |
| crashes in which road conditions contributed to crash frequency or severity | 5.3 M | 31.4 | 2.2 M | 38.2 | 22.5 k | 52.7 |

Both statistics clearly indicate a connection between potholes and accidents. The connection might be only indirect and explained by drivers slowing down, evading potholes or being frightened after hitting undetected potholes due to poor (weather/darkness) or blocked (vehicle in front) visibility.[18]

Considering these statistical numbers, the constantly growing traffic volume, and constantly aging road conditions, the extent and importance of the overall research topic becomes clear.

## 1.2 State of the Art

Most sources classify automotive suspension systems into three main categories:

- passive suspension systems,
- semi-active/adaptive suspension systems, and
- active suspension systems.[19, 20]

Figure 1-1 shows a mechanical diagram of a vehicle with a modular suspension system, including three placeholders, ❶, ❷, and ❸, per axis between the vehicle's chassis and its wheels. Figure 1-2 shows five mechanical components for the suspension system, namely: spring Ⓐ, shock absorber Ⓑ adaptive spring Ⓒ, adaptive shock absorber Ⓓ, and force generator/actuation system Ⓔ. By putting different combinations of the components from Figure 1-2 into the placeholders in Figure 1-1, each of the above-mentioned categories can be generated.

14 Cf. Dash, K. D.: Bad roads killed over 10k people in 2015; 3,416 deaths due to potholes, 2016.

15 Cf. Zaloshnja, E. and Miller, T. R.: Cost of Crashes Related to Road Conditions, United States, 2006, 2009, pp. 143 & 149.

16 Cf. Zaloshnja, E. and Miller, T. R.: Cost of Crashes Related to Road Conditions, United States, 2006, 2009, pp. 143.

17 Cf. Zaloshnja, E. and Miller, T. R.: Cost of Crashes Related to Road Conditions, United States, 2006, 2009, p. 149.

18 Cf. Hegde, S., Mekali, H. V., and Varaprasad, G.: Pothole Detection and Inter Vehicular Communication, 2014, p. 84.

19 Cf. Aboud, W. S., Haris, S. M., and Yaacob, Y.: Advances in the control of mechatronic suspension systems, 2014, pp. 849-851.

20 Cf. Fischer, D. and Isermann, R.: Mechatronic semi-active and active vehicle suspensions, 2003, pp. 1353-1357.

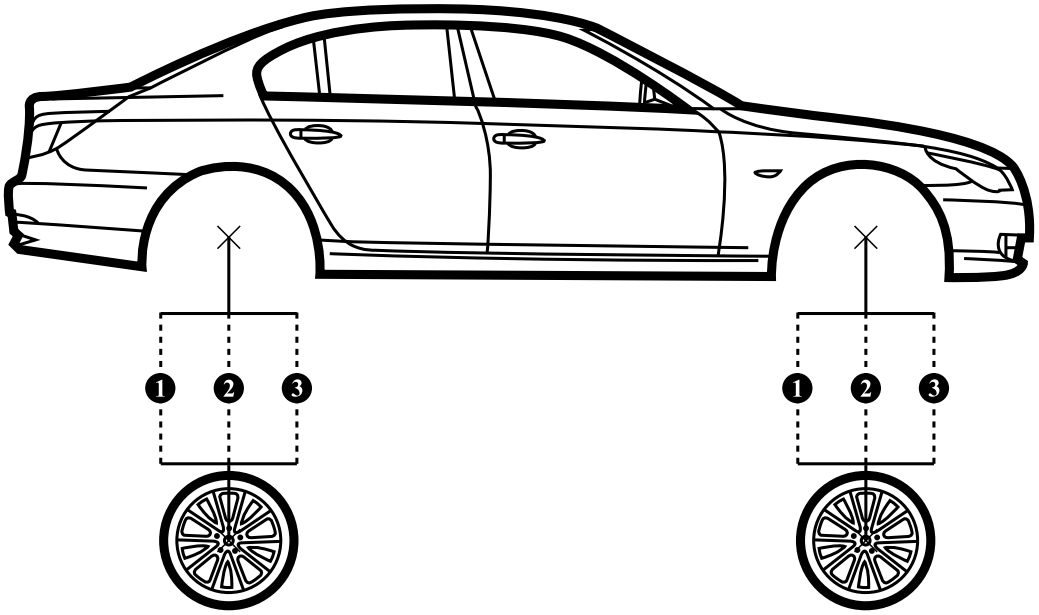


Figure 1-1: Mechanical Diagram of a Vehicle with a Modular Suspension System[21]

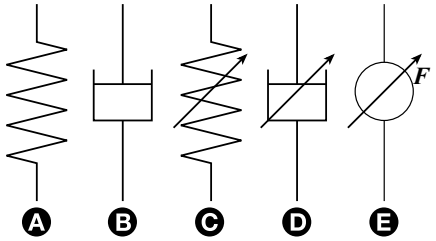


Figure 1-2: Mechanical Components of a Vehicle Suspension Systems

Most vehicles currently on the road are still equipped with passive suspension systems[22], even though a tremendous amount of research on non-passive suspension systems has been done over the last decades. A passive suspension system consists of a parallel combination of springs Ⓐ and shock absorbers Ⓑ; Ⓐ in ❶ and Ⓑ in ❷.[23] Spring stiffness and damping coefficients are constant, which leads to the well-known trade-off between ride comfort and handling. Soft suspensions are installed to provide good ride comfort for the occupants, while the handling performance decreases. Good handling performance on the other hand requires a stiff suspension, which results in a decreased ride comfort.[24]

21 Cf. Golovanov, A.: BMW 5 Series (5th generation) icon, 2017.

22 Cf. ot. Mitschke, M. and Wallentowitz, H.: Dynamik der Kraftfahrzeuge, 2014, p. 426.

23 Cf. Aboud, W. S., Haris, S. M., and Yaacob, Y.: Advances in the control of mechatronic suspension systems, 2014, p. 851.

24 Cf. Ikenaga, S., Lewis, F. L., and Davis, L.: Active Suspension Control of Ground Vehicle based on a Full-Vehicle Model, 2000, p. 4019.

In order to reduce this impact of the trade-off, an increasing number of automakers have made semi-active/adaptive suspension systems available for some of their models, mostly in the luxury segment.[25, 26] These suspension systems are able to change their spring stiffness and/or damping coefficient by putting together a suspension system consisting of parallel combinations of adjustable and non-adjustable springs Ⓐ/Ⓒ and dampers Ⓑ/Ⓓ, in which at least one component is adjustable; Ⓐ or Ⓒ in ❶ and Ⓑ or Ⓓ in ❷. Also a combination of a non-adjustable spring Ⓐ in series with a force generator/actuating system Ⓔ in parallel with a non-adjustable shock absorber Ⓑ is possible, used in order to create a low bandwidth adaptive suspension system; Ⓐ parallel with Ⓔ in ❶ and Ⓑ in ❷.[27, 28] Examples for these kinds of suspension systems are Audi's Adaptive Air Suspension[25] and Adaptive Drive from BMW.[26] Audi's Air Suspension system is able to adjust the vehicle's height in order to provide more ground clearance in rough terrain (Audi A6 Allroad Quattro), and can adjust the damping coefficients at each wheel by using electromagnetic valves.[25] BMW's Adaptive Drive system's main goal is to improve driving stability by adjusting damping coefficients as well.[26] With these products the driver is able to adjust the suspension's behavior by switching from a stiff to a soft suspension characteristic. Thus, the driver benefits from good handling performance, for example on highways and interstates, as well as from increased ride comfort, for example on uneven roads.

Beside from these two categories, active suspensions require a force generator/actuation system Ⓔ which can be combined with springs Ⓐ and shock absorbers Ⓑ. In the case of an active fully loaded suspension, the force generator/actuation system Ⓔ is the only component between the vehicle's chassis and wheel, and it handles all tasks performed by springs and shock absorbers; Ⓔ in ❶. Active partial loaded suspensions consist of a force generator/actuation system Ⓔ parallel to springs Ⓐ and shock absorbers Ⓑ; Ⓐ in ❶, Ⓑ in ❷, and Ⓔ in ❸.[27, 28] The force generator/actuation system generates forces between the vehicle's chassis and wheel (positive and negative) and is the main differentiator between active suspensions and the other categories. Active suspension systems are able to adapt to varying road conditions with a high bandwidth and make use of the entire suspension travel range. This way they are able to satisfy both ride comfort and handling performance simultaneously.[29] Another and well explained way to look at the application differences is the followed citation from "Advances in the control of mechatronic suspension systems" by Aboud, Haris, and Yaacob:

"To understand apparently the subtle difference between semi-active and active suspensions, consider a hypothetical conflict with a known pothole. A semi-active system will make the suspension softer when hitting the pothole and stiff after the pothole. An active suspension could feasibly lift the wheel over the pothole, and thereby will improve both ride comfort and safety."[30]

---

25 Cf. ot. Audi Technology Portal: adaptive air suspension, 2017.

26 Cf. ot. BMW Techniklexikon: Adaptive Drive, 2017.

27 Cf. Aboud, W. S., Haris, S. M., and Yaacob, Y.: Advances in the control of mechatronic suspension systems, 2014, pp. 849-851.

28 Cf. Fischer, D. and Isermann, R.: Mechatronic semi-active and active vehicle suspensions, 2003, pp. 1355-1357.

29 Cf. Aboud, W. S., Haris, S. M., and Yaacob, Y.: Advances in the control of mechatronic suspension systems, 2014, pp. 851-854.

30 Aboud, W. S., Haris, S. M., and Yaacob, Y.: Advances in the control of mechatronic suspension systems, 2014, p. 852.

Until now, active suspension systems can rarely be found in standard vehicles. Magic Body Control from Mercedes Benz is one of the few available systems. It is able to generate forces between the vehicle's chassis and wheels to, among other things, level out vehicle movements during steering, breaking and accelerating, as well as smooth out low frequency road disturbances.[31] Figure 1-3 shows an image of the active suspension system from Mercedes Benz, a.k.a Magic Body Control.

Figure 1-3: Active Suspension from Mercedes Benz, a.k.a. Magic Body Control[32]

Bose Corp. has been conducting research since 1980 on developing and designing an active suspension system in order to eliminate the tradeoff between ride comfort and handling. They were able to develop an active fully loaded suspension. It uses linear electromagnetic motors to compensate road disturbances and can be used in generator mode as well. Bose Corp. was also able to reduce the required power to run the active suspension system to one-third of the power needed for a standard car air conditioning.[33]

Active suspension systems can be realized using a variety of system designs and actuation systems. Aboud, Wajdi S., Haris, Sallehuddin Mohamed, and Yaacob,Yuzita have summarized different types of actuation systems used in active suspension systems: oleo-pneumatic actuators, hydraulic actuators, magnetic, and electromagnetic actuators.[34]

31 Cf. ot. Mercedes-Benz Techcenter: Magic Body Control, 2017.

32 Cf. Dyer, E: 3 Technologies That Are Making Car Suspensions Smarter Than Ever, 2017.

33 Cf. ot Auto Motor und Sport: Aktives Fahrwerk von Bose, 2004.

34 Cf. Aboud, W. S., Haris, S. M., and Yaacob, Y.: Advances in the control of mechatronic suspension systems, 2014, pp. 852-854.

Another way to look at the differences of suspension categories is from an energy perspective. Passive suspensions are only able to store energy in their springs for a very limited time, while the shock absorbers dissipate the energy.[35] Even though semi-active/adaptive suspensions put external energy into the system, this energy is mainly used for the adaptation process of the passive components, meaning the energy does not have direct influence on the overall system behavior. Active suspensions on the other hand are able to take advantage of supplied energy and transform it into forces inside the system in order to actively control the overall system behavior, without the need of earlier stored energy[35].

In summary, active suspensions clearly offer the best possibility for controlling ride comfort and handling simultaneously, mitigating road disturbances, using the entire range of the suspensions, and providing a high bandwidth reaction. That said, they are expensive, complex, require more space, and still have the need for additional research in the areas of design, power consumption, and control algorithms[36].

While currently available and designed systems vary in functionality and design, it gives the impression that the overall system and actuator design process is still in a phase that requires additional iterations, maybe with support from additional design tools. From the controls' point of view, several different approaches were made in the past concerning controlling active suspensions.

Thompson showed an approach to use an optimal linear state feedback to obtain a practical solution on a tracking problem. A road input in the form of a PSD was used to represent a variety of road profiles. He concludes that it is possible to evolve a physically realizable and controllable active suspension system, but more instrumentations and sensors are needed for his approach.[37]

Ab. Talib and Mat Darns have investigated the use of PID control in order to tune vehicle responses due to bumps/holes, sine waves, and random road profiles. The methods they used for tuning were heuristic, Ziegler-Nichols, and iterative learning algorithm (ILA) tuning. Best results were shown to be had using iterative learning algorithm (ILA) tuning. Compared to passive suspension systems, all of the three tuning methods were able to reduce the impact of road disturbances to the vehicle.[38]

PID control was then compared to fuzzy logic control by Changizi and Rouhani. By using 75 rules for deriving the fuzzy terms, they were able to provide better performance than the PID control approach.[39]

[35] Cf. Rao, A. M.: A Structured Approach to Defining Active Suspension Requirements, 2016, p. 1.

[36] Cf. Tseng, H. E. and Hrovat, D.: State of the art survey: active and semi-active suspension control, 2015, pp. 1034-1035.

[37] Cf. Thompson, A. G.: An Active Suspension with Optimal Linear State Feedback, 2007, pp. 187-203.

[38] Cf. Ab. Talib, M. H. and Mat Darus, I. Z.: Self-Tuning PID Controller for Active Suspension System with Hydraulic Actuator, 2013, pp. 86-91.

[39] Cf. Changizi, N. and Rouhani, M.: Comparing PID and Fuzzy Logic Control a Quarter Car Suspension System, 2011, pp. 559-564.

More approaches for controlling active suspensions can be found in the literature. Ghazaly and Moaaz[40] as well as Aboud, Haris and Yaacob[41] reviewed and summarized the state of the art. To name some more: optimal control, robust control, adaptive control, robust adaptive control, switching control, combinations of different control approaches, etc., also by using different theoretical approaches like skyhook, etc.[42]

So far, none of the above-mentioned approaches made use of preview information, even though Bender proposed and showed the significant impact of preview information in active suspension systems as early as 1968.[43] Preview information of the road can be collected using different kinds of sensors. Mercedes Benz uses a system which they call Road Surface Scan for its Magic Body Control system. A stereo camera mounted close to the inside mirror enables the system to scan the road profile ahead of the vehicle and use this signal for controlling purpose.[44] Looking at the ongoing research in the field of autonomous driving vehicles, a tremendous number of new and additional sensors are being added to vehicles. It might be conceivable to use one of these new sensor approaches in order to get preview information of the road ahead of the vehicle. While HAĆ summarizes some of the previous work done in order to generate new control strategies using preview information, he states that preview information is not only able to improve ride comfort and handling, but also reduces power requirements and energy consumption[45].

Recapping the current state of the art, most of the approaches tried to close the gap between the ride comfort vs. handling trade-off using some kind of feedback control. None of the found attempts so far tried to find the ideal force profile, which can be used as a tracking signal for the force generator/actuation system in order to mitigate single event disturbances, and which would also be a great tool for the design purpose of active suspension systems. Rao started this approach with his Master's Thesis research and therefore began the overall research project at PERL VT[46].

## 1.3 Previous Work

As stated above, previous work was done at PERL VT in order to mitigate single event disturbances by using preview information in order to generate force profiles, which can then be used as tracking signal for force generators/actuation systems of an active suspensions. The approach should also be able to serve as a design tool for future work in the area of hardware design.[47]

---

40 See Ghazaly, N. M. and Moaaz, A. O.: The Future Development and Analysis of Vehicle Active Suspension Systems, 2014, pp. 19-25.

41 See Aboud, W. S., Haris, S. M., and Yaacob, Y.: Advances in the control of mechatronic suspension systems, 2014, pp. 848-860.

42 Cf. Aboud, W. S., Haris, S. M., and Yaacob, Y.: Advances in the control of mechatronic suspension systems, 2014, pp. 854-857.

43 Cf. HAĆ, A.: Optimum Linear Preview Control of Active Vehicle Suspension, 1992, pp. 167-168.

44 Cf. ot. Mercedes-Benz Techcenter: Magic Body Control, 2017.

45 HAĆ, A.: Optimum Linear Preview Control of Active Vehicle Suspension, 1992, pp. 167-195.

46 See Rao, A. M.: A Structured Approach to Defining Active Suspension Requirements, 2016.

47 Cf. Rao, Ashwin M.: A Structured Approach to Defining Active Suspension Requirements, 2016, pp. 1-68.

The overall research project was started by Rao, a former graduate student at PERL VT, in 2015 and is documented in his Master's Thesis with the title "A Structured Approach to Defining Active Suspension Requirements"[48], submitted to the faculty of Virginia Polytechnic Institute and State University in 2016-07. Rao's work was done using a quarter car model with a partial loaded active suspension system, using an ideal force generator/actuation system. As a basis, that will be used throughout the overall research project, Rao identified a set of standardized single event disturbance signals, which will further be called road profiles. He also set up a preprocessing procedure in order to use these road profiles as an input signal to his quarter car model.[49]

The quarter car with active suspension system was set up parametrical, in order to make quick changes and apply the research to different kind of vehicles and active suspension systems. Standardized single even disturbance signals, a.k.a road profiles, were chosen in order to simplify and reduce the complexity of the evaluation processes determining the impact of each road profile to the vehicle response and the generated force profiles.[49]

For generating force profiles, which are able to mitigate single event disturbances, an iterative FX-LMS algorithm approach was determined to be valid and suitable. Rao implemented this approach in his research project and was able to extract force profile signals from previewed road profile signals using offline simulations. He performed several test studies using a set of different road profiles and vehicle velocities in order to determine peak force requirements for the force generator/actuation system. In the end, he concluded that peak force requirements depend on the shape of the road profile, vehicle velocity as well as on the preview time. While all have an impact on the peak force, he determined vehicle velocity has the most.[49]

The outcome and success from this first research project provided enough information to start a second project at PERL VT. Using the determined peak force requirements, a research project in the form of an Advanced Design Project (ADP) was started with the target to prove the concept of implementing pneumatic actuation systems in active suspension systems.[50]

Compared to other systems, the advantages of pneumatic force generators/actuation systems are low cost, the availability of components, the ease of maintenance, the relatively high power to weight ratio as well as the readily available and cheap power sources. However, pneumatic driven actuation systems have highly nonlinear characteristics due to the compressibility of air, complex friction laws, and the nonlinearity of air valves, which makes the research and design process more complicated.[50]

Five main components were determined to be needed for a working system design: pneumatic cylinders, electromagnetic valves, an air compressor, air tanks, and supply hoses. Iterating through several system designs considering low, middle, and high pressure systems, a system design with 10 bar (1 MPa) cylinder operating pressure and 50 bar (5 MPa) air tank pressure was determined to be suitable and implementable. In the end, a set of suitable commercial off-the-shelf parts were suggested in order to build a test rack, which can be used for further research. A more detailed and individual

48 See Rao, A. M.: A Structured Approach to Defining Active Suspension Requirements, 2016, p. 1.

49 Cf. See Rao, A. M.: A Structured Approach to Defining Active Suspension Requirements, 2016, pp. 1-68.

50 Cf. Kappes, C: ME 5964 – Advanced Design Project, 2016.

component design would be needed in order to implement those components into a standard passenger car. Power requirements were determined to be less than the power needed for a vehicle air conditioning unit.[51]

All in all, the first research project determined a way to extract force profiles from preview information of road profiles in order to mitigate single event disturbances and predict peak force requirements using offline LMS algorithms. The second research project determined that a pneumatic actuation system is suitable for an active suspension system and gave a first set of key requirements for a possible system design.

## 1.4 Research Objectives

Until now, active suspension systems are still fairly rare to find in commercial vehicles, while still more research on system designs and control strategies is conducted. State of the art control strategies mostly use some kind of feedback control strategies in order to close the trade-off between ride comfort and handling.

The main research objective of the overall research project at PERL VT is to use preview information and LMS algorithms to extract ideal force profiles, which can be used as a tracking signal for a force generator/actuation system, controlled by a separated inner controller. For a new system design, pneumatic actuators are considered.

The research objective of this Master's Thesis will contribute to the overall research project by examining and building on outcomes of previous work by Rao. One of the main goals is to find relationships in the filter models, which extract force profiles from the previewed road profiles. Depending on whether relationships can be found and depending on the kind and strength of these relationships, the offline LMS algorithm approach will be transformed into a real-time control law. An open-loop control law is desired, but may be replaced or merged with a closed-loop control law. It is important to mention that this research project is a proof of concept whether relationships can be found and if a real-time control law based on LMS algorithms is realizable.

Eventually, the goal is to find a suitable control law that can be used for further research. It can also be used as a design tool for future active suspension systems, extracting key specifications from the different chosen environmental conditions. This research project will then also work on a real-time and real-world implementation by adjusting the found control law, discussing other system requirements, and suggesting further steps in the overall research and design process.

[51] Cf. Kappes, C.: ME 5964 – Advanced Design Project, 2016.

# 2 Methodology

To achieve the set research objectives, a structured methodology was developed and will be introduced in this chapter.

As mentioned above, this research project is part of the overall research project at PERL VT and builds on the outcomes of Rao's Master's Thesis and one Advanced Design Project. The methodology for this research project is split up into four main sections: Application Set Up[52], Data Generation and Evaluation[53], Controller Design[54], and Real-Time Realization[55]; Figure 2-1 visualizes the overall methodology in a flowchart. The Application Set Up section covers theoretical background information and implements it into a software application (Matlab script library), so that in section two different data sets can be generated and evaluated. This generation and evaluation process is done according to a predefined operational test plan. The controller design process in section three highly depends on the kind of relationships found in section two. The same is true for section four, in which the developed control law is adjusted to work in a real-time application and where the adjustments depend on the chosen controller design in section three.

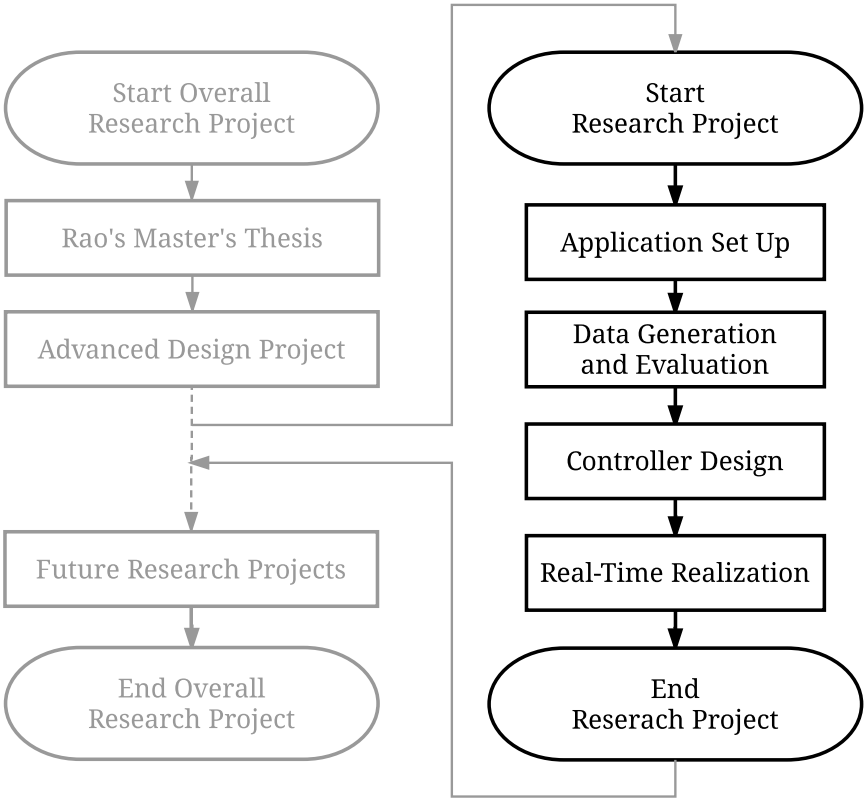


Figure 2-1: Flow Chart Methodology Overall Research Project

[52] See chapter 2.1 Application Set Up.

[53] See chapter 2.2 Data Generation and Evaluation.

[54] See chapter 2.3 Controller Design.

[55] See chapter 2.4 Real-Time Implementation.

## 2.1 Application Set Up

At the beginning of the research project a software application in form of a Matlab script library must be developed and set up. The application extracts force profiles from previewed road profile information ahead of the vehicle. The purpose of these force profiles is to mitigate single event disturbances by using an active suspension system. The application uses a realistic vehicle model, a road profile preprocessor and an LMS algorithm.

The developed and implemented realistic vehicle model is a quarter car model with a partial loaded active suspension system. It is used for simulating the uncontrolled and controlled vehicle response due to road and force excitations, and also serves as a discrete plant model for the LMS algorithm. The next step is to choose and implement appropriate standard road profiles, which represent common single event disturbances. The use of a set of standardized road profiles simplifies the search for relationships in the outcome signals. As Rao showed in his research, a preprocessing of these road profiles is necessary[56] and is therefore also implemented into the application. The approach from previous research is continued by using an LMS algorithm, which will use the quarter car model and the preprocessed road profiles to extract the force profiles. Figure 2-2 shows a flow chart of the Application Set Up methodology. Note: The application is based on and extends the previous script library from PERL VT.

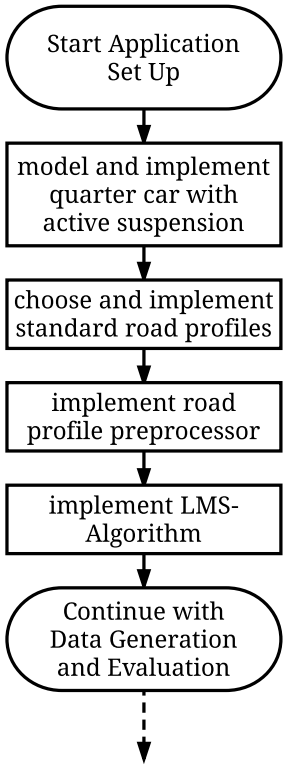


Figure 2-2: Flow Chart Methodology Application Set Up

[56] Cf. Rao, A. M.: A Structured Approach to Defining Active Suspension Requirements, 2016, pp. 14-34.

## 2.2 Data Generation and Evaluation

In order to find and determine relationships in the application outcomes, a properly planned operational test plan is of importance. The focus during the plan development process is on generating a plan were the relations between different road profiles and vehicle velocities is easy to understand and clearly to see. This simplifies and lowers the complexity of the data evaluation process in later steps where coherence in different LMS filters and force profiles are examined for existing relationships.

Before all data sets can be processed by the application, it is critical to tune and evaluate the performance of the LMS algorithm first. The LMS algorithm must be tuned accordingly to the fixed set of vehicle and road profile parameters. The tuning process and its variables will be covered in later chapters.[57] The importance of this process is high because it directly influences all further steps in this research project. The LMS algorithm must fully converge, and the reduction in its mean square error needs to be big enough to mitigate the disturbance signals well. This also generates more accurate filter profiles, which are easier to examine for correlations and relationships. Because a well-tuned LMS algorithm is so important a significant amount of time was spent on this step, which paid off eventually.

Afterwards all data sets are processed and visualized by the application according to the operational test plan using the tuned version of the LMS algorithm.

The following analysis and evaluation process is clearly one of the main parts of this research project. The evaluation process is based on both subjective and objective judgements. The subjective evaluation uses the earlier generated plots, while the objective part makes use of correlation coefficients in order to determine the level of correlation. Figure 2-3 shows a flow chart of the methodology for the data generation and evaluation process. First, the correlation between a fixed profile over different vehicle velocities is examined, since it is estimated that these correlate the most. Next, the correlation for one fixed vehicle velocity over different road profiles will be examined and evaluated. As is it shown below there are five possible outcomes from the evaluation process.

While outcome ❶ is clearly a worst-case scenario where no correlation or relationships can be found, it does not mean the end of the research project. In this case the LMS approach can still be transformed into a real-time solution[58], however, it would not be as efficient and require more work compared to the other outcomes. Outcomes ❷ and ❸ contain correlations and relationships between a variation of at least one variable, and outcome ❹ has correlations in both variables. These outcomes can be realized using a real-time gain scheduling control approach. Outcome ❺, from which a universal filter model can be derived from the data sets, is the best case and would lead to a controller design which can be easily realized in a very efficient way, without the need of a lot for additional hardware.[58] Outcomes ❷, ❸, and ❹ were estimated to be most likely after examining Rao's research outcomes.

[57] See chapter 4.2 iFX-LMS Tuning and Performance.

[58] See chapter 5 Controller Design.

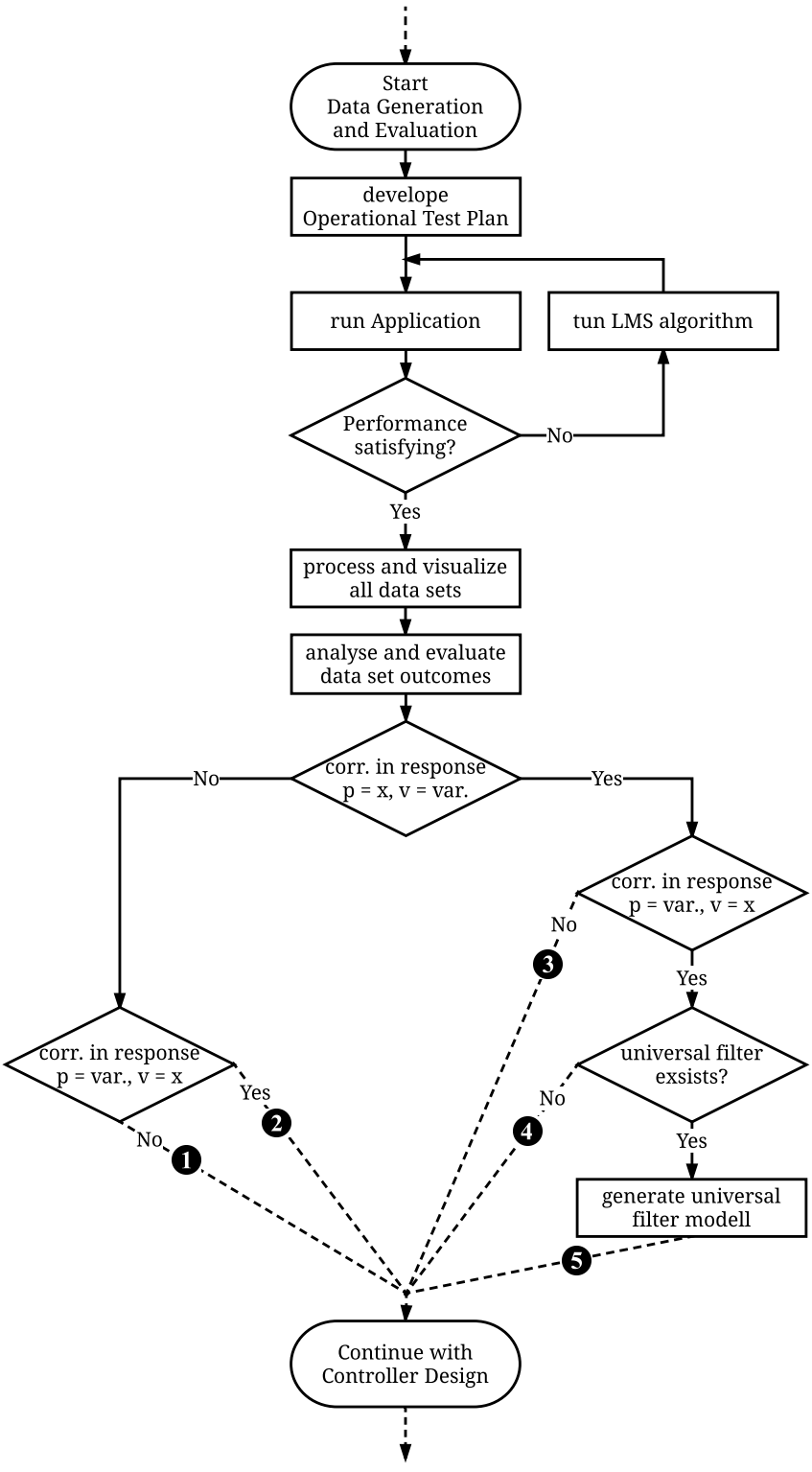


Figure 2-3: Flow Chart Methodology Data Generation and Evaluation

## 2.3 Controller Design

In this section a real-time controller is designed that ideally emulates the performance of the tuned offline LMS algorithm as best as it can, since a real-time version of the LMS algorithm is difficult to implement. Based on the found relationships the procedure is nearly the same for each of the five outcomes discussed in the previous section. The first attempt is to design an open-loop non-adaptive control law using gain-scheduling for road profiles or vehicle velocities, or a universal filter model. Depending on the performance of the open-loop controller, it might be necessary to also design a closed-loop adaptive control law which, either way, is merged with or without the open-loop control law. However, an open-loop controller design is preferred due to its general characteristics, i.e. less expensive, higher stability, and being easier to realize while being lesser complex. The methodology of this section is visualized in a flow chart diagram as well and shown in Figure 2-4.

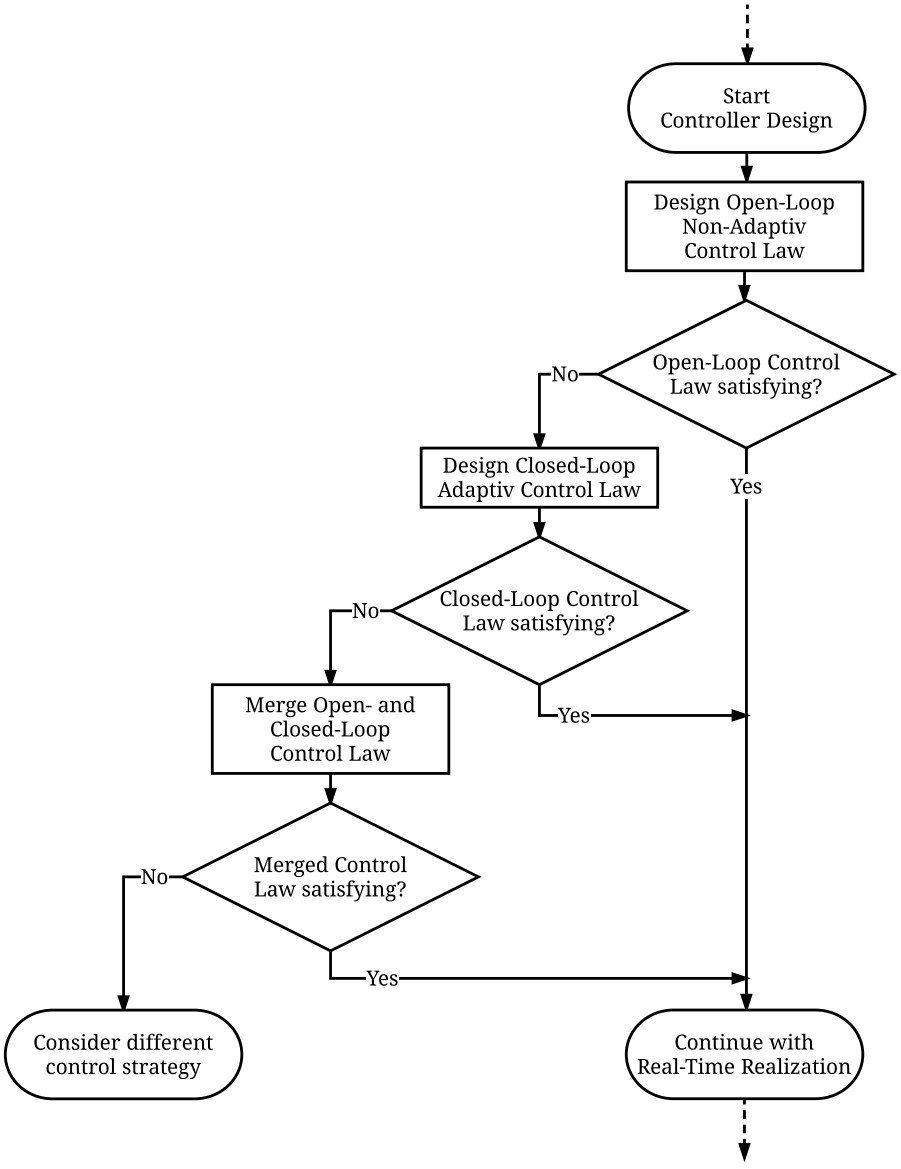


Figure 2-4: Flow Chart Methodology Controller Design

## 2.4 Real-Time Implementation

The final goal of this research project is to develop a control law which is based on the performance of the LMS algorithm approach and can be used in a real-time application. During the entire research project several simplifications and assumptions were made in order to develop the new control law in the following sections. To make sure the made simplifications and assumptions do not conflict with the final version of the control law and its real-time realization, this section reiterates to adjust the control law accordingly. The method for this section depends on all the simplifications and assumptions made throughout this research project, which is why a more detailed version of the methodology is not provided. Instead, some of the following questions will be asked later:

- Does the system behavior of a force generator/actuation system needs to be taken into account for the controller design?
- What kind of supporting hardware and software components are needed for a real-time realization and can they deliver the required in-/outputs accordingly?
- What are the limitations of the controller and do they require any additional safety features?

# 3 Application Set Up

As stated in chapter 2.1, this chapter provides information on the theoretical background of the conducted research and implements it into a software application (Matlab script library). First, the underlying vehicle model is explained and its equations are derived.[59] Second, the set of chosen road profiles representing common single event disturbances are introduced.[60] Afterwards, the necessary road profile preprocessing is explained.[61] These road profiles, along with the vehicle model, serve as inputs for the used LMS algorithm, which is explained next, along with its specific set up for this research project.[62] It is explained again in this chapter, because the underlying theoretical background is not trivial and because it is necessary to have this background knowledge in order to design an appropriate controller. Lastly, a relatively short overview is given about the chosen software and the realization/implementation of the application.[63]

## 3.1 Quarter Car Model with Active Suspension System

Vehicles can be represented mechanically using various kinds of mechanical models. The model chosen for this research is a quarter car model. As the name indicates, this model only represents a quarter of the overall vehicle, including a quarter mass of the vehicle's body, one suspension system, and one wheel in contact with the ground.

Sharp and Crolla state in their review paper the advantages and disadvantages of using quarter car models. Even though quarter car models do not contain some of the geometric effects of a full car model and do not allow for the study of longitudinal interconnections, they contain the most basic real problem features of a vehicle, like wheel load and suspension forces.[64] "It is the simplest model which has these features and possesses particular advantages over more complex models in terms of

(a) being described by few design parameters,

(b) having few performance parameters,

(c) having only a single input, leading to ease of computation of performance and ease of application of optimal control theory to derive control laws, and

(d) ease of mapping and understanding of the relationships between design and performance."[65]

After the research problem is solved using a quarter car model, it has to be applied again to a full car model to examine the impact of the ignored effects.

---

59 See chapter 3.1 Quarter Car Model with Active Suspension System.

60 See chapter 3.2 Road Profiles.

61 See chapter 3.3 Road Profile Preprocessing.

62 See chapter 3.4 iFX-LMS Algorithm.

63 See chapter 3.5 Software and Implementation.

64 Cf. Sharp, R. S. and Crolla, D. A.: Road Vehicle Suspension System Design - a review, 1987, pp. 171-172.

65 Sharp, R. S. and Crolla, D. A.: Road Vehicle Suspension System Design - a review, 1987, p. 172.

Before the quarter car model and its equation are derived, the effects of tire damping are discussed. Maher and Young outlined in their publication some of the current views about the importance and impact of tire damping.[66] Some authors argue that tire damping is not worth to be added to vehicle models. The main reasons given are the fact that it increases complexity of the model, and that the impact of tire damping is low compared to damping caused by the shock absorber.[67] On the other hand Türkay and Akçay concluded that tire damping has a significant impact on the performance of closed-loop controlled active suspension systems.[68] Therefore, in order to increase the accuracy of the model, and because closed-loop control is considered to be realized in this research project, tire damping is included in the quarter car model.

Figure 3-1 shows the mechanical diagram of the earlier introduced vehicle (left) and its quarter car model representation (right) with an active suspension system.

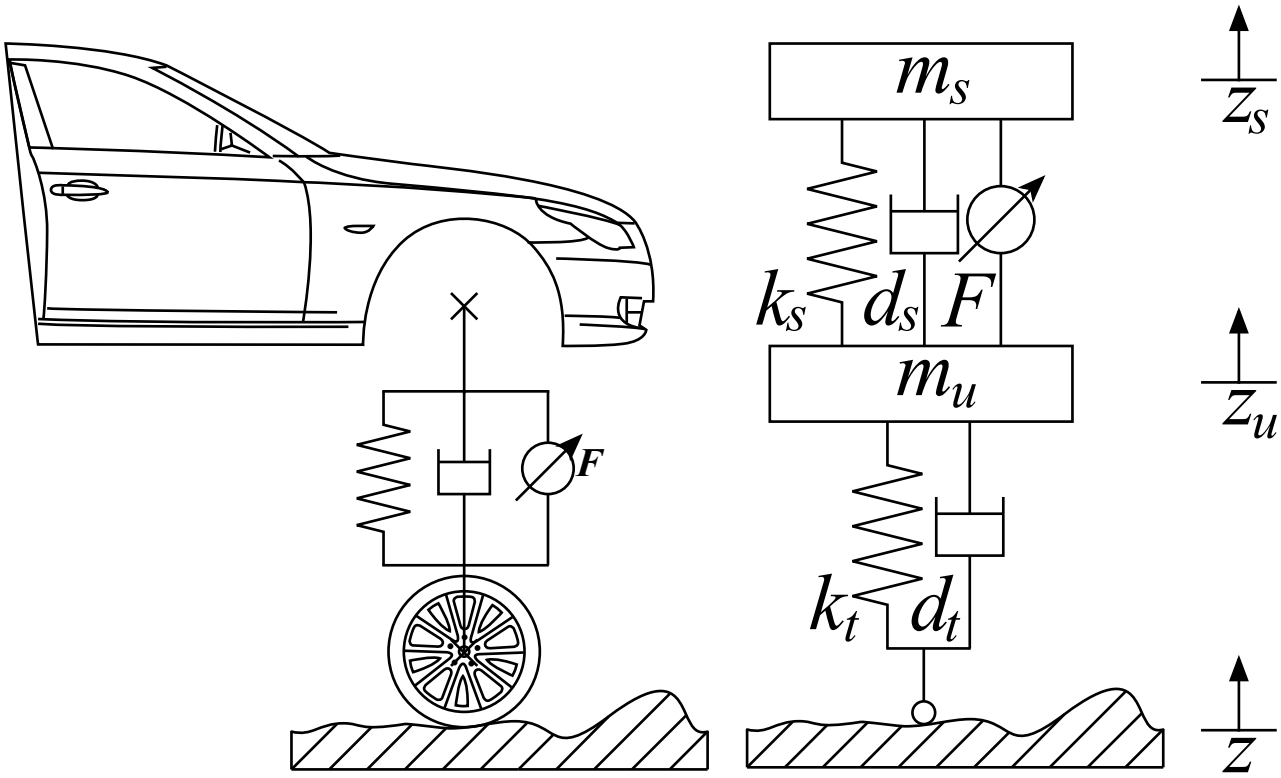


Figure 3-1: Mechanical Diagram Vehicle Model (left) and Quarter Car Model (right) with Active Suspension[69]

The model is a two-degree of freedom system with two masses. The upper mass $m_s$ is called the system's sprung mass and represents the mass of the quarter vehicle. The lower mass $m_u$ is called the system's unsprung mass and represents the mass of the tire. The partial loaded active suspension

66 See Maher, D. and Young, P.: An insight into linear quarter car model accuracy, 2011, pp. 465-466.

67 Cf. Maher, D. and Young, P.: An insight into linear quarter car model accuracy, 2011, pp. 465-466.

68 Cf. Türkay, S. and Akçay, H.: Influence of tire damping on the ride performance potential of quarter-car active suspensions, 2008, pp. 4390-4395.

69 Cf. Golovanov, A.: BMW 5 Series (5th generation) icon, 2017.

system is placed between the chassis and wheel of the vehicle. It is represented by a spring with stiffness $k_s$, a shock absorber with damping coefficient $d_s$, and the force generator/actuation system $F$. Tire behavior is modeled using a spring with stiffness $k_t$ and a damper with damping coefficient $d_t$. The coordinate systems are shown on the right side of Figure 3-1. The global coordinate system $z$ is given by the road profile, while the vertical vehicle and tire displacement are measured in the two local coordinate systems $z_s$ and $z_u$.

The behavior of the vehicle, suspension system, and tire is assumed to be linear, which simplifies the design process and holds to be valid and accurate enough for this research project. In Figure 3-2 the free body diagram of the quarter car model is shown in order to derive the system equations.

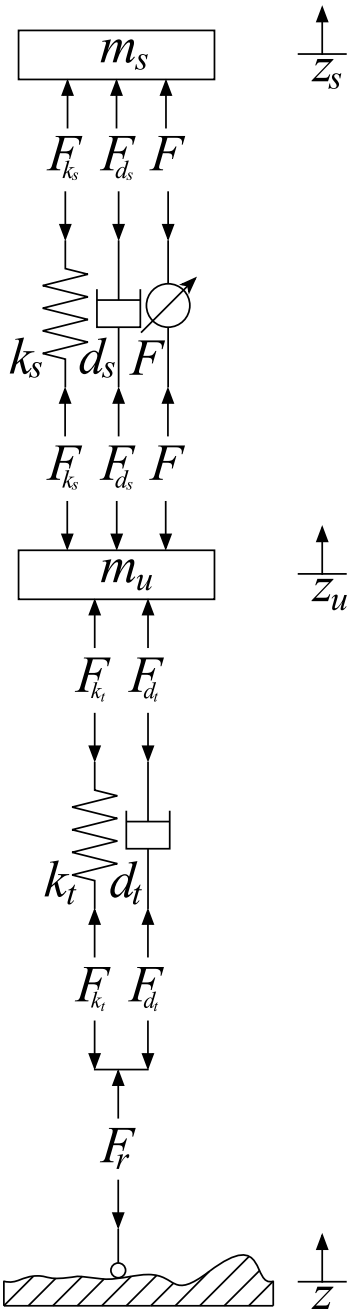


Figure 3-2: Free Body Diagram Quarter Car Model

Using the free body diagram the following system equations and equations of motion are derived.
Sprung mass:

$$F_{k_s} = k_s(z_u - z_s) \quad (3\text{-}1)$$

$$F_{d_s} = d_s(\dot{z}_u - \dot{z}_s) \quad (3\text{-}2)$$

$$F = F \quad (3\text{-}3)$$

$$m_s\ddot{z}_s = F_{k_s} + F_{d_s} + F \quad (3\text{-}4)$$

Unsprung mass:

$$F_{k_u} = k_t(z - z_u) \quad (3\text{-}5)$$

$$F_{d_u} = d_t(\dot{z} - \dot{z}_u) \quad (3\text{-}6)$$

$$m_u\ddot{z}_u = -F_{k_s} - F_{d_s} + F_{k_u} + F_{d_u} + F \quad (3\text{-}7)$$

Putting equations ( 3-1 ) - ( 3-3 ) and ( 3-5 ) - ( 3-6 ) in ( 3-4 ) and ( 3-7 ):

$$m_s\ddot{z}_s = k_s(z_u - z_s) + d_s(\dot{z}_u - \dot{z}_s) + F \quad (3\text{-}8)$$

$$m_u\ddot{z}_u = -k_s(z_u - z_s) - d_s(\dot{z}_u - \dot{z}_s) + k_t(z - z_u) + d_t(\dot{z} - \dot{z}_u) + F \quad (3\text{-}9)$$

The excitation signals (inputs) of the system are the road disturbance signal $z$ and $\dot{z}$ and the force of the force generator/actuation system $F$. The performance of the system (output) is measured using the vertical acceleration $a$ of the vehicle, i.e. the sprung mass $\ddot{z}_s$. This is due to the fact that ride comfort is mostly measured and influenced by the vehicle's vertical acceleration. In order to calculate the vehicle response due to its excitation given these two inputs and one output, the system can be represented using a state-space realization or transfer-function system.

The state-space realization is a so-called MISO system (Multiple Input Single Output). State-Space realizations allow one to reduce second or higher order differential equations to first order differential equation systems, which are easier to work with. The process to get the state-space realization of the system is not trivial for the given model due to the effects of tire damping. As can be seen, the equations of motion need the road disturbance signal in form of a vertical displacement $z$ and vertical velocity $\dot{z}$. However, state-space realizations for two-mass oscillators normally work only with four states. One way to handle the requirement of two extra inputs from the road profiles is to add a fifth state and only have the vertical road velocity $\dot{z}$ as an input. Using one input will also be easier for a later real-time application, since the road profile only needs to be scanned for one signal instead of two. The state vector then holds the states for $z_s$, $\dot{z}_s$, $z_u$, $\dot{z}_u$, and $z$ and the state-space realization has the following form:

Input-Equation:

$$\begin{bmatrix} \dot{z}_s \\ \ddot{z}_s \\ \dot{z}_u \\ \ddot{z}_u \\ \dot{z} \end{bmatrix} = \begin{bmatrix} 0 & 1 & 0 & 0 & 0 \\ -\frac{k_s}{m_s} & -\frac{d_s}{m_s} & \frac{k_s}{m_s} & \frac{d_s}{m_s} & 0 \\ 0 & 0 & 0 & 1 & 0 \\ \frac{k_s}{m_u} & \frac{d_s}{m_u} & -\frac{(k_s+k_t)}{m_u} & -\frac{(d_s+d_t)}{m_u} & \frac{k_t}{m_u} \\ 0 & 0 & 0 & 0 & 0 \end{bmatrix} \begin{bmatrix} z_s \\ \dot{z}_s \\ z_u \\ \dot{z}_u \\ z \end{bmatrix} + \begin{bmatrix} 0 & 0 \\ 0 & \frac{1}{m_s} \\ 0 & 0 \\ \frac{d_t}{m_u} & -\frac{1}{m_u} \\ 1 & 0 \end{bmatrix} \begin{bmatrix} \dot{z} \\ F \end{bmatrix} \quad (3\text{-}10)$$

Output-Equation:

$$[a] = \begin{bmatrix} -\frac{k_s}{m_s} & -\frac{d_s}{m_s} & \frac{k_s}{m_s} & \frac{d_s}{m_s} & 0 \end{bmatrix} \begin{bmatrix} z_s \\ \dot{z}_s \\ z_u \\ \dot{z}_u \\ z \end{bmatrix} + \begin{bmatrix} 0 & \frac{1}{m_s} \end{bmatrix} \begin{bmatrix} \dot{z} \\ F \end{bmatrix} \quad (3\text{-}11)$$

This state-space realization allows the application to get the vertical vehicle acceleration (sprung mass) $a = \ddot{z}_s$ by using only the vertical velocity of the road profile $\dot{z}$ and the force created by the force generator/actuation system. Figure 3-3 shows the block diagram of the state-space realization.

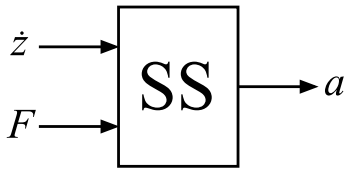


Figure 3-3: Block Diagram State-Space Realization[70]

The derived and shown state-space realization is generally valid, is set up the same way as earlier research at PERL VT[71], and is used for the software application. However, the model can also be handled using a transfer-function representation. Therefore the Laplace-Transformation of ( 3-8 ) and ( 3-9 ) is needed and shown below:

Sprung mass:

$$Z_s(m_s s^2 + d_s s + k_s) = Z_u(d_s s + k_s) + F \quad (3\text{-}12)$$

Unsprung mass:

$$Z_u\big(m_u s^2 + (d_s + d_t)s + (k_s + k_t)\big) = Z_s(d_s s + k_s) + Z(d_t s + k_t) - F \quad (3\text{-}13)$$

[70] Cf. Rao, A. M.: A Structured Approach to Defining Active Suspension Requirements, 2016, p. 10.

[71] See Rao, A. M.: A Structured Approach to Defining Active Suspension Requirements, 2016, pp. 10-11.

Plugging ( 3-13 ) in ( 3-12 ):

$$Z_s \qquad \text{( 3-14 )}$$

$$= Z\frac{(d_s d_t)s^2 + (d_s k_t + d_t k_s)s + (k_s k_t)}{(m_s m_u)s^4 + (m_s(d_s + d_t) + m_u d_s)s^3 + (m_s(k_s + k_t) + m_u k_s + d_s d_t)s^2 + (d_s k_t + d_t k_s)s + (k_s k_t)}$$
$$+ F\frac{(m_u)s^2 + (d_t)s + (k_t)}{(m_s m_u)s^4 + (m_s(d_s + d_t) + m_u d_t)s^3 + (m_s(k_s + k_t) + m_u k_s + d_s d_t)s^2 + (d_s k_t + d_t k_s)s + (k_s k_t)}$$

Using ( 3-14 ) two separate transfer-functions, one for each input, can be generated and the output transformed into the needed vertical acceleration:

( 3-15 )

$$\frac{\ddot{z}_s}{\dot{z}} = \frac{(d_s d_t)s^3 + (d_s k_t + d_t k_s)s^2 + (k_s k_t)s}{(m_s m_u)s^4 + (m_s(d_s + d_t) + m_u d_t)s^3 + (m_s(k_s + k_t) + m_u k_s + d_s d_t)s^2 + (d_s k_t + d_t k_s)s + (k_s k_t)}$$

( 3-16 )

$$\frac{\ddot{z}_s}{F} = \frac{(m_u)s^4 + (d_t)s^3 + (k_t)s^2}{(m_s m_u)s^4 + (m_s(d_s + d_t) + m_u d_t)s^3 + (m_s(k_s + k_t) + m_u k_s + d_s d_t)s^2 + (d_s k_t + d_t k_s)s + (k_s k_t)}$$

Figure 3-4 shows the system's block diagram using transfer-functions, with $TF_{a\dot{z}} = \frac{\ddot{z}_s}{\dot{z}}$, $TF_{aF} = \frac{\ddot{z}_s}{\dot{z}}$.

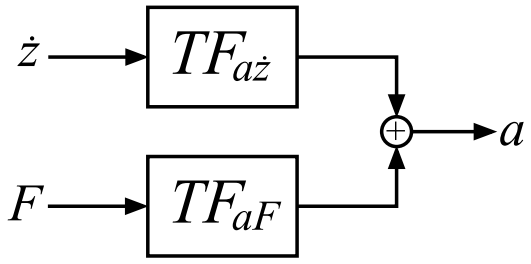


Figure 3-4: Block Diagram Transfer-Function Realization[72]

For consistency and comparison purposes a set of vehicle parameters are used during this research project which were chosen and fixed during earlier research at PERL VT.[73] The values of those are shown in Table 3-1.

[72] Cf. Rao, A. M.: A Structured Approach to Defining Active Suspension Requirements, 2016, p. 10.

[73] See Rao, A. M.: A Structured Approach to Defining Active Suspension Requirements, 2016, p. 12.

Table 3-1: Vehicle Parameter Quarter Car with Active Suspension[74]

| Vehicle Parameter | Value |
|---|---|
| $m_s$ | 400 kg |
| $m_u$ | 40 kg |
| $k_s$ | 21 kN/m |
| $k_t$ | 150 kN/m |
| $d_s$ | 1.50 kNs/m |
| $d_t$ | 1.47 kNs/m |

Using this set of parameters and the introduced state-space realization of the quarter car with active suspension system, the natural frequencies of the sprung and unsprung mass are calculated, which are 10.28 Hz and 1.1 Hz.

The state-space realization is implemented in the Matlab script library using an LTI (linear time invariant) object.

## 3.2 Road Profiles

The main research objective is to mitigate single event disturbances which are part of virtually every road. In general, all roads vary in their shape and condition. Variations exist not only between different countries, but also within countries comparing highway and city streets. For example, Germany has very solid and straight highways for high speed driving capabilities, while many other countries do not have the need for such a structure and do not maintain their highways to such standards.

Even though so many variations in shape and condition of roads exist, the quarter car model requires a set of single event disturbances which represents real world situations scanned by a road scanner. One way to implement these in the software application is by generating arbitrary (random) road profiles, which cover the whole range of different disturbances. This option is used quite often and results can be found in the literature. The disadvantage of using arbitrary road profiles, though, is that correlations and relationship in the LMS algorithm are more difficult to find and determine.

Therefore, a second approach is used for this research project. A set of differently shaped and commonly found single event disturbances are predefined and used as excitation signals for the quarter car model. These standardized road profiles have the advantage of being generally shaped differently, but also show correlations in subsets, which simplifies the evaluation process.

The same approach was already used during previous work at PERL VT, were a set of standard road profiles were defined.[75] In order to stay consistent throughout the overall research project and allow comparisons in the performance values and research output, a subset of these road profiles is used. These are namely curbs, potholes, speed humps, and uneven road profiles, which also represent these

[74] Cf. Rao, A. M.: A Structured Approach to Defining Active Suspension Requirements, 2016, p. 12.

[75] See Rao, A. M.: A Structured Approach to Defining Active Suspension Requirements, 2016, pp. 14-27.

kind of road situations mentioned in the introduction part. In the next section, all road profiles are introduced. A more detailed description of the decision making and design process can be found in "A Structured Approach to Defining Active Suspension Requirements".[76]

### 3.2.1 Curbs

Curbs are commonly used and can mostly be found at either side of a road. "The purposes of curbs are to provide drainage, delineate the edge of the pavement, support the pavement edge, provide the edge for a pedestrian walkway, and possibly provide some redirective capacity for low-speed impacts."[77] Interaction with curbs can cause loss of control and crashes on higher-speed roadways. Therefore, the American Association of State Highway and Transportation Officials discourages the use of curbs on higher-speed roadways, but they are often required.[78]

In their report 537 "Recommended Guidelines for Curb and Curb–Barrier Installations" the National Cooperative Highway Research Program lists seven typical AASHTO highway curbs.[79] These seven curbs represent a subset of common single event disturbances on roads and are therefore implemented as road profiles into the software application.

Figure 3-5 shows the road profile of Curb A (ratio 1:1), which is called a vertical curb. One purpose of it is to redirect errant vehicles. However, if vehicle velocity and approach angle are too large, they can make a vehicle unstable due to an introduced roll moment.[78] Causing a vehicle to make use of the redirecting purpose of the curb may not be recommended for a real-time application, but the road profile can serve as a test for single event disturbance signals.

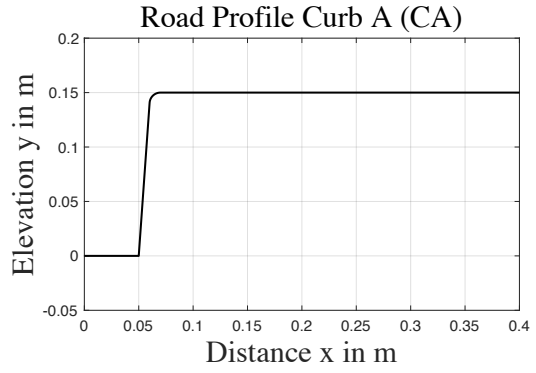


Figure 3-5: Road Profile Curb A (CA)[78]

[76] See Rao, A. M.: A Structured Approach to Defining Active Suspension Requirements, 2016, pp. 14-27.

[77] Plaxico, C. A., Ray, M. H., Orengo, F., Tiso, P., McGee, H., Council, F., and Eccles, K.: Recommended Guidelines for Curb and Curb–Barrier Installations, 2005, p. 1.

[78] Cf. Plaxico, C. A., Ray, M. H., Orengo, F., Tiso, P., McGee, H., Council, F., and Eccles, K.: Recommended Guidelines for Curb and Curb–Barrier Installations, 2005, p. 1-2.

[79] See Plaxico, C. A., Ray, M. H., Orengo, F., Tiso, P., McGee, H., Council, F., and Eccles, K.: Recommended Guidelines for Curb and Curb–Barrier Installations, 2005, p. 2.

Figure 3-6 to Figure 3-11 show Curb B through Curb G (ratio 1:1) which are called sloping curbs. These curbs are mainly installed for draining purposes and at locations where redirecting is undesirable due to traffic. Thus, they have a sloped face so vehicles can drive over them.[80]

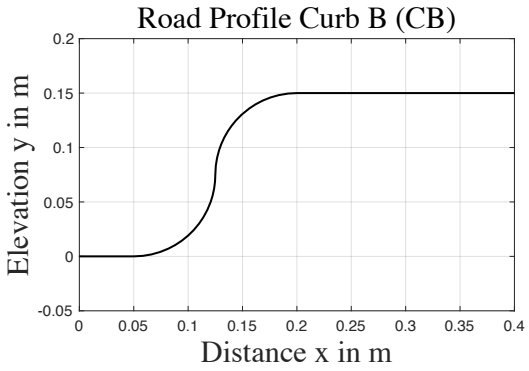


Figure 3-6: Road Profile Curb B (CB)[81]

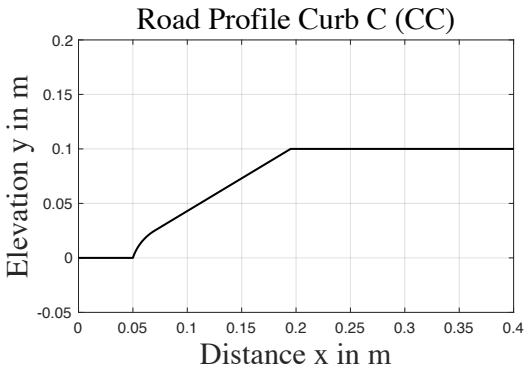


Figure 3-7: Road Profile Curb C (CC)[81]

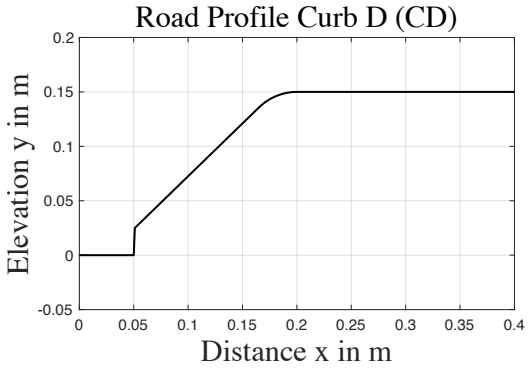


Figure 3-8: Road Profile Curb D (CD)[81]

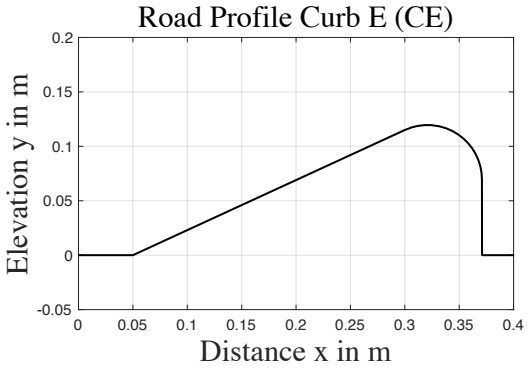


Figure 3-9: Road Profile Curb E (CE)[81]

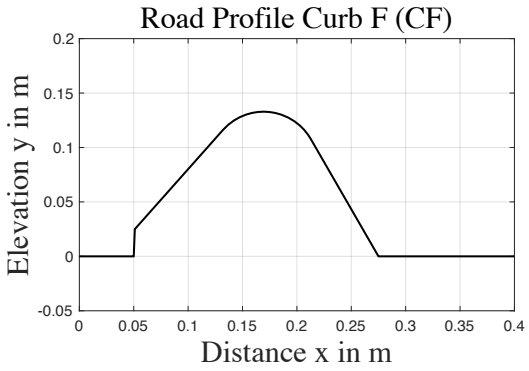


Figure 3-10: Road Profile Curb F (CF)[81]

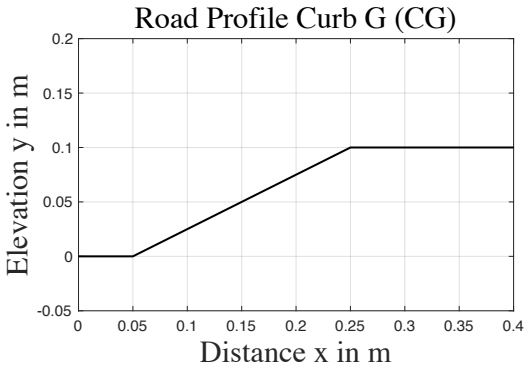


Figure 3-11: Road Profile Curb G (CG)[81]

[80] Cf. Plaxico, C. A., Ray, M. H., Orengo, F., Tiso, P., McGee, H., Council, F., and Eccles, K.: Recommended Guidelines for Curb and Curb–Barrier Installations, 2005, p. 1.

[81] Cf. Plaxico, C. A., Ray, M. H., Orengo, F., Tiso, P., McGee, H., Council, F., and Eccles, K.: Recommended Guidelines for Curb and Curb–Barrier Installations, 2005, p. 2.

In most situations, vehicles do not drive orthogonally towards and over these kinds of profiles. However, considering an orthogonal drive-over generates a more difficult situation for the active suspension system, since the shape is sharper than an elongated version of the profile. In this way, the application will be tuned in order to mitigate rather more stressful than to facile situations.

Comparing all seven curbs visually, they can be categorized into three classes with equal shape:

1. Sharpe edge profile: Curb A and Curb B
2. Gentle slope profile: Curb C, Curb D, Curb G
3. Override profile: Curb E and Curb F

### 3.2.2 Potholes

Even though the phenomenon of potholes is commonly known, there is no clear definition.[82] Potholes normally refer to defects in the road surface which can grow several $10^{ths}$ of a cm in width and a few cm in depth. They are mainly caused by expanding water in the soil structure during winter time, and can continue to grow due to passing traffic.[83]

Since no standard definition for potholes exists, experimental data is used. This data was generated and discretized during previous work at PERL VT.[84] Three of them are implemented in the software application and are shown in Figure 3-12 through Figure 3-14 (ratio 1:5). All potholes have approximately the same shape, mostly differing in slope, depth, and length. Pothole 1 is most likely to require the most force from the active suspension due to is sharpness, while pothole 2 seems to be the most gentlest one.

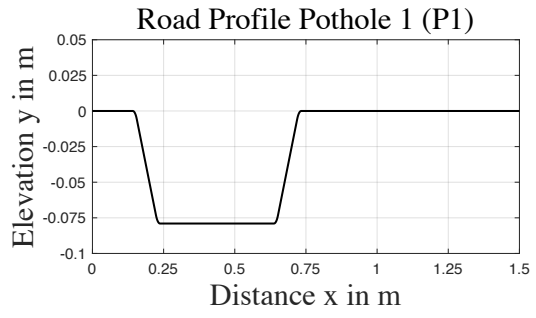


Figure 3-12: Road Profile Pothole 1 (P1)[85]

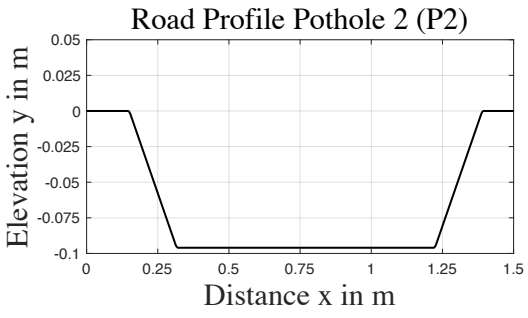


Figure 3-13: Road Profile Pothole 2 (P2)[85]

[82] Cf. Robinson, H.: National Definition Of Pothole Called For, 2016.

[83] Cf. Rao, A. M.: A Structured Approach to Defining Active Suspension Requirements, 2016, p. 18.

[84] See Rao, A. M.: A Structured Approach to Defining Active Suspension Requirements, 2016, pp. 18-20.

[85] Cf. Rao, A. M.: A Structured Approach to Defining Active Suspension Requirements, 2016, pp. 19-20.

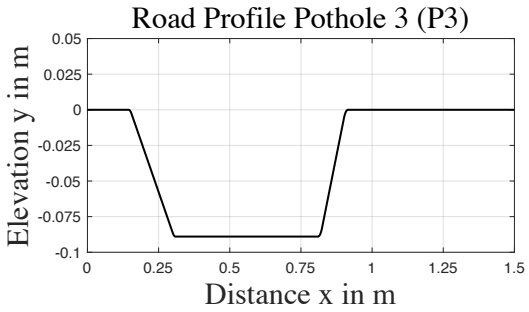


Figure 3-14: Road Profile Pothole 3 (P3)[86]

### 3.2.3 Speed Humps

Speed bumps and humps are both designed to slow down traffic and were first introduced in the 1970s by the Transport and Road Research Laboratory (TRRL) in Great Britain. While speed bumps and speed humps are different in specific design parameters, both are elevated areas in the roadway pavement. Speed bumps are mainly implemented in private roadways and parking lots, while speed humps on the other hand are mainly used in residential local streets. Speed bumps slow vehicles down to an approximate vehicle velocity of 2.2 m/s (8 km/h, 5mph) and speed humps to a velocity around 9 m/s (32 km/h, 20 mph).[87]

Both designs are equal in shape but vary in their characteristic geometry. Speed bumps are shorter and higher while speed humps are lower and longer.[88] Because there are no standards for speed bumps, and because they are mainly inverse potholes with a smoother design, only speed humps are considered for this research project.

In the United States both the Seminole Profile Hump and Watts Profile Hump are commonly used[88] and are shown in Figure 3-15 and Figure 3-16 (ratio 1:23.3).

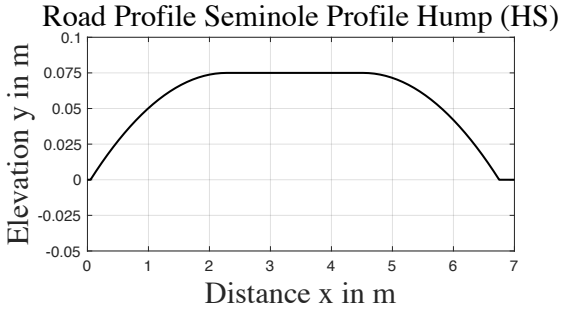


Figure 3-15: Road Profile Seminole Profile Hump (HS)[89]

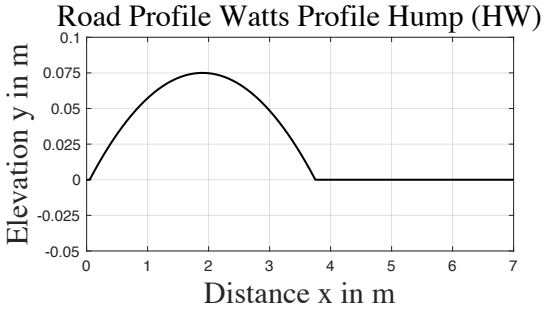


Figure 3-16: Road Profile Watts Profile Hump (HW)[89]

As can be seen both designs are equally shaped and mainly only differ in their length.

86 Cf. Rao, A. M.: A Structured Approach to Defining Active Suspension Requirements, 2016, pp. 19-20.

87 Cf. Parkhill, M., Sooklall, R., & Bahar, G.: Updated Guidelines for the Design and Application of Speed Humps, 2007, pp. 1-2.

88 Cf. Weber, P. A. & Braaksma, J. P.: Towards a North American Geometric Design Standard for Speed Humps, 2000, pp. 30-34.

89 Cf. Rao, A. M.: A Structured Approach to Defining Active Suspension Requirements, 2016, pp. 17-18.

### 3.2.4 Uneven Roads

Apart from the three other categories, a set of additional uneven road profiles offer great opportunities, too. Later, the system behavior and LMS solution of the other road profiles, which are relatively rough and have a sharp profile, can be compared to those rather smooth and gentle uneven road profiles.

In previous research at PERL VT an approach was used to overlay road profiles with unevenness to make them more realistic.[90] While this would make the search for correlations and relationships in this research project more difficult, the approach can be used, as before, to generate uneven road profiles.[90] Three uneven roads are shown in Figure 3-17 through Figure 3-19 (ratio 1:3) and are used as a set of road profiles for the LMS approach in this research project.

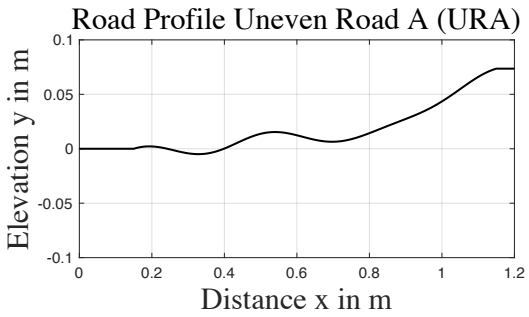


Figure 3-17: Road Profile Uneven Road A (URA)[91]

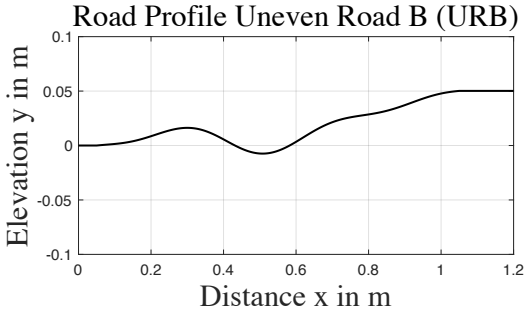


Figure 3-18: Road Profile Uneven Road B (URB)[91]

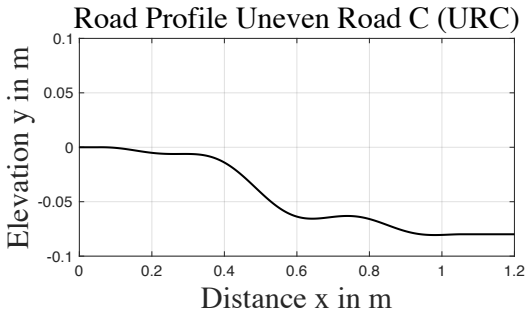


Figure 3-19: Road Profile Uneven Road C (URC)[91]

[90] See Rao, A. M.: A Structured Approach to Defining Active Suspension Requirements, 2016, pp. 20-27.

[91] Cf. Rao, A M.: A Structured Approach to Defining Active Suspension Requirements, 2016, pp. 20-27.

## 3.3 Road Profile Preprocessing

Before the generated road profiles[92] can be used as excitation signals to the quarter car model[93], signal preprocessing is necessary. This preprocessing is needed due to the tire geometry, the discretization of the road profiles[94] and the required velocity input for the state-space system[93]. The following three subchapters cover all three steps of preprocessing.

### 3.3.1 Geometric Filtering

The quarter car model, including the vehicle tire, is set up to be excited by the road profile assuming a point contact. The point contact together with the generated road profiles, which partially include relatively high frequencies, make geometric filtering necessary. The rule of thumb for geometric filtering is that it is necessary as soon as the wavelength of the excitation signal is two to three times smaller than the contact length of the tire[95].

The technique, called "Tandem-Cam Model", used to generate effective road surfaces for profiles containing high frequency disturbance signals was developed by Schmeitz and is explained in his dissertation "a semi-empirical three-dimensional model of the pneumatic tire rolling over arbitrarily uneven road surfaces"[96] from Delft University. He validated his technique by comparing it to measured data and proved it to be qualitative for small low and high frequency signals, independent of the axle load.[97] His model is often used in vehicle dynamics and tire modeling.[98, 99]

The Tandem-Cam Model builds on the basic function and two-point follower from Bandel and Zegelaar and is considered a further development of these. The basic function and two-point follower method determines the effective height, $w(x)$, of a road profile by using a single basic function $f_b(x)$ and a two-point follower with a horizontal length $l_s$. The basic function $f_b(x)$ is represented by a quarter sine wave with height $h_t$ equal to the step height $h_{step} = h_t$, a curve length $l_b$, and an offset parameter $l_f$ which marks the beginning of the step in the road profile.[100] Figure 3-20 shows a visual representation of the basic function and two-point follower model.

92 See chapter 3.2 Road Profiles.

93 See chapter 3.1 Quarter Car Model with Active Suspension System.

94 Cf. Rao, A. M.: A Structured Approach to Defining Active Suspension Requirements, 2016, pp. 27-34.

95 Cf. Pacejka, H.: Dynamic Tire Response to Short Road Unevennesses, 2012, p. 475.

96 See Schmeitz, A. J. C.: A Semi-Empirical Three-Dimensional Model of the Pneumatic Tire Rolling over Arbitrarily Uneven Road Surfaces, 2004.

97 Cf. Schmeitz, A. J. C.: A Semi-Empirical Three-Dimensional Model of the Pneumatic Tire Rolling over Arbitrarily Uneven Road Surfaces, 2004, pp. 91-140.

98 Cf. Pacejka, H.: Dynamic Tire Response to Short Road Unevennesses, 2012, pp. 485-487.

99 Cf. Houben, L. W. L.: Run flat tires versus conventional tires, 2006, pp. 10-12.

100 Cf. Schmeitz, A. J. C.: A Semi-Empirical Three-Dimensional Model of the Pneumatic Tire Rolling over Arbitrarily Uneven Road Surfaces, 2004, pp. 104-111.

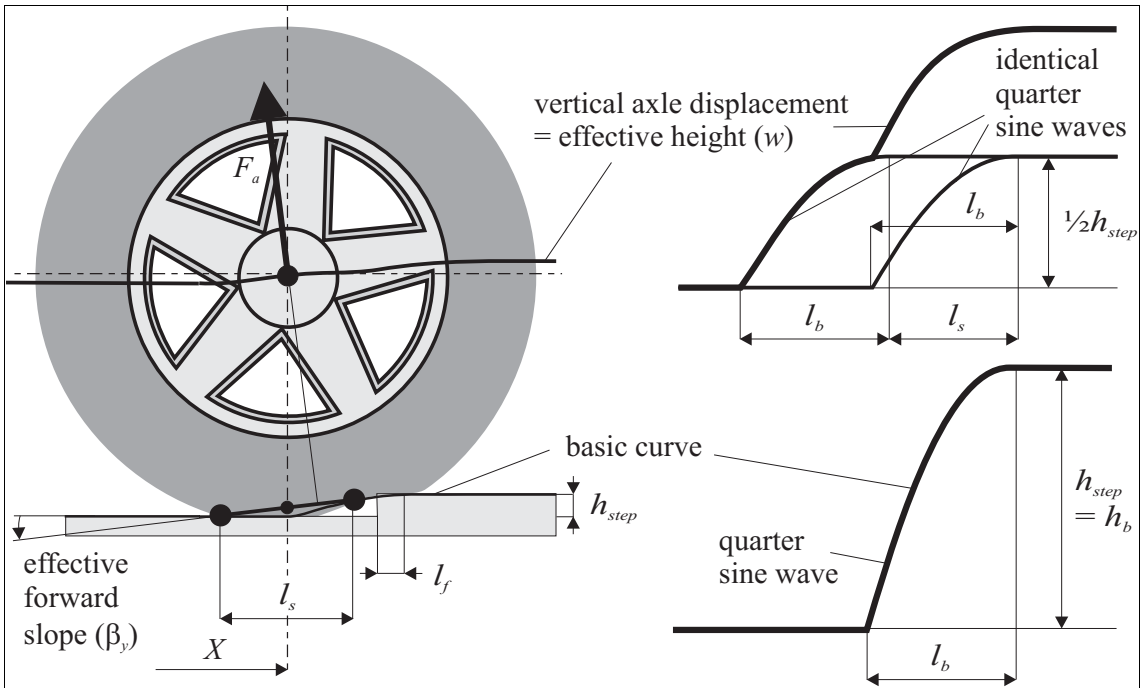


Figure 3-20: Basic Function and Two-Point Follower Model[101]

The effective road surface $w(x)$ can be calculated using the following equation for the effective height, calculating the midpoint of two points on the follower.[102]

$$w(x) = \frac{f_b\left(X - \frac{l_s}{2}\right) + f_b(X + \frac{l_s}{2})}{2} \qquad (3\text{-}17)^{103}$$

In principle, the basic function and two-point follower method can be used for any other obstacle surfaces as well, however, it has two main issues. The offset parameter $l_f$ is described as a mysterious parameter for which no physical explanation is known and the shape of the basic curve is apparently far from ideal. These issues and their impact can be illustrated by comparing three effective road surfaces which only differ in their step height. No matter how deep the step is, they should all follow the same path until they hit flat ground again. As Figure 3-21 indicates, they do not when using the basic curve and two-point follower method.[104]

[101] Schmeitz, A. J. C.: A Semi-Empirical Three-Dimensional Model of the Pneumatic Tire Rolling over Arbitrarily Uneven Road Surfaces, 2004, p. 105 from Houben, L. W. L.: Run flat tires versus conventional tires, 2006, p. 9.

[102] Cf. Schmeitz, A. J. C.: A Semi-Empirical Three-Dimensional Model of the Pneumatic Tire Rolling over Arbitrarily Uneven Road Surfaces, 2004, p. 105.

[103] Schmeitz, A. J. C.: A Semi-Empirical Three-Dimensional Model of the Pneumatic Tire Rolling over Arbitrarily Uneven Road Surfaces, 2004, p. 105.

[104] Cf. Schmeitz, A. J. C.: A Semi-Empirical Three-Dimensional Model of the Pneumatic Tire Rolling over Arbitrarily Uneven Road Surfaces, 2004, pp. 104 -111.

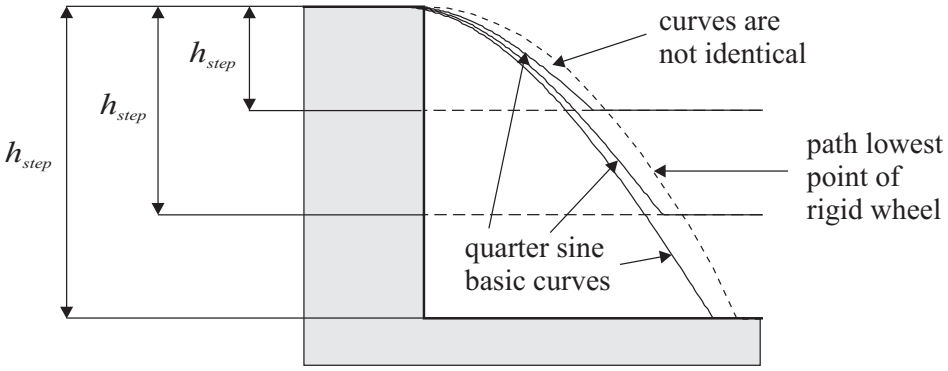


Figure 3-21: Path Comparison for Three Basic Curves[105]

Schmeitz developed the Tandem-Cam Model in order to address these issues. His approach generates a basic curve by using the path of the lowest point of an elliptical cam, shown in Figure 3-22. The shape of the ellipse in form of a standing egg is due to the dropped offset parameter and to have an identical starting point each time.[106]

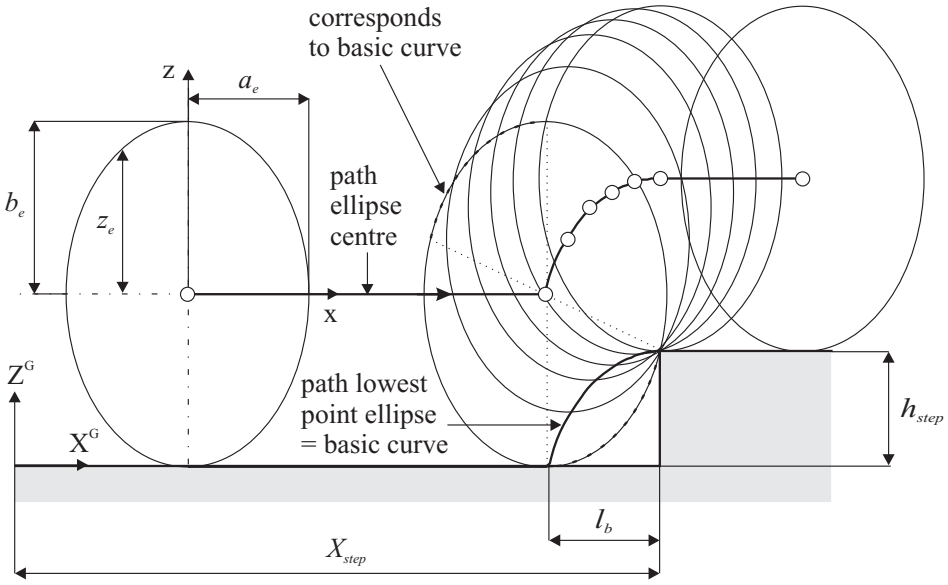


Figure 3-22: Basic Curve with Tandem-Cam Model[107]

[105] Schmeitz, A. J. C.: A Semi-Empirical Three-Dimensional Model of the Pneumatic Tire Rolling over Arbitrarily Uneven Road Surfaces, 2004, p. 111 from Houben, L. W. L.: Run flat tires versus conventional tires, 2006, p. 10.

[106] Cf. Schmeitz, A. J. C.: A Semi-Empirical Three-Dimensional Model of the Pneumatic Tire Rolling over Arbitrarily Uneven Road Surfaces, 2004, pp. 104-140.

[107] Schmeitz, A. J. C.: A Semi-Empirical Three-Dimensional Model of the Pneumatic Tire Rolling over Arbitrarily Uneven Road Surfaces, 2004, p. 112 from Houben, L. W. L.: Run flat tires versus conventional tires, 2006, p. 10.

The shapes of the elliptical cams are defined by $a_e$, $b_e$, and $c_e$, the shape parameters, and in terms of the local coordinates x and z by[108]:

$$\left(\frac{x}{a_e}\right)^{c_e} + \left(\frac{z}{b_e}\right)^{c_e} = 1 \qquad (3\text{-}18)^{109}$$

The length $l_b$ of the basic curve is given by[108]:

$$l_b = a_e \left(1 - \left(1 - \frac{|h_{step}|}{b_e}\right)^{c_e}\right)^{\frac{1}{c_e}} \qquad (3\text{-}19)^{109}$$

The distance $z_e$ between local $x$ axis and the elliptical cam is given by[108]:

$$z_e = \left| b_e \left(1 - \left(\frac{|x|}{a_e}\right)^{c_e}\right)^{\frac{1}{c_e}} \right| \qquad (3\text{-}20)^{109}$$

$X_{step}$ marks the global position of the step in x direction. Therefore, the basic curve using an elliptical cam in terms of global coordinates is a section-wise defined function[108]:

$$Z = \begin{cases} 0 & \text{if } X \leq -l_b + X_{step} \\ h_{step} - b_e + \left| b_e \left(1 - \left(\frac{|X - X_{step}|}{a_e}\right)^{c_e}\right)^{\frac{1}{c_e}} \right| & \text{if } -l_b + X_{step} < X < X_{step} \\ h_{step} & \text{if } X \geq X_{step} \end{cases} \qquad (3\text{-}21)^{110}$$

In the tandem configuration, shown in Figure 3-23, the center of the front and rear ellipse in global coordinates is given by[111]:

$$Z_f = \max\left[Z_{road}\left(X_f + x_f\right) + z_e(x_f)\right] \qquad (3\text{-}22)^{112}$$

[108] Cf. Schmeitz, A. J. C.: A Semi-Empirical Three-Dimensional Model of the Pneumatic Tire Rolling over Arbitrarily Uneven Road Surfaces, 2004, p. 112.

[109] Schmeitz, A. J. C.: A Semi-Empirical Three-Dimensional Model of the Pneumatic Tire Rolling over Arbitrarily Uneven Road Surfaces, 2004, p. 112.

[110] Schmeitz, A. J. C.: A Semi-Empirical Three-Dimensional Model of the Pneumatic Tire Rolling over Arbitrarily Uneven Road Surfaces, 2004, p. 113.

[111] Cf. Schmeitz, A. J. C.: A Semi-Empirical Three-Dimensional Model of the Pneumatic Tire Rolling over Arbitrarily Uneven Road Surfaces, 2004, pp. 113-116.

[112] Schmeitz, A. J. C.: A Semi-Empirical Three-Dimensional Model of the Pneumatic Tire Rolling over Arbitrarily Uneven Road Surfaces, 2004, p. 115.

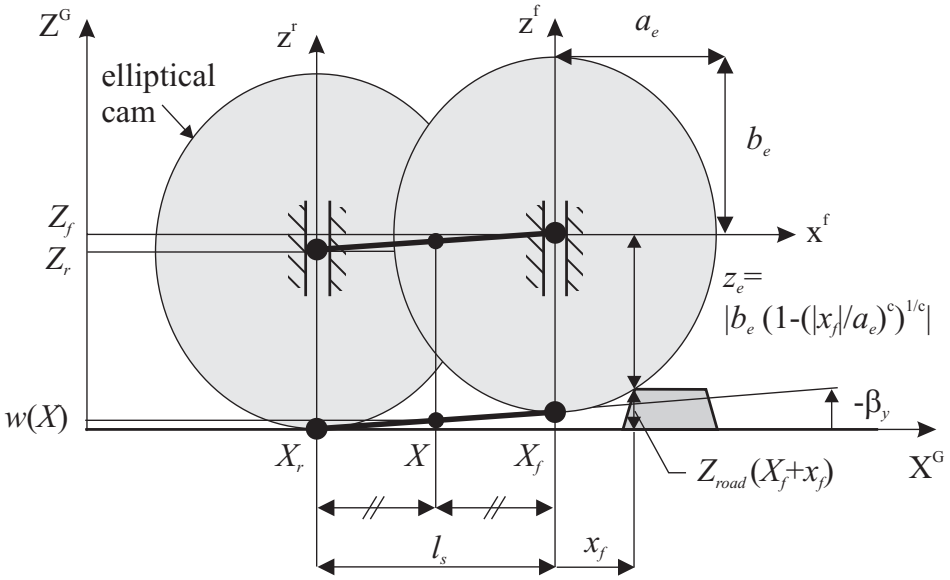


Figure 3-23: Tandem Configuration Tandem-Cam Model[113]

Using the Tandem-Cam Model the effective road surface can finally be generated by using[114]:

$$w(X) = \frac{Z_f + Z_r}{2} - b_e \qquad (3\text{-}23)^{115}$$

The Tandem-Cam Model is implemented in the software application and uses a set of parameters which were used in earlier research at PERL VT[116], see Table 3-2.

Table 3-2: Vehicle Tire Parameter Quarter Car with Active Suspension[117]

| **Vehicle Tire Parameter** | **Value** |
|---|---|
| Unloaded Radius $r_o$ | 0.3100 m |
| Effective rolling radius $r_{eo}$ | 0.3050 m |
| Half contact length $a$ | 0.0603 m |
| Half ellipse length/unloaded radius $p_{ae}$ | 1.0325 |
| Half ellipse height/unloaded radius $p_{be}$ | 1.0306 |
| Ellipse exponent $p_{ce}$ | 1.8230 |
| Shift length/contact length $p_{sh}$ | 0.8773 |

113 Schmeitz, A. J. C.: A Semi-Empirical Three-Dimensional Model of the Pneumatic Tire Rolling over Arbitrarily Uneven Road Surfaces, 2004, p. 115 from Houben, L. W. L.: Run flat tires versus conventional tires, 2006, p. 11.

114 Cf. Schmeitz, A. J. C.: A Semi-Empirical Three-Dimensional Model of the Pneumatic Tire Rolling over Arbitrarily Uneven Road Surfaces, 2004, p. 115.

115 Schmeitz, A. J. C.: A Semi-Empirical Three-Dimensional Model of the Pneumatic Tire Rolling over Arbitrarily Uneven Road Surfaces, 2004, p. 115.

116 See Rao, A. M.: A Structured Approach to Defining Active Suspension Requirements, 2016, p. 31.

117 Cf. Rao, A. M.: A Structured Approach to Defining Active Suspension Requirements, 2016, p. 31.

### 3.3.2 Road Disturbance to Velocity Signal

As derived earlier, the state-space realization of the used quarter car model with active suspension requires a vertical velocity instead of vertical displacement road profile input signal due to tire damping.[118] Until now, the road profiles and their geometric filtered versions are still in the form of a vertical displacement over a distance in the *x* direction. In order to put the input signal in the required form, the signal must first be translated into vertical displacement over time and then the first derivate must be taken. The first problem is basically just a scaling operation with respect to the vehicle velocity, while the second is done by using the built-in Matlab derive function.

### 3.3.3 Low-Pass Filtering

Taking the derivate of the preprocessed road profiles will cause peaks in the output signal. This is mainly due to the discretization process when the profiles were sampled from the literature. These peaks would greatly increase the force requirements for mitigating the single event disturbances, and thus are filtered out using a low-pass filter. A Butterworth filter with a break frequency of 150 Hz was determined to be appropriate for the given profiles and model of the quarter car.[119]

Figure 3-24 shows a flow chart diagram of the overall road profile preprocessing procedure.

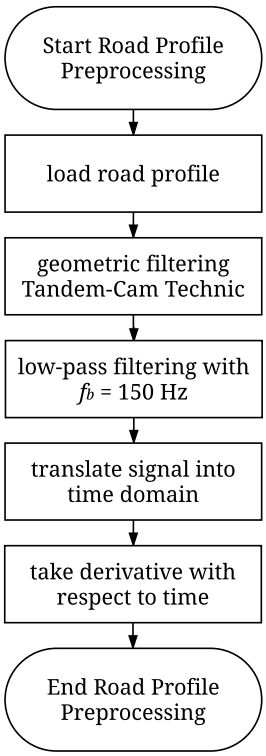


Figure 3-24: Flow Chart Road Profile Preprocessing

[118] See chapter 3.1 Quarter Car Model with Active Suspension System.

[119] Cf. Rao, A. M.: A Structured Approach to Defining Active Suspension Requirements, 2016, p. 32-33.

Figure 3-25 through Figure 3-27 show three road profiles and the interim steps transforming from raw road profiles to the processed velocity profiles. Low-pass filtering and the translation into the time domain are not shown, because the differences from the step ahead are marginal.

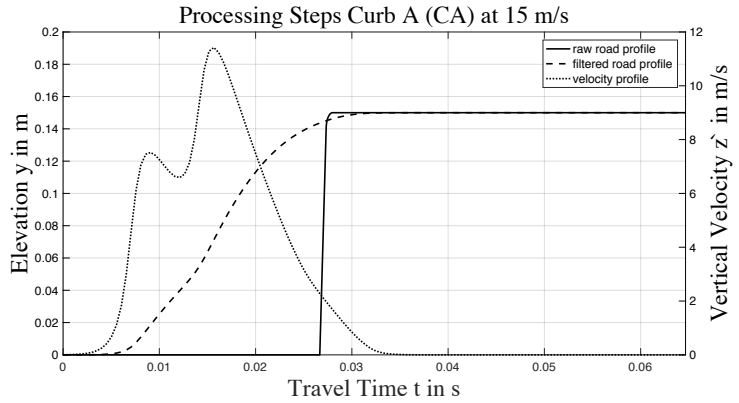


Figure 3-25: Processing Steps Curb A (CA) at 15 m/s

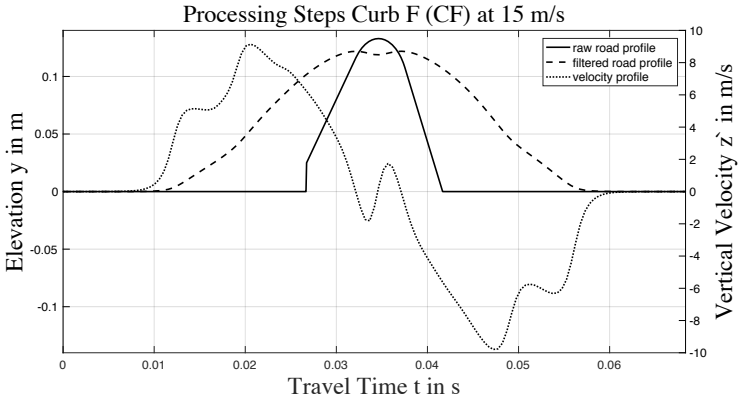


Figure 3-26: Processing Steps Curb B (CB) at 15 m/s

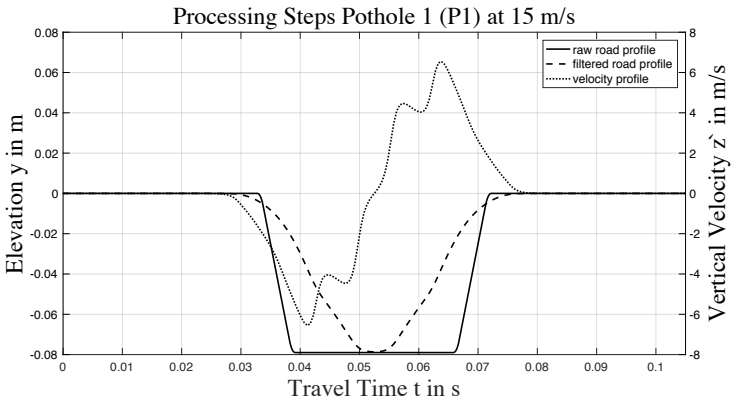


Figure 3-27: Processing Steps Pothole 1 (P1) at 15 m/s

## 3.4 iFX-LMS Algorithm

The preprocessed road profiles are then applied to the state-space realization of the quarter car model with active suspension system by using it as the first element of the input vector of the state-space system. Due to this excitation, the system will then begin oscillating uncontrolled. Using the state-space or the introduced transfer-function system, the response of the uncontrolled system is analytically calculated in continuous time. The vertical sprung mass acceleration was chosen as an evaluation parameter in order to accomplish the research goal of mitigating single event disturbances and to evaluate the performance of the new control strategy. Vertical vehicle acceleration and its root-mean-square value are often used as valid parameters to evaluate ride comfort[120]. This is mainly due to the fact that acceleration causes forces, that the human body can detect.

The proposed control strategy is to design a controller which uses preview information about the road in order to generate a force profile. This force profile can then be used as a tracking signal for the force generator/actuation system. In the ideal case the vehicle excitation caused by the road (first input state-space system) and from the force generator/actuation system (second input state-space system) tracking the force profile, compensate themselves and the effective vehicle response goes down to zero. Unfortunately, there is no obvious and trivial way to extract those force profiles analytically from the predefined, preprocessed road profile signals, and later real-time sampled real road signals since they are sampled discrete, do not follow any basic functions, and will later be overlaid with noise and disturbances.

Adaptive systems are a great tool to generate those force profiles instead. These systems are commonly used in different applications and promise to be applicable for this problem. To this point, previous research proved adaptive LMS filtering to be valid for extracting and generating force profiles. This offline study used an iterative FX-LMS (iFX-LMS) algorithm which showed reasonable performance and potential for further research.[121] This algorithm is explained in this subchapter in order to provide a better overall understanding and enable the design of an appropriate controller.

Adaption has several meanings, depending on the area of use. In general it means a system is adjusted or adjusts itself in order to perform better.[122] In their book “Adaptive Signal Processing”, Widrow and Stearns give a good overview of the different applications and system designs of adaptive systems.[123] They “think of adaption as a procedure for moving generally downhill on a “performance surface””[124], in order to adjust the system to produce an ideal or optimal response.[125] Uncini states that “[…], an adaptive system autonomously changes its internal parameters for achieving a certain processing goal […]”.[126]

---

120 Cf. Hrovat, D.: Survey of Advanced Suspension Developments and Related Optimal Control Applications, 1997, p. 1783.

121 See Rao, A. M.: A Structured Approach to Defining Active Suspension Requirements, 2016.

122 Cf. Widrow, B., and Stearns, S. D.: Adaptive Signal Processing, 1985, p. 3.

123 See Widrow, B., and Stearns, S. D.: Adaptive Signal Processing, 1985.

124 Widrow, B., and Stearns, S. D.: Adaptive Signal Processing, 1985, p. 1.

125 Cf. Widrow, B., and Stearns, S. D.: Adaptive Signal Processing, 1985, p. 1.

126 Uncini, A.: Fundamentals of Adaptive Signal Processing, 2015, p. 55.

The iFX-LMS algorithm effectively iterates the FX-LMS specified amount of time, while, on the other hand, the FX-LMS algorithm is an extension of the basic LMS algorithm, which is based on an adaptive linear combiner.[127]

"The Adaptive Linear Combiner, or nonrecursive adaptive filter, is fundamental to adaptive signal processing. It appears, in one form or another, in most adaptive filters and systems, and it is the single most important element in "learning" systems and adaptive processes in general. … In essence it is a time-varying, nonrecursive digital filter [...]".[128] A schematic diagram of a single input adaptive linear combiner (or adaptive transversal filter with four weights), the desired response, and error signal is shown in Figure 3-28.

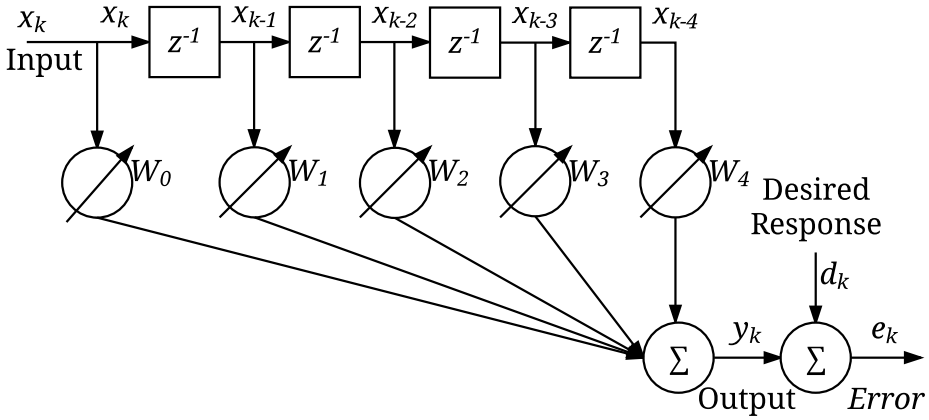


Figure 3-28: Adaptive Linear Combiner: Time *k*, Single Input, 4 Fixed Weights *W*, Desired Response *d*, and Error Signal *e*[129]

In the figure above *x* is the input signal, which is delayed through the following unit delays $z^{-1}$ and multiplied by the adjustable weights $w_l$. The linear combination of these signals represents the output signal *y*. In the ideal case the weights $w_k$ are adjusted in a way such that the output signal *y* is as close as possible to the desired response signal *d*, while the error signal *e* is minimized. In reality, a linear combiner can have as many weights as needed and the weights can vary over time.[129] The system's equations of the linear combiner are as followed:

$$y_k = \sum_{l=0}^{L=4} w_l \, x_{k-l} \qquad (3\text{-}24)^{130}$$

$$e_k = d_k - y_k = d_k - W^T X_k \qquad (3\text{-}25)^{131}$$

127 Cf. Widrow, B., and Stearns, S. D.: Adaptive Signal Processing, 1985, chapter 1, 2, 6, and 11.

128 Widrow, B., and Stearns, S. D.: Adaptive Signal Processing, 1985, p. 15.

129 Cf. Widrow, B., and Stearns, S. D.: Adaptive Signal Processing, 1985, pp. 17-19.

130 Cf. Widrow, B., and Stearns, S. D.: Adaptive Signal Processing, 1985, p. 17.

131 Cf. Widrow, B., and Stearns, S. D.: Adaptive Signal Processing, 1985, p. 19.

The following relationships between the linear combiner and quarter car model with active suspension can be drawn while keeping in mind that this is still a very low-level system:

- input signal *x*: vertical road velocity profile in m/s
- output signal *y*: generated force profile signal
- desired response *d*: ideal force profile signal ($a = 0$)
- error signal $e$: error between generated and ideal force profile signal, i.e. sprung mass acceleration
- weights *w*: iFX-LMS algorithm must adjust these properly to make e as small as possible.

As stated above, the objective is to adjust the weights *w* in a way so that the vehicle mitigates the excitation due to the road as best as it can by generating a force profile signal where the excitation due to the road profile and force generator/actuation system are compensated.

The mean-square-error (MSE), which is the squared error signal, provides information about the performance of the current system design.[132]

$$MSE = e^2 = d_k^2 + W^T X_k X_k^T W - 2 d_k X_K{}^T W \qquad (3\text{-}26)^{132}$$

Recalling Widrow and Stearns' statement about adaptive systems and their target of moving down on a performance surface[133], Figure 3-29 visualizes such a performance surface for ( 3-26 ) by assuming two weights and a quadratic function. Again, the purpose of adaptive systems is to adjust the weight w in the weight vector *W* in a way to reduce the error and therefore MSE. The goal is to be as close as possible to the global minimum, which is marked as $W^*$, the Wiener-Filter.[134]

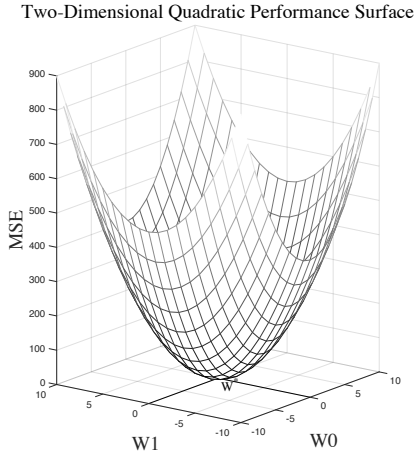


Figure 3-29: Two-Dimensional Quadratic Performance Surface[134]

132 Cf. Widrow, B., and Stearns, S. D.: Adaptive Signal Processing, 1985, pp. 19-20.

133 Cf. Widrow, B., and Stearns, S. D.: Adaptive Signal Processing, 1985, p. 1.

134 Cf. Widrow, B., and Stearns, S. D.: Adaptive Signal Processing, 1985, pp. 19-21.

Over time several different algorithms have been introduced in order to descend on the performance surface and to find the global minimum. These include Newton's algorithm and the steepest descent method, both of which require offline gradient estimation at every iteration step. Another algorithm, the Least-Mean-Square (LMS) algorithm, does not require offline gradient estimation and is simple and easy to compute. Widrow and Stearns consider the LMS algorithm the generally best choice for applications where the input vector *X* and desired response signal *d* are available the whole time.[135]

The method of steepest descent generates a new set of adjusted weights by using the following equation:[136]

$$W_{k+1} = W_k + \mu(-\nabla_k) \qquad (3\text{-}27)^{137}$$

In this equation $\mu$ is a constant and regulates the step size of the adjustment process. Where in other methods the gradient $\nabla_k$ is calculated by taking offline differences, the LMS algorithm estimates $\nabla_k$ using the error signal:[138]

$$\nabla_k = -2e_k X_k \qquad (3\text{-}28)^{138}$$

From that follows:

$$W_{k+1} = W_k + 2\mu e_k X_k \qquad (3\text{-}29)^{138}$$

As ( 3-29 ) indicates, the LMS algorithm uses the input signal *X* as well as the calculated error signal *e* in order to adjust the linear combiner weights. Figure 3-30 shows the block diagram of the LMS algorithm, where the same can be seen.

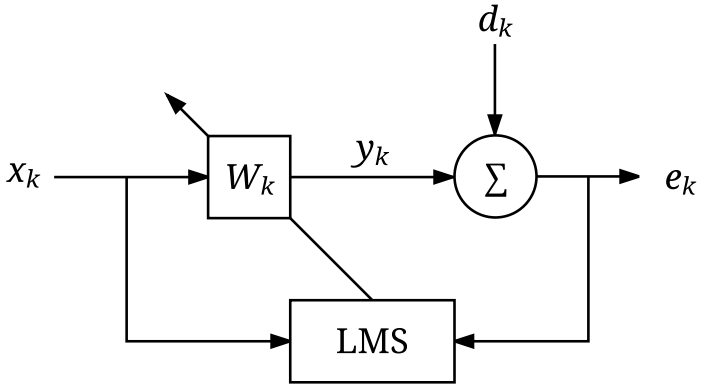


Figure 3-30: Block Diagram LMS Algorithm[139]

135 Cf. Widrow, B., and Stearns, S. D.: Adaptive Signal Processing, 1985, p. 99 and chapter 4.

136 Cf. Widrow, B., and Stearns, S. D.: Adaptive Signal Processing, 1985, p. 57.

137 Widrow, B., and Stearns, S. D.: Adaptive Signal Processing, 1985, p. 57.

138 Cf. Whidrow, B., and Stearns, S. D.: Adaptive Signal Processing, 1985, p. 100.

139 Cf. Rao, A. M.: A Structured Approach to Defining Active Suspension Requirements, 2016, p. 37.

The desired signal *d* represents vertical sprung mass acceleration a, which is the acceleration signal due to the road excitation. Therefore, *y* must be a signal of acceleration, too, meaning a change must be made to the block diagram in Figure 3-30. For problems like this an extension of the regular LMS algorithm can be used, called a Filtered-X LMS (FX-LMS) algorithm. A block diagram of the FX-LMS algorithm is shown in Figure 3-31.[140]

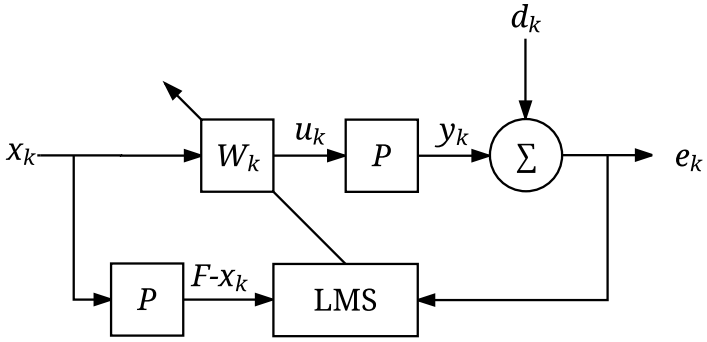


Figure 3-31: Block Diagram FX-LMS Algorithm[141]

As can be seen in the block diagram, the FX-LMS algorithm requires and takes advantage of known or estimated plant models *P* of the system. These models are implemented using discrete time transfer-functions of the quarter car model with active suspension, and filter the input signal *x* and control signal *u*.[142] A tuned filter model of the quarter car model with active suspension system is implemented in the application at PERL VT.[143]

Starting with a set of initial values for the weights vector *W*, the FX-LMS algorithm adjusts the weights vector and generates a new set of weights closer to the optimal solution, i.e. the global minimum on the performance surface. In order to obtain a solution which is as close as possible to the global, the FX-LMS algorithm iterates multiple times in loops. Each iteration starts with the former weights vector *W* from the previous loop. The method is called iterative FX-LMS algorithm (iFX-LMS) and was proven in previous work to have a positive impact on finding the optimal solution.[144]

Using an iFX-LMS algorithm instead of the basic LMS algorithm requires more performance tuning. This heavy tuning process and the different tuning parameters are covered in later chapters.[145]

Finally, Figure 3-32 shows the block diagram of all systems combined; preprocessing, quarter car model, and iFX-LMS algorithm. It starts on the left with the raw road profile $z_{kr}$, which is then processed through a geometric $z_{kgf}$ and low-pass $z_k$ filter. The first order time derivative of this signal $\dot{z}_k$ is then passed into the three subpaths. In the lower path the signal is filtered using the

140 Cf. Widrow, B., and Stearns, S. D.: Adaptive Signal Processing, 1985, pp. 288-292.

141 Cf. Rao, A. M.: A Structured Approach to Defining Active Suspension Requirements, 2016, p. 37.

142 Cf. Rao, A. M.: A Structured Approach to Defining Active Suspension Requirements, 2016, pp. 42-45.

143 See. Rao, A. M.: A Structured Approach to Defining Active Suspension Requirements, 2016, pp. 42-45.

144 Cf. Rao, A. M.: A Structured Approach to Defining Active Suspension Requirements, 2016, pp. 38-42.

145 See chapter 4.2 iFX-LMS Tuning and Performance.

transfer-function $TF_{a\dot{z}}$ which generates the filtered x signal $\dot{z}_{kx}$, with $\dot{z}_{kx} = a_{zk}$. In the middle pass the signal is weighted with the weight vector and represents afterwards the needed force profile signal $F_k$. Using a plant model of the quarter car $P_{aF}$ the vertical acceleration $a_{Fk}$ due to the force profile is calculated. This signal should ideally be the inverse of the desired signal $a_{\dot{z}k}$ coming from the top and calculated using the delayed version $\dot{z}_{k-1}$and passed through the plant model $P_{az} = TF_{a\dot{z}}$. The acceleration error signal $e_{ak}$ should be as small as possible.

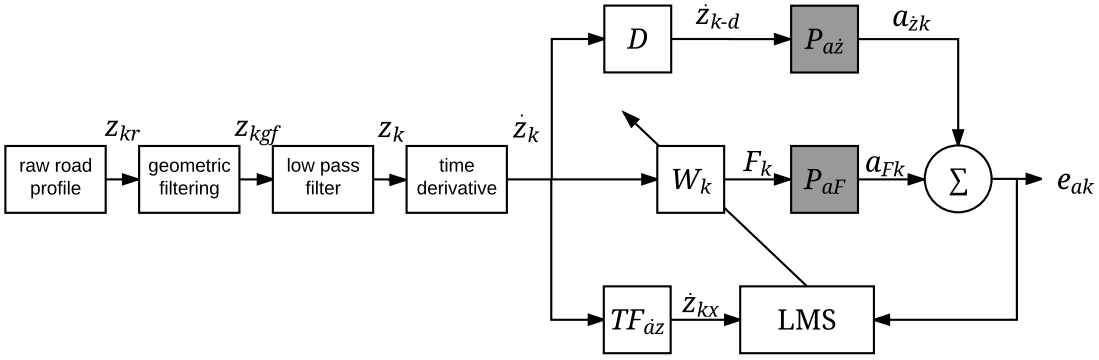


Figure 3-32: Block Diagram Quarter Car Model with Active Suspension System and iFX-LMS Algorithm[146]

The basis of Figure 3-32 is "Figure 5.7: FX-LMS algorithm applied to quarter-car model" from Rao.[147] Throughout this Master's Thesis the figure will be further developed, adjusted, and differ more and more from his idea. Therefore, it will not further be referenced.

## 3.5 Software and Implementation

The software used for this research project and the introduced application steps is Matlab R 2016 A. Matlab has great capabilities and opportunities to handle the data files and process them using Linear-Time Invariant (LTI) Objects and predefined functions included in Matlab. The whole application is set up as a script/function library.

In addition to the main library, several support scripts/functions are written for simplifying the process steps, to visualize and store the generated data sets, and for the controller design process performed later.

[146] Cf. Rao, A. M.: A Structured Approach to Defining Active Suspension Requirements, 2016, pp. 41.

[147] Rao, A. M.: A Structured Approach to Defining Active Suspension Requirements, 2016, pp. 41.

# 4 Data Generation and Evaluation

Once the application is set up and ready to use, this chapter outlines the generated data sets and evaluates them. First an appropriate operational test plan is developed in order to simplify the following evaluation process.[148] Before all data sets can then be generated, processed, and visualized,[149] the iFX-LMS algorithm must be tuned in order to make sure it and its outcomes converge to their optimal solution.[150] After the generated data sets and their outcomes are evaluated,[151] this chapter closes by using them to create a universal filter model.[152]

*Note:* A large amount of time of this research project was spent on the work presented in this chapter. The additional time spent on designing an operational test plan, tuning the iFX-LMS algorithm, and the evaluation process turned out to be well spent. Through the findings in this chapter the rest of the research project was positively influenced.

## 4.1 Operational Test Plan

Previous research proved the iFX-LMS algorithm approach to be valid. Even though this earlier research did not investigate in the correlation of its outcomes, no easily identifiable correlation between different data sets was determined.[153] Therefore, a well-designed operational test plan is outlined in this chapter to allow correlations to be found easier, and to draw conclusions between the outcomes of the iFX-LMS algorithm and its inputs, i.e. road profiles and vehicle velocity.

Recalling from chapter 3.2 Road Profiles, a total of 15 different road profiles in four categories (curbs, potholes, speed humps, and uneven roads) were derived. All 15 road profiles are taken into account for the operational test plan. Since the road profiles' shapes change depending on the desired vehicle velocity, each road profile must be tested over a set of different vehicle velocities. The army solicitation specified a maximum operational vehicle velocity of 65 mph for their requested system, which is about ~29.1 m/s or ~104.6 km/h[154]. However, Rao concluded in his research project that high vehicle velocities dramatically increase the system requirements of the active suspension system, in particular peak force requirements[155]. Nevertheless, the maximum vehicle velocity for the operational test plan is set at 30 m/s, which is 108 km/h or about ~67.1 mph. 30 m/s covers the specification from the army solicitation, and is in the range of common highway travel velocities on highways in the

148 See chapter 4.1 Operational Test Plan.

149 See chapter 4.3 Data Sets Generating, Processing, and Visualization.

150 See chapter 4.2 iFX-LMS Tuning and Performance.

151 See chapter 4.4 Analysis and Evaluation of Data Sets.

152 See chapter 4.5 Universal Filter Model.

153 See Rao, A. M.: A Structured Approach to Defining Active Suspension Requirements, 2016, p. 39, 40, 47.

154 Cf. US Army Research, Development, and Engineering Command (RDECOM): ARMY 14.1 Small Business Innovation Research (SBIR) Proposal Submission Instructions, 2013, pp. 94-95.

155 Cf. Rao, A. M.: A Structured Approach to Defining Active Suspension Requirements, 2016, p. 57.

USA and Europe – excluding Germany. However, it must be kept in mind that higher vehicle velocities will have a negative impact on the system.

To determine correlations between different vehicle velocities from 0 to 30 m/s, a difference of 5 m/s, which is 18 km/h or 1.4 mph, is chosen as a first trial. Lowering the difference between those vehicle velocities was one of the options to increase visibility of correlations in different data sets. These values lead to a set of six different vehicle velocities considered for the operational test plan: 5 m/s, 10 m/s, 15 m/s, 20 m/s, 25 m/s, and 30m/s. Table 4-1 visualizes the operational test plan and shows all 90 data sets.

Table 4-1: Operational Test Plan

| Velocity / Profile | 5 m/s | 10 m/s | 15 m/s | 20 m/s | 25 m/s | 30 m/s |
|---|---|---|---|---|---|---|
| **CA** | # 1 | # 2 | # 3 | # 4 | # 5 | # 6 |
| **CB** | # 7 | # 8 | # 9 | # 10 | # 11 | # 12 |
| **CC** | # 13 | # 14 | # 15 | # 16 | # 17 | #18 |
| **CD** | # 19 | # 20 | # 21 | # 22 | # 23 | # 24 |
| **CE** | # 25 | # 26 | # 27 | # 28 | # 29 | # 30 |
| **CF** | # 31 | # 32 | # 33 | # 34 | # 35 | # 36 |
| **CG** | # 37 | # 38 | # 39 | # 40 | # 41 | # 42 |
| **P1** | # 43 | # 44 | # 45 | # 46 | # 47 | # 48 |
| **P2** | # 49 | # 50 | # 51 | # 52 | # 53 | # 54 |
| **P3** | # 55 | # 56 | # 57 | # 58 | # 59 | # 60 |
| **HS** | # 61 | # 62 | # 63 | # 64 | # 65 | # 66 |
| **HW** | # 67 | # 68 | # 69 | # 70 | # 71 | # 72 |
| **URA** | # 73 | # 74 | # 75 | # 76 | # 77 | # 78 |
| **URB** | # 79 | # 80 | # 81 | # 82 | # 83 | # 84 |
| **URC** | # 85 | # 86 | # 87 | # 88 | #89 | # 90 |

All 90 data sets are generated, processed, and visualized throughout this chapter.[156] As mentioned in the methodology for this chapter, two approaches were determined in order to evaluate the generated data sets.[157] The first evaluation approach compares all data sets for a given road profile over all examined vehicle velocities. The second approach compares a variety of road profiles over a given vehicle velocity. Because comparing 15 data sets at the same time can be very difficult, the second approach first compares each subcategory internally and afterwards all together.

Table 4-2 visualizes the first evaluation approach. Using this approach, the overall data set will be evaluated using 15 different setups. Table 4-3 visualizes the second approach, part one. Here, all subcategories or road profiles will be compared internally for a given vehicle velocity. In Table 4-4 the second part of the second approach is visualized, where all data sets are compared at once for a given vehicle velocity. The second evaluation approach results in 24 and 6, a total of 30 different setups. All in all, 45 different evaluation setups are created.

156 See chapter 4.3 Data Sets Generating, Processing, and Visualization.

157 See chapter 2.2 Data Generation and Evaluation.

This operational test plan is considered to be appropriate in order to determine whether correlation in the outcomes exists or not. However, depending on the results of the first correlation analysis, the operation test plan might be changed if necessary.

Table 4-2: Evaluation Approach 1

| Evaluation | Velocity Profile | 5 m/s | 10 m/s | 15 m/s | 20 m/s | 25 m/s | 30 m/s |
|---|---|---|---|---|---|---|---|
| **E1** | **CA** | # 1 | # 2 | # 3 | # 4 | # 5 | # 6 |
| **E2** | **CB** | # 7 | # 8 | # 9 | # 10 | # 11 | # 12 |
| **E3** | **CC** | # 13 | # 14 | # 15 | # 16 | # 17 | #18 |
| **E4** | **CD** | # 19 | # 20 | # 21 | # 22 | # 23 | # 24 |
| **E5** | **CE** | # 25 | # 26 | # 27 | # 28 | # 29 | # 30 |
| **E6** | **CF** | # 31 | # 32 | # 33 | # 34 | # 35 | # 36 |
| **E7** | **CG** | # 37 | # 38 | # 39 | # 40 | # 41 | # 42 |
| **E8** | **P1** | # 43 | # 44 | # 45 | # 46 | # 47 | # 48 |
| **E9** | **P2** | # 49 | # 50 | # 51 | # 52 | # 53 | # 54 |
| **E10** | **P3** | # 55 | # 56 | # 57 | # 58 | # 59 | # 60 |
| **E11** | **HS** | # 61 | # 62 | # 63 | # 64 | # 65 | # 66 |
| **E12** | **HW** | # 67 | # 68 | # 69 | # 70 | # 71 | # 72 |
| **E13** | **URA** | # 73 | # 74 | # 75 | # 76 | # 77 | # 78 |
| **E14** | **URB** | # 79 | # 80 | # 81 | # 82 | # 83 | # 84 |
| **E15** | **URC** | # 85 | # 86 | # 87 | # 88 | #89 | # 90 |

Table 4-3: Evaluation Approach 2-1

| Velocity Profile | 5 m/s | 10 m/s | 15 m/s | 20 m/s | 25 m/s | 30 m/s |
|---|---|---|---|---|---|---|
| **Evaluation** | **E16** | **E17** | **E18** | **E19** | **E20** | **E21** |
| **CA** | # 1 | # 2 | # 3 | # 4 | # 5 | # 6 |
| **CB** | # 7 | # 8 | # 9 | # 10 | # 11 | # 12 |
| **CC** | # 13 | # 14 | # 15 | # 16 | # 17 | #18 |
| **CD** | # 19 | # 20 | # 21 | # 22 | # 23 | # 24 |
| **CE** | # 25 | # 26 | # 27 | # 28 | # 29 | # 30 |
| **CF** | # 31 | # 32 | # 33 | # 34 | # 35 | # 36 |
| **CG** | # 37 | # 38 | # 39 | # 40 | # 41 | # 42 |
| **Evaluation** | **E22** | **E23** | **E24** | **E25** | **E26** | **E27** |
| **P1** | # 43 | # 44 | # 45 | # 46 | # 47 | # 48 |
| **P2** | # 49 | # 50 | # 51 | # 52 | # 53 | # 54 |
| **P3** | # 55 | # 56 | # 57 | # 58 | # 59 | # 60 |
| **Evaluation** | **E28** | **E29** | **E30** | **E31** | **E32** | **E33** |
| **HS** | # 61 | # 62 | # 63 | # 64 | # 65 | # 66 |
| **HW** | # 67 | # 68 | # 69 | # 70 | # 71 | # 72 |
| **Evaluation** | **E34** | **E35** | **E36** | **E37** | **E38** | **E39** |
| **URA** | # 73 | # 74 | # 75 | # 76 | # 77 | # 78 |
| **URB** | # 79 | # 80 | # 81 | # 82 | # 83 | # 84 |
| **URC** | # 85 | # 86 | # 87 | # 88 | #89 | # 90 |

Table 4-4: Evaluation Approach 2-2

| Velocity / Profile | 5 m/s | 10 m/s | 15 m/s | 20 m/s | 25 m/s | 30 m/s |
|---|---|---|---|---|---|---|
| **Evaluation** | **E40** | **E41** | **E42** | **E43** | **E44** | **E45** |
| **CA** | # 1 | # 2 | # 3 | # 4 | # 5 | # 6 |
| **CB** | # 7 | # 8 | # 9 | # 10 | # 11 | # 12 |
| **CC** | # 13 | # 14 | # 15 | # 16 | # 17 | #18 |
| **CD** | # 19 | # 20 | # 21 | # 22 | # 23 | # 24 |
| **CE** | # 25 | # 26 | # 27 | # 28 | # 29 | # 30 |
| **CF** | # 31 | # 32 | # 33 | # 34 | # 35 | # 36 |
| **CG** | # 37 | # 38 | # 39 | # 40 | # 41 | # 42 |
| **P1** | # 43 | # 44 | # 45 | # 46 | # 47 | # 48 |
| **P2** | # 49 | # 50 | # 51 | # 52 | # 53 | # 54 |
| **P3** | # 55 | # 56 | # 57 | # 58 | # 59 | # 60 |
| **HS** | # 61 | # 62 | # 63 | # 64 | # 65 | # 66 |
| **HW** | # 67 | # 68 | # 69 | # 70 | # 71 | # 72 |
| **URA** | # 73 | # 74 | # 75 | # 76 | # 77 | # 78 |
| **URB** | # 79 | # 80 | # 81 | # 82 | # 83 | # 84 |
| **URC** | # 85 | # 86 | # 87 | # 88 | #89 | # 90 |

## 4.2 iFX-LMS Tuning and Performance

Before varying road profiles and vehicle velocities for a correlation analysis in the outcomes of the iFX-LMS algorithm, it must be made sure that the iFX-LMS algorithm is properly tuned. In this chapter the tuning process of the algorithm is described to make sure it generates outputs which are in an acceptable range, close to the ideal solution, mitigate the road disturbance well, and are accurate enough for the following correlation analysis. The tunable performance parameters and the system/model they belong to are as follows:

- quarter car model and road profiles: sample frequency $F_s$
- linear combiner: number of weights in $W$ vector
- LMS algorithm: step size $\mu$
- iFX-LMS algorithm: filter models and number of iterations *nloops*

All other vehicle and application parameters are held constant over all data sets as they were defined in earlier chapters.

### 4.2.1 Sample Frequency $F_s$

The required sample frequency $F_s$ mainly depends on two factors, the quarter car model with active suspension system and the input signals. It is important to ensure the Nyquist-Shannon sampling theorem is not violated, meaning the sample frequency must be at least double the highest frequency in the system.[158] Therefore, the sample frequency $F_s$ must be at least double the highest eigenvalue of the quarter car model with active suspension system or if bigger the highest occurring frequency in the input signal (vertical road velocity).

While the highest eigenvalue of the quarter car model is with a value of about 10 Hz,[159] rather low, the input signals do contain much higher frequencies. By comparing each of the used road profiles signal's frequency spectrum, the highest occurring frequency is determined to be approximately 400 Hz, considering a maximum vehicle velocity of 30 m/s. Therefore, the minimum sample frequency, $F_s$, should be at least 800 Hz.

Because the offline calculation process is not time and resource critical, a sampling frequency, $F_s$, of 2000 Hz is chosen in order to have a safety buffer, and in case higher vehicle velocities or higher frequency signals are considered later.

### 4.2.2 Number of Weights in $W$ vector

As Figure 3-28 in chapter 3.4 shows, the linear combiner, which is the base of the iFX-LMS algorithm, weighs the input signal using a weight vector. In the given example the vector had five elements/weights. In general, the linear combiner can have as many weights as are required by the system or as can be processed.

The number of weights does have an important impact on the overall performance of the algorithm and its mitigation ability. If the number of weights is too small, the algorithm is not able to generate a force profile close to the optimal solution. In this case the mean-square error signal (MSE) would show only a small amount in reduction. Secondly, as the number of weights decreases, the harder it will be to find correlations. This problem is analogous to taking the average of a population. The smaller the sample size is, the farther the average of the sample is from the population. Thus, the more weight values are considered in the algorithm, the more accurate a later created Finite-Impulse-Response Filer (FIR) will be, and the easier it will be to determine correlations.

Most of the tools and parameters for evaluating the mitigation performance of the iFX-LMS algorithm will be introduced in the following chapter. However, in order to tune and set a number of weights, some of the easier to evaluate performance parameters are calculated below. The evaluated road profile is curb A with a vehicle velocity of 15 m/s, and uses three different numbers for the weight vector: 100, 500, and 2000 weights. These parameters and their outcomes are shown in Table 4-5.

[158] Cf. Wikipedia: Nyquist–Shannon sampling theorem, 2017.

[159] See chapter 3.1 Quarter Car Model with Active Suspension System.

Table 4-5: Performance Evaluation for Variations in the Number of Weights

| | 100 weights | 500 weights | 2000 weights |
|---|---|---|---|
| **MSE reduction** | - 4.5 dB | - 8.6 dB | - 25.7 dB |
| **max. acceleration reduction** | 73 % | 81 % | 98 % |
| **evaluation ability W vector** | hard | middle | easy |

As can be seen, a higher number of weights reduces the MSE better than a lower number of weights. It also increases the reduction of maximum acceleration and makes it easier to evaluate the weight vector. For the final design 2000 weights is chosen to be appropriate. Even though the number could be reduced without the loss of much accuracy, it is kept that high for safety reasons and because the offline study provides nearly unlimited calculation and computing resources.

*Note:* The above shown data set is just an example for illustrative purposes. In the real tuning process many more numbers of weights were used and evaluated. A lot of trials were necessary because all tuned performance parameters influence each other and must be tuned simultaneously.

### 4.2.3 Step Size $\mu$

The step size $\mu$ is a constant used from the LMS algorithm and regulates the difference between each weight adjustment step. It influences the algorithm's stability, controls the convergence speed and impacts the MSE reduction.[160]

The goal of the LMS algorithm is to move downwards on the performance surface as introduced in chapter 3.4. In order to do so, the LMS algorithm adjusts the weights in each step using a gradient estimation. This estimation is then multiplied with the step size $\mu$. The process should be performed as quickly as possible, while simultaneously reaching the lowest point possible, i.e. as close to the global minimum as possible. Unfortunately, these two wishes contradict each other. In order to move down quickly on the performance surface the step size should be large. On the other hand, the step-size should be small enough in order to reach down close to the global minimum. Another way to think about this problem is with the analogy of both a small and big ball thrown into a performance surface like the one shown in Figure 3-29. A large ball will relatively quickly reach its final settling point in the surface, meaning it is stuck at the point where its radius has the same size as the minimum horizontal distance between two points on the surface. A smaller ball, however, will need longer to reach its settling point, because it can move around more due to its smaller radius. Therefore, it is able to reach further down. Because processing time is not a limiting factor at this stage of the research, a smaller step size is chosen and more appropriate.

Table 4-6 again shows the performance of three samples, the evaluated road profile is curb A again with a vehicle velocity of 15 m/s. Three different step sizes are used for $\mu$: 5, 100, 500. All sets are calculated using 5000 iterations. As can be seen the set with $\mu = 5$ converges very slowly and has not

[160] Cf. Widrow, B., and Stearns, S. D.: Adaptive Signal Processing, 1985, pp. 54-60.

converged yet after 5000 iterations, hence its performance is fairly poor. Both other sets converged quickly with a sufficient MSE reduction.

Table 4-6: Performance Evaluation for Variations in Step Size μ

| | $\mu = 5$ | $\mu = 100$ | $\mu = 500$ |
|---|---|---|---|
| **MSE reduction** | - 14 dB* | - 25.7 dB | - 25.7 dB |
| **convergence rate** | not conv. yet | quick | quick |
| **max. acceleration reduction** | 85% | 98% | 98% |

A final step size of $\mu = 100$ is chosen because there is virtually no difference between the set which uses $\mu = 500$ instead.

*Note:* The same note stated in chapter 4.2.2 is true for tuning the step size $\mu$.

### 4.2.4 Filter Models and Number of Iterations *nloops*

As indicated in chapter 3.4, the filtered-X version of the LMS algorithm requires well-tuned filter models of the plant in order to work properly. Further, these filters were tuned in previous research at PERL VT.[161] The fact that they must be tuned is only mentioned here for completeness.

Using the iterative version of the FX-LMS algorithm requires one to choose an appropriate number of iterations, called *nloops*. Each iteration of the FX-LMS algorithm starts with initial conditions from the previous iteration in order to further improve the results. This factor interlinks heavily with the step size $\mu$. If the step size $\mu$ is chosen to be too small, the number of iterations clearly needs to be bigger in order to give the algorithm more steps for moving down on the performance surface. The same logic holds for the opposite case. Table 4-7 shows the performance evaluation for curb A with a vehicle velocity of 15 m/s and a step size $\mu = 100$. The number of iterations varies from 100, to 1000, and 5000 iterations.

Table 4-7: Performance Evaluation for Variations in the Number of Iterations *nloops*

| | ***nloops* = 100** | ***nloops* = 1000** | ***nloops* = 5000** |
|---|---|---|---|
| **MSE reduction** | - 9.3 dB* | - 22.6 dB | - 25.7 dB |
| **convergence** | not conv. yet | not conv. yet | converged |
| **max. acceleration reduction** | 65% | 95% | 98% |

The table indicates that the algorithm does not converge using a number of weights which is 100 or 1000, considering a chosen step size $\mu = 100$. As a result, both of these data sets show poor performance. 5000 iterations are chosen for the final set of parameters.

*Note:* The same note stated in chapter 4.2.2 and 4.2.3 is true for tuning the number of iterations *nloops*.

[161] See Rao, A. M.: A Structured Approach to Defining Active Suspension Requirements, 2016, pp. 42-44.

### 4.2.5 Final Set of Performance Parameters

The final set of performance parameters consists of those derived and introduced in this chapter, and are shown again in Table 4-8.

Table 4-8: Final Set of Performance Parameters

| Performance Parameter | Value |
|---|---|
| Sample Frequency $F_s$ | 2000 Hz |
| Number of Weights $W$ | 2000 |
| Step size $\mu$ | 100 |
| Number of Iterations *nloops* | 5000 |

Even though Widrow and Stearns present techniques in their book "Adaptive Signal Processing"[162] for how to derive or calculate some of the performance parameters, it is most common to tune these by hand. The overall tuning process of the iFX-LMS algorithm is still an expensive, time-intense, sometimes non-transparent, and over all iterative trial and error process. This is mostly due to the interlink between each performance parameter. The iteration process also includes to start the correlation analysis as shown below, searching for correlations, going back, and tuning again. Fortunately, power and efficiency requirements are not critical for this offline simulation study. Therefore, the final parameters were ramped up at the end of the tuning process in order to have a lager safety zone.

The tuning process is carried out considering a set of performance parameters which fit to all road profiles. This is important in order to be able to proceed with the following correlation analysis. As will be explained later, the tuned LMS algorithm performed very well and was one of the key points which guided the search for the correlation model in the right direction.

## 4.3 Data Sets Generating, Processing, and Visualization

Using the final set of performance parameters[163] and taking the operational test plan into account,[164] all 90 data sets are generated, processed by the iFX-LMS algorithm, and finally their results are visualized and analyzed.

For each of the 90 data sets a struct data file is generated, each of which contains the set of different initial conditions. Afterwards, these files are put into the application which then processes them using the iFX-LMS algorithm. In the end, all outputs are combined in a struct data file again. For the following analysis process a subset of these outputs are extracted and visualized. The following outcomes from 4.3.1.1 to 4.3.1.6 are determined to show an appropriate overview of the systems behavior in order to search for correlations in between different data sets.

[162] See Widrow, B., and Stearns, S. D.: Adaptive Signal Processing, 1985.

[163] See chapter 4.2.5 Final Set of Performance Parameters.

[164] See chapter 4.1 Operational Test Plan.

#### 4.3.1.1 MSE at each Iteration Step

As stated above, the MSE signal indicates whether the algorithm has converged yet and, if so, how big the reduction is. A non-converged MSE, meaning it still has a negative slope, indicates that step size $\mu$ and the number of iterations *nloops* is not chosen appropriately for the specific data set. Ideally this should not happen for the generated data sets due to the earlier tuning process, however it is still important to check for convergence and MSE reduction first. The MSE reduction should be around -20 dB, which is a value commonly used in controls engineering.

#### 4.3.1.2 Uncontrolled Sprung Mass Acceleration

In order to evaluate the mitigation performance of the iFX-LMS algorithm, the controlled sprung mass acceleration (smaller) needs to be compared relatively to the uncontrolled sprung mass acceleration (larger). In this context, the uncontrolled sprung mass acceleration is understood as the acceleration of the sprung mass only caused by the road excitation.

#### 4.3.1.3 Controlled Sprung Mass Acceleration

Afterwards the controlled sprung mass acceleration, which is the acceleration of the sprung mass caused by the road excitation and the force generator/actuation system together, can be compared to the uncontrolled sprung mass acceleration. This comparison will indicate how well the iFX-LMS algorithm performs and mitigates the road excitation.

#### 4.3.1.4 Weights in *W* Vector

After it was made sure that the iFX-LMS works appropriately and the mitigation performance is satisfying, the weights in the *W* vector from different data sets can be compared. Looking only at the weights will give a first impression whether correlation exists and if so, how strongly.

#### 4.3.1.5 FIR Filter

The introduced linear combiner, which weights the input signal with the set of adjusted weights, is also called a digital filter. Without the use of feedback it is a non-recursive digital filter. Instead of weighting the input signal, an equivalent procedure is to filter it digitally using a Finite Impulse Response (FIR) Filter. This filter is given by a transfer-function which contains all weights in the numerator and a 1 in the denominator. Comparing the filter model of each data set is the second stage comparison and search for correlations in the weights vector/filter model.[165] It basically is the same as 4.3.1.4, however, it better shows and provides information about the filter shape.

[165] Cf. Widrow, B., and Stearns, S. D.: Adaptive Signal Processing, 1985, pp. 120-124.

#### 4.3.1.6 Correlation Coefficient

Comparing and searching for correlations in the weights vector by comparing the weight values and its FIR filter representation is rather subjective. In order to make a more objective statement about the kind and strength of correlation, the correlation coefficients are calculated. Comparing signals using their correlation coefficients provides both information about how close both two signals are and whether a correlation is likely or not.

In total, three visualization plots for the above-mentioned outcomes are generated: Overview Plot, FIR Filter Plot, Correlation Coefficient Plot. They are introduced in the following subchapters.

### 4.3.2 Overview Plot

As the name indicates, the Overview Plot provides a visual overview of the overall system performance. Figure 4-1 shows an example Overview Plot for curb A over the whole set of chosen vehicle velocities (5 m/s, 10 m/s, 15 m/s, 20 m/s, 25 m/s, and 30 m/s).

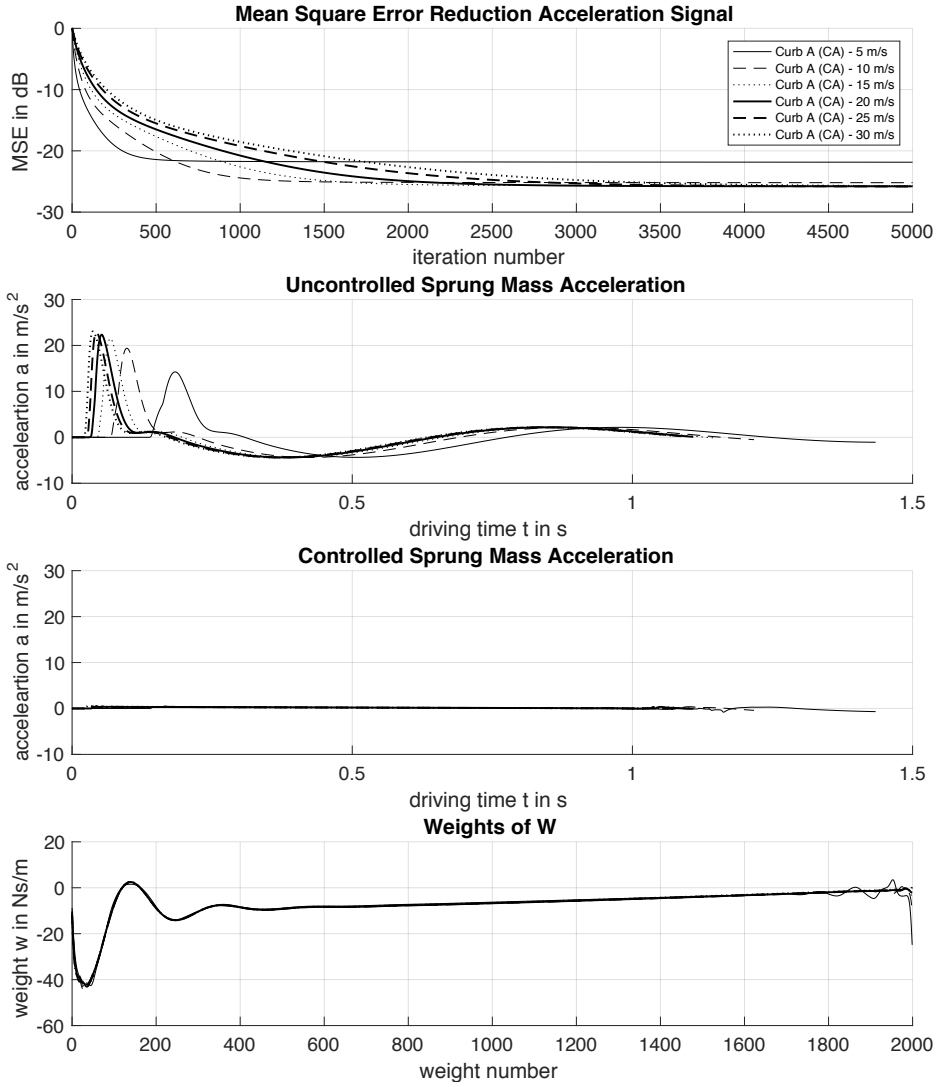


Figure 4-1: Overview Plot Curb A (CA) Over Whole Set of Vehicle Velocities (E1)

At the top of the plot the MSE value at each iteration step is shown. As is common in controls engineering, it is displayed on a dB scale. At the beginning of the evaluation process, looking at this subplot will be the first step. If the signal has not converged yet, i.e. it still has a major negative slope, or if the overall reduction in the signal is too small, i.e. above or not close to -20 dB, the processing needs to be redone with a new set of performance parameters. In the shown example all signals are fully converged and the MSE is reduced well enough.

The MSE signal is followed by the uncontrolled and controlled sprung mass acceleration. Both signals have the same scale on the y axis for comparison purpose. In order to make a qualitative statement about the mitigation performance of the iFX-LMS solution, it is necessary to compare the controlled (road and force excitation) sprung mass acceleration relatively to the uncontrolled (road excitation only) one. The example above from curb A already indicates how well the algorithm works. It is tuned well enough so that the peak acceleration sprung mass acceleration drops from above 20 $m/s^2$ to a value close to 0 $m/s^2$, making a reduction in acceleration by about 96.25 %. The different signals are shifted to the right due to different vehicle velocities. Due to this as well, all signals have a different signal length.

*Note:* The algorithm adds to each road profile signal a 1 m flat road in front and after the disturbance. Also, a 1 second settling time is added to the signal after the extended road profile ends.

After the performance of the iFX-LMS algorithm and its mitigation performance is evaluated using the first three subplots, the evaluation of the weights can be started. The values of each weight are shown in the last subplot (weight value over weight number). While it is difficult to read anything out of the signal shape, it is more important to compare the shape of each signal to all of the others. In this example, all weight vectors have a very similar weight vector/shaped signal. This indicates that correlation between those exists. This last evaluation is the most important one, since it indicates that a universal filter for curb A over the whole set of vehicle velocities exists.

The Overview Plot was also used as a tool during the tuning process.

### 4.3.3 FIR Filter Plot

After the overview plot provides some information about the weights of the *W* vectors and their correlation, the FIR Plot is used to further investigate the correlation of the different signals and the general filter shape. An example of the FIR Plot is given in Figure 4-2 for curb A over the whole set of vehicle velocities.

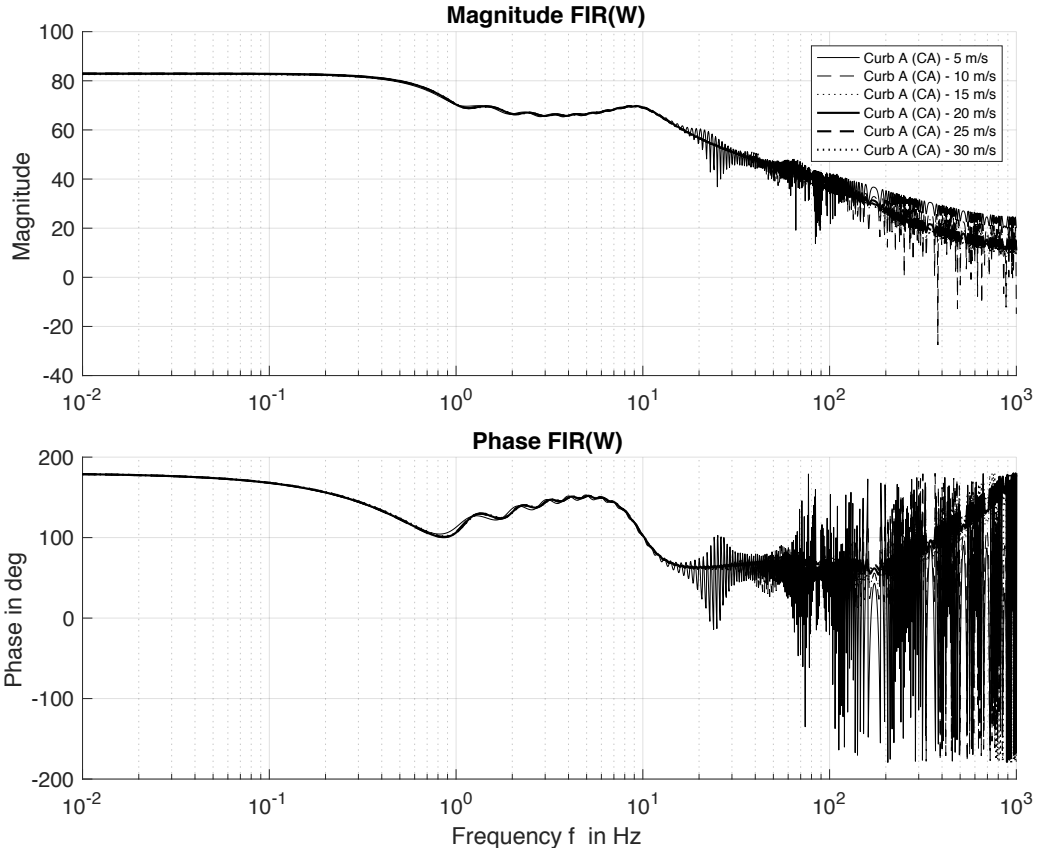


Figure 4-2: FIR Filter Plot Curb A (CA) Over Whole Set of Vehicle Velocities (E1)

As can be seen, the plot provides a Bode Diagram of the earlier introduced FIR filter, on top the magnitude over frequency and on the bottom phase over frequency. From the plot two aspects of the weight vector can be examined. First, the shapes of all filter models seem to follow the same filter, meaning they are very close to each other and seem to correlate well. The deviations in the end of the frequency range (over 100 Hz) are not of high importance, due to two reasons. First, compared to the margin magnitude they are relatively small; a reduction of -40 dB is a factor of 100 times smaller. Second, most of the road and velocity input signals contain frequency signals in the range from 0 to approximately 100 Hz. Few signals contain high frequency signals, which caused the iFX-algorithm to not perform that well in this range. The phase signal also contains several 180° and 360° phase shifts, which is due to the visualization tool. On the other hand, the plot also provides information by showing the general shape of the filter. This information will be used in later chapters during the evaluation and analysis process in order to derive a new and universal filter model.

### 4.3.4 Correlation Coefficients Plot

Even though both the Overview Plot and FIR Plot already showed all weights to be very similar and correlated, each of these judgments is rather subjective. In order to provide a more objective statement about the level of correlation for these different signals, correlation coefficients are calculated. While auto and cross correlations can be plotted and compared as well, correlation coefficients are more appropriate. The advantage of these coefficients is that they are already normalized and provide only a single value (shift 0 s). Figure 4-3 shows a Correlation Plot for curb A over the whole set of vehicle velocities.

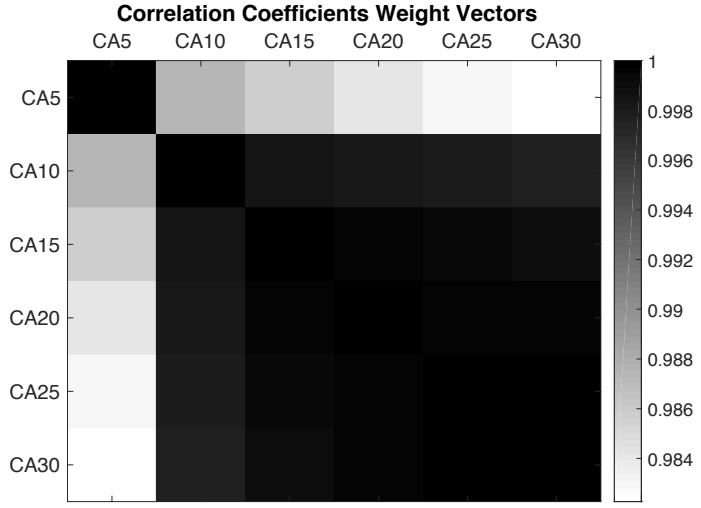


Figure 4-3: Correlation Coefficient Plot Curb A (CA) Over Whole Set of Vehicle Velocities (E1)

Instead of showing the values of the correlation coefficients, the plot visualizes them in an image with scaled colors using the Matlab imagesc function. The road profiles and the corresponding vehicle velocities are displayed on the top and left side of the plot. Each square represents a correlation coefficient, for example the square in the top left corned represents the correlation of curb A at 5 m/s with curb A at 5 m/s, since both signals are identical the correlation coefficient must be 1. The same is true for all squares on the main diagonal, which are basically auto correlations at a shift of 0 s. The square in the top right corner represents the correlation of curb A with 5 m/s compared to curb A with 30 m/s. As can be seen this value is the lowest in the whole plot, but still as high as 0.984. Since the upper right and lower left part of the matrix beside the main diagonal show the same values, only one of these must be evaluated.

For the given example, the Correlation Plot shows very high correlations as indicated by the legend on the right which shows that the values are in the range from 0.984 to 1. Also, lower correlation coefficients correspond to larger differences in vehicle velocities.

## 4.4 Analysis and Evaluation of Data Sets

The outcomes of the data sets are analyzed and evaluated from two points of views. First, their outcomes and correlations are checked comparing the outcomes for a given profile over the whole set of vehicle velocities. Afterwards the same will be done comparing different profiles for a given vehicle velocity. This procedure is according to the operational test plan.[166]

Even though all data sets are evaluated and analyzed, only a subset of the results is shown in this chapter. This is due to the fact that the plots require a lot of space and because most of the data sets show the same result and repeat earlier statements. Therefore, only the most interesting data sets are presented, but at least one for each subcategory of road profiles.

In order to present the results in a clean and easily readable way, a table for each presented data set is created. An example table is shown in Table 4-9. Additional comments are only provided if the data sets show anomalies.

Table 4-9: Example Outcome Evaluation and Analysis Table

| **Evaluation and Analysis** | **Value/Score** |
|---|---|
| MSE signal converged? | yes/no |
| MSE reduction satisfying? | yes/no, reduction value in dB |
| subjective acceleration mitigation | scores 1: poor, 2: neutral, 3: well |
| maximum acceleration reduction | from ~x $m/s^2$ to ~y $m/s^2$, ~y/x % reduction |
| subjective weight vector correlation | scores 1: poor, 2: neutral, 3: well |
| correlation coefficients | high, > z |
| FIR filter model adequate? | scores 1: poor, 2: neutral, 3: well |
| overall algorithm performance satisfying? | yes/no |
| correlation exists? | yes/no |

[166] See chapter 4.1 Operational Test Plan.

### 4.4.1 Analysis and Evaluation of Data Sets for a Given Road Profile Over Whole Set of Vehicle Velocities

#### 4.4.1.1 Curbs

The results of Curb A (E1) were already presented, analyzed, and evaluated in the previous chapter, which is why they are not represented here again. The two subcategories of curb profiles (sharp and gentle edges) all show approximately the same results as curb A. Therefore, E2, E3, E4, and E7 are not presented. The result of the override profile curb F (E6) is presented because it differs from the other categories, however, due to their close shape it is equal to curb E (E5). Figure 4-4 through Figure 4-6, and Table 4-10 present the data set, analysis, and evaluation of curb F (E6).

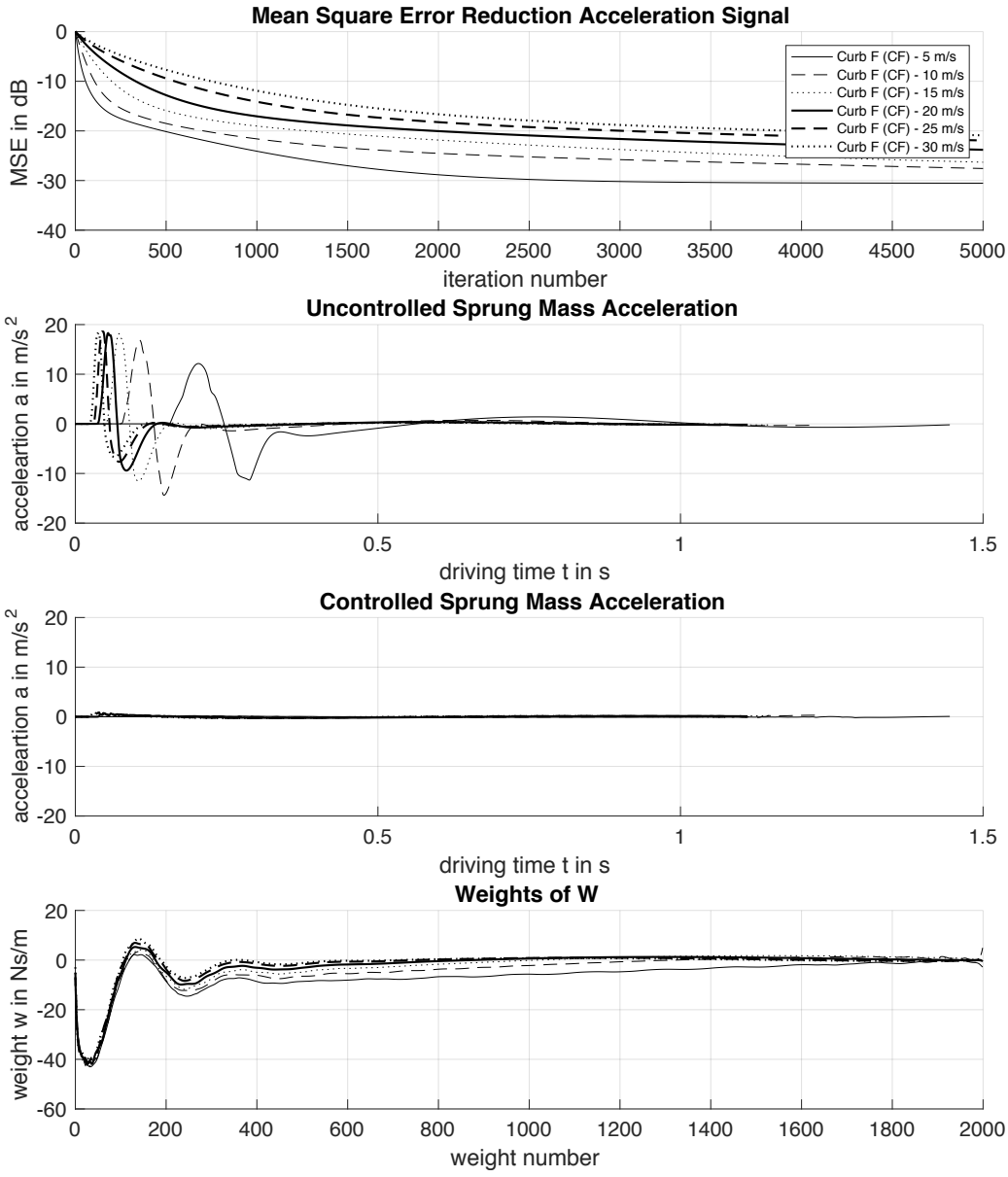


Figure 4-4: Overview Plot Curb F (CF) Over Whole Set of Vehicle Velocities (E6)

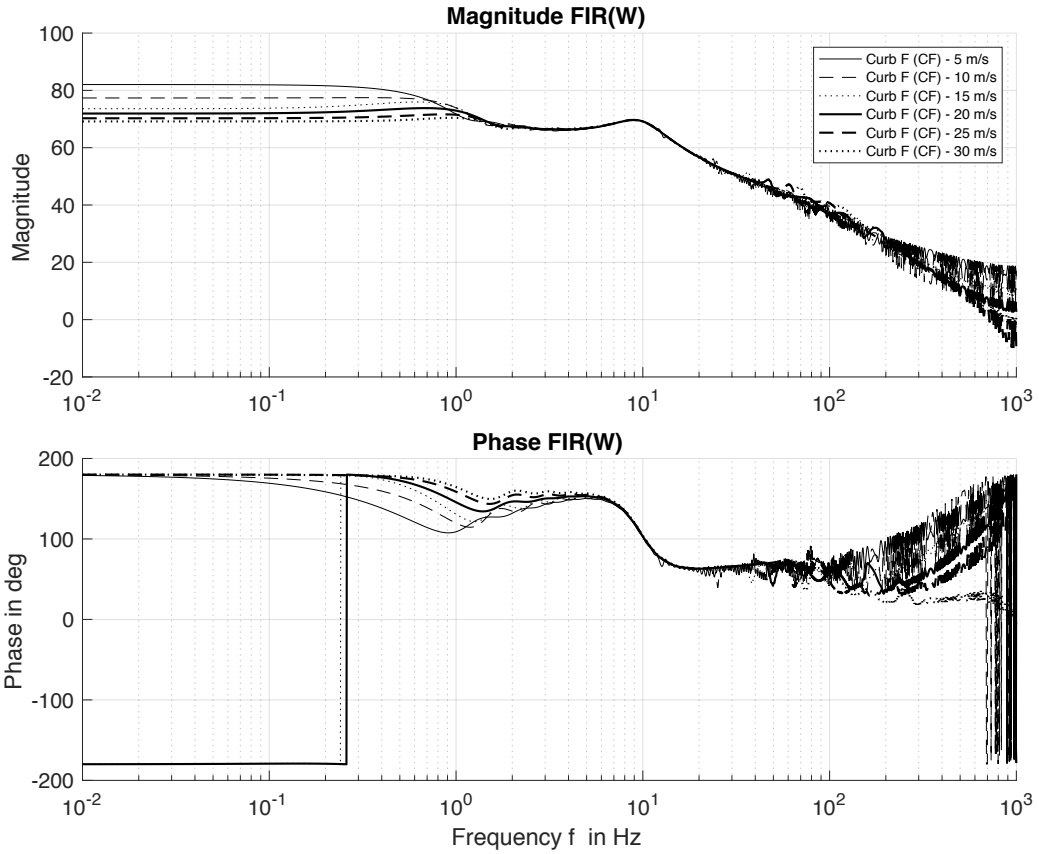


Figure 4-5: FIR Filter Plot Curb F (CF) Over Whole Set of Vehicle Velocities (E6)

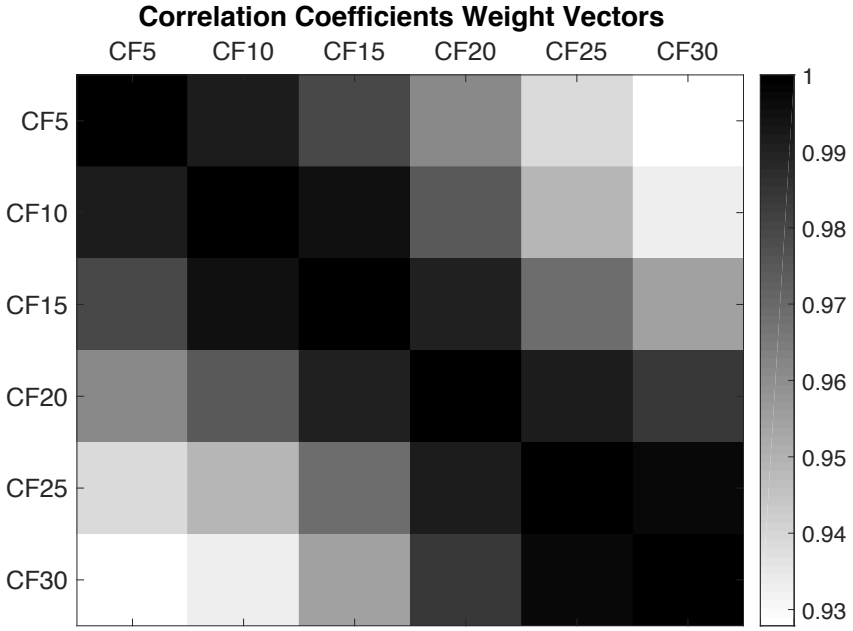


Figure 4-6: Correlation Coefficient Plot Curb F (CF) Over Whole Set of Vehicle Velocities (E6)

Table 4-10: Outcome Evaluation and Analysis Table Curb F (CF) Over Whole Set of Vehicle Velocities (E6)

| **Evaluation and Analysis** | **Value/Score** |
|---|---|
| MSE signal converged? | yes |
| MSE reduction satisfying? | yes, > -20db |
| subjective acceleration mitigation | 3 |
| maximum acceleration reduction | from ~18 $m/s^2$ to ~0.93 $m/s^2$, ~95 % reduction |
| subjective weight vector correlation | 2.5 |
| correlation coefficients | high, > 0.92 |
| FIR filter model adequate? | 2.5 |
| overall algorithm performance satisfying? | yes |
| correlation exists? | yes |

#### 4.4.1.2 Potholes

The results of all potholes follow nearly the same path and shape. However, pothole 2 seems to be the most stressful for the vehicle and requires the most action from the active suspension system, therefore it is presented here. Figure 4-7 through Figure 4-9, and Table 4-11 present the data set, analysis, and evaluation of pothole 2 (E9).

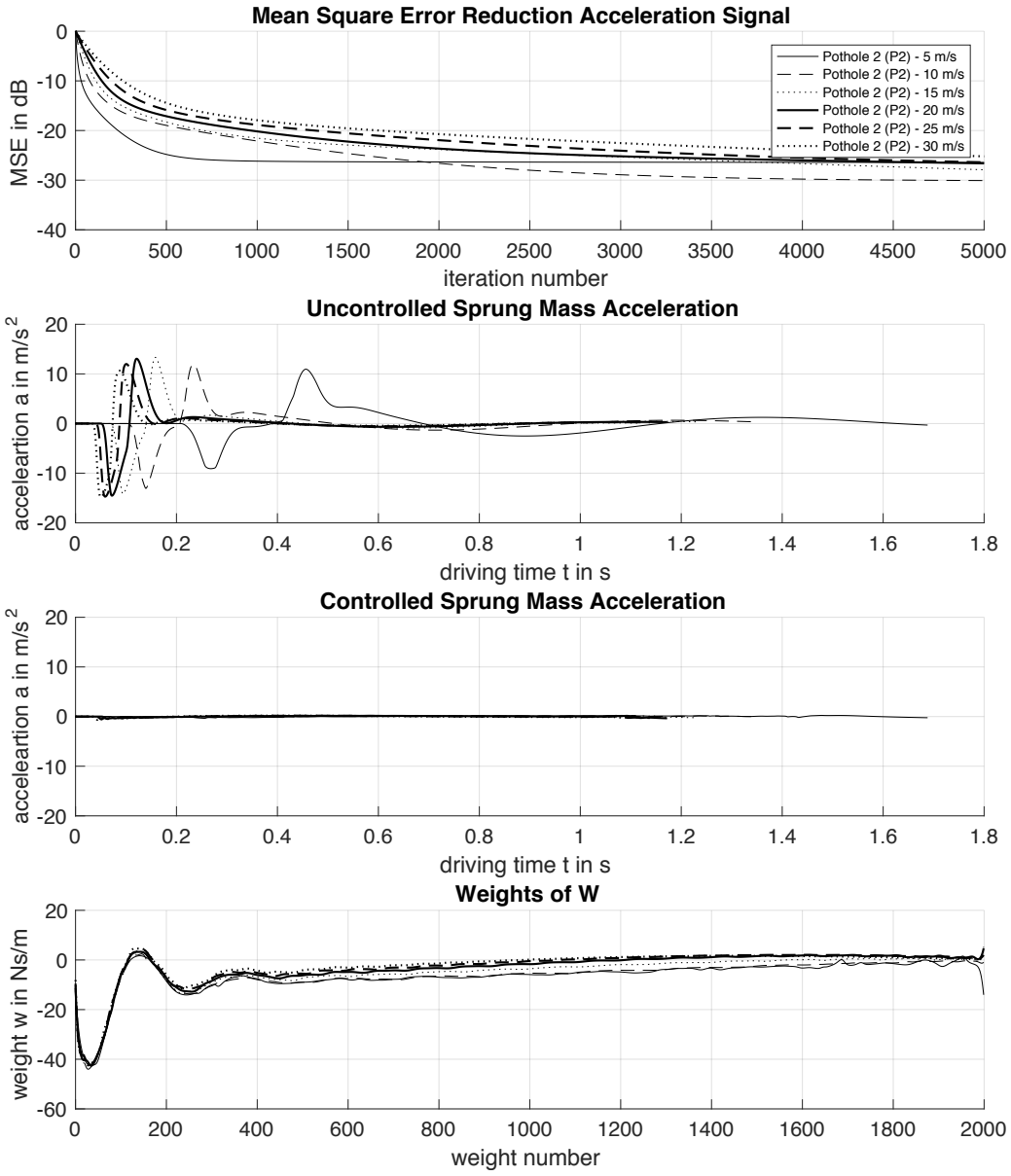


Figure 4-7: Overview Plot Pothole 2 (P2) Over Whole Set of Vehicle Velocities (E9)

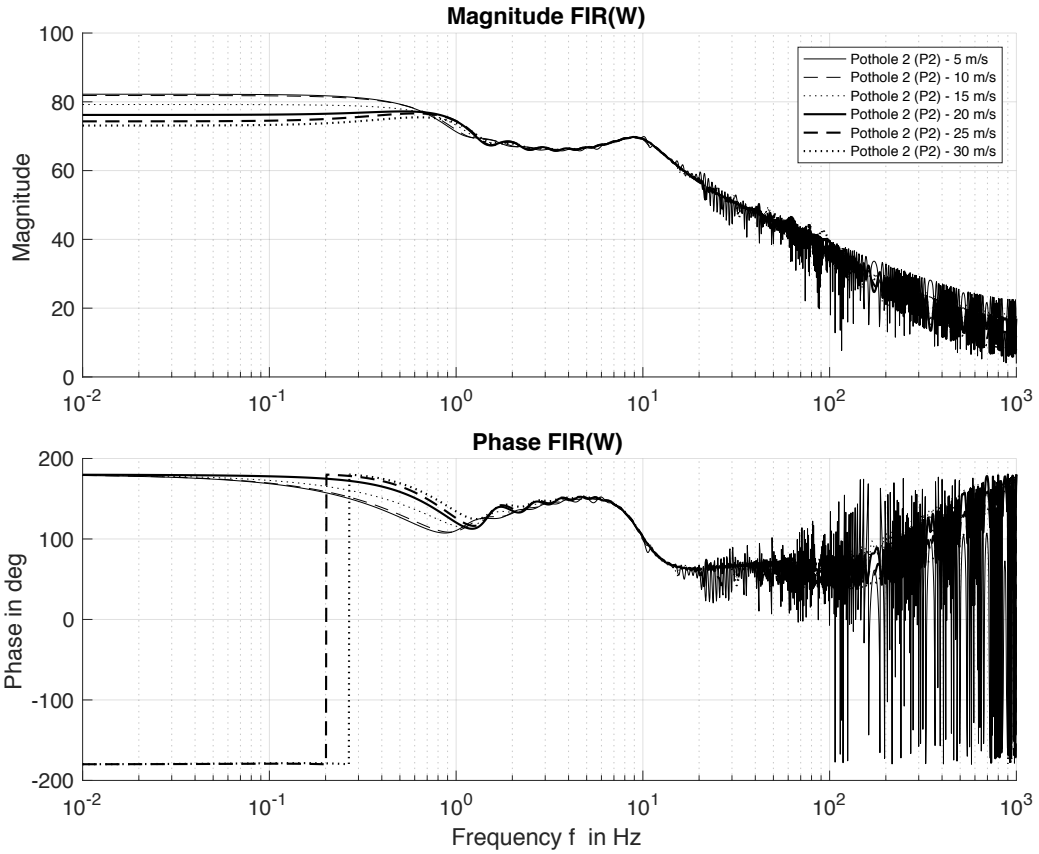


Figure 4-8: FIR Filter Plot Pothole 2 (P2) Over Whole Set of Vehicle Velocities (E9)

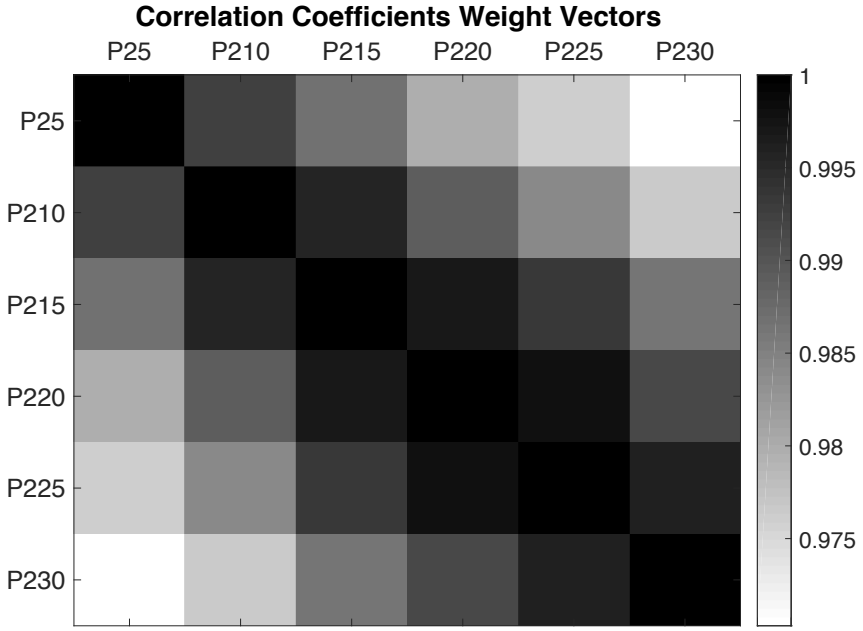


Figure 4-9: Correlation Coefficient Plot Pothole 2 (P2) Over Whole Set of Vehicle Velocities (E9)

Table 4-11: Outcome Evaluation and Analysis Table Pothole 2 (P2) Over Whole Set of Vehicle Velocities (E9)

| **Evaluation and Analysis** | **Value/Score** |
|---|---|
| MSE signal converged? | yes |
| MSE reduction satisfying? | yes, > -25db |
| subjective acceleration mitigation | 3 |
| maximum acceleration reduction | from ~13.3 $m/s^2$ to ~0.15 $m/s^2$, ~99 % reduction |
| subjective weight vector correlation | 3 |
| correlation coefficients | high, > 0.97 |
| FIR filter model adequate? | 2.5 |
| overall algorithm performance satisfying? | yes |
| correlation exists? | yes |

#### 4.4.1.3 Speed Humps

Both the Seminole and Watts Profile Hump show similar results. Because the results of the Watts Profile Hump require slightly more action from the active suspension system and cause a larger acceleration of the sprung mass, it is presented below. Figure 4-10 through Figure 4-12, and Table 4-12 present the data set, analysis, and evaluation of the Watts Profile Hump (E12).

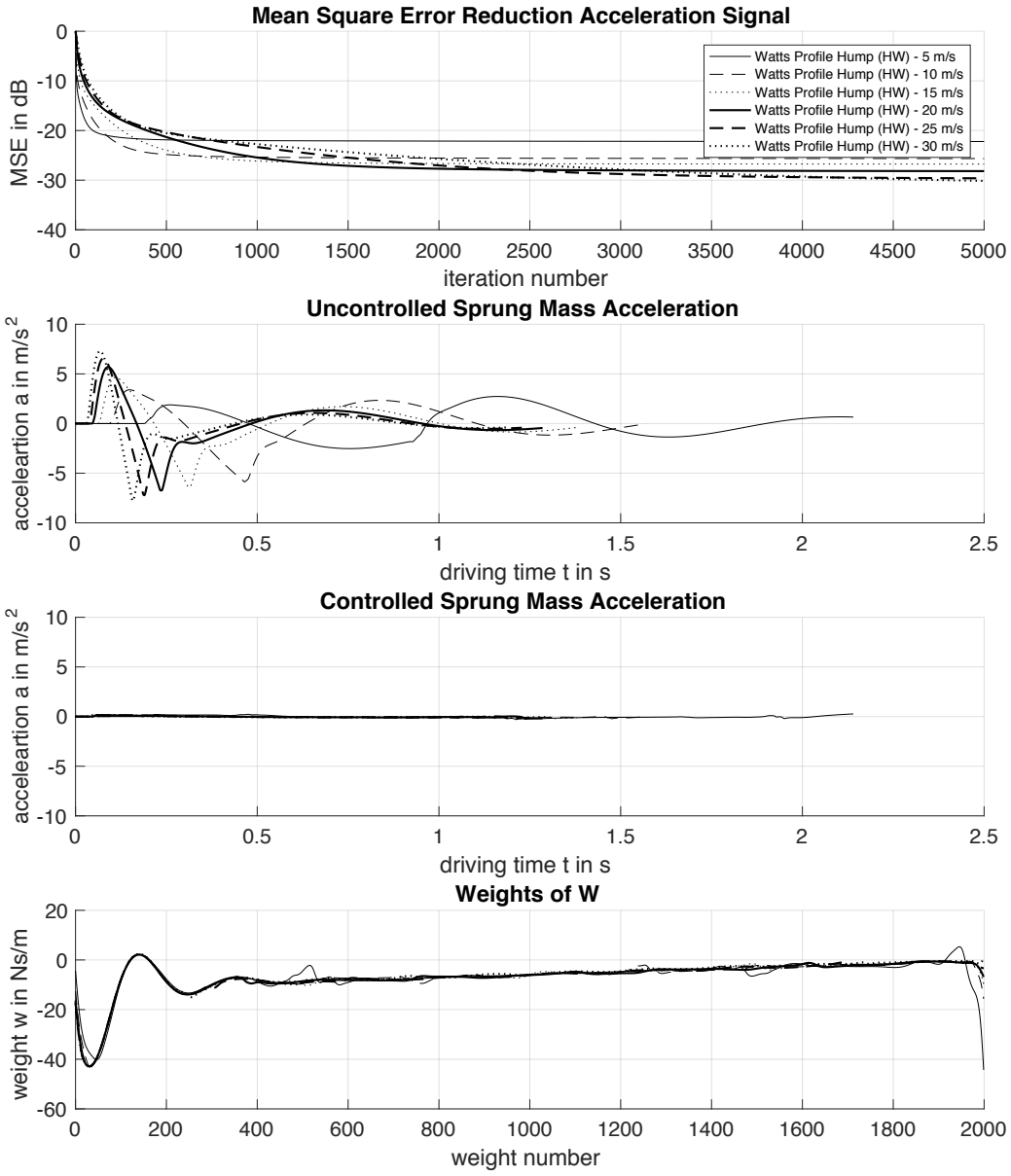


Figure 4-10: Overview Plot Watts Profile Hump (HW) Over Whole Set of Vehicle Velocities (E12)

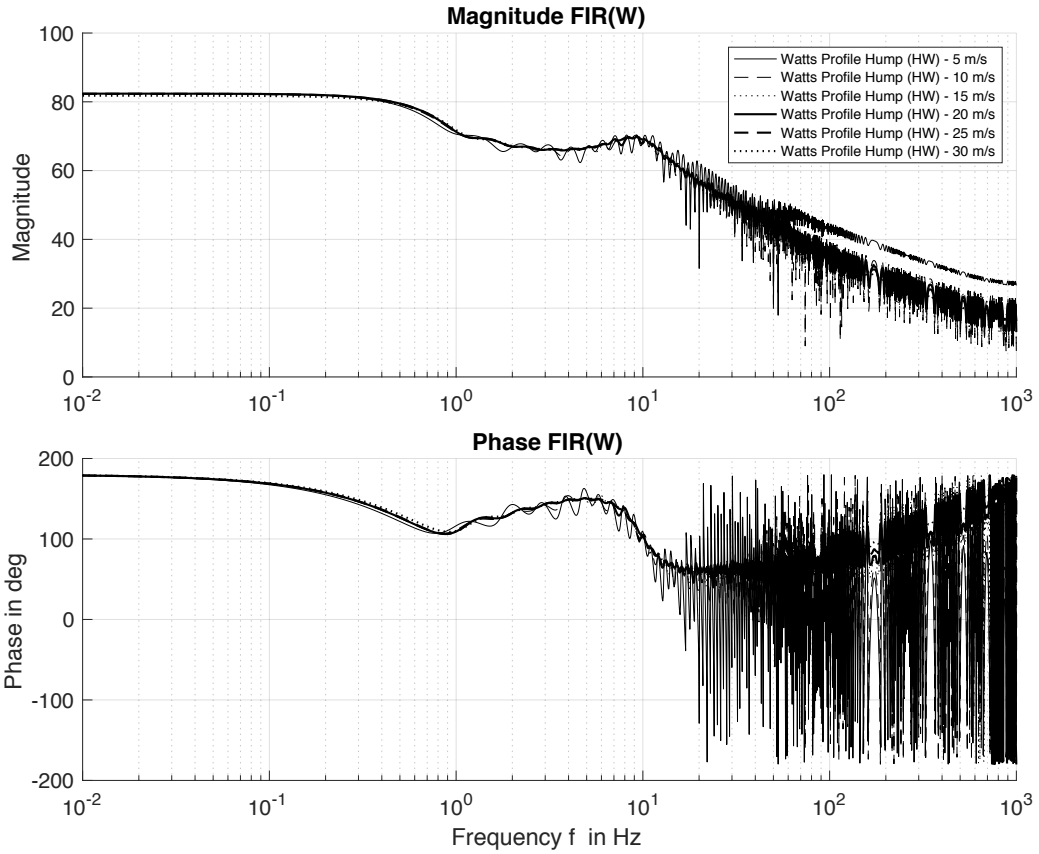


Figure 4-11: FIR Filter Plot Watts Profile Hump (HW) Over Whole Set of Vehicle Velocities (E12)

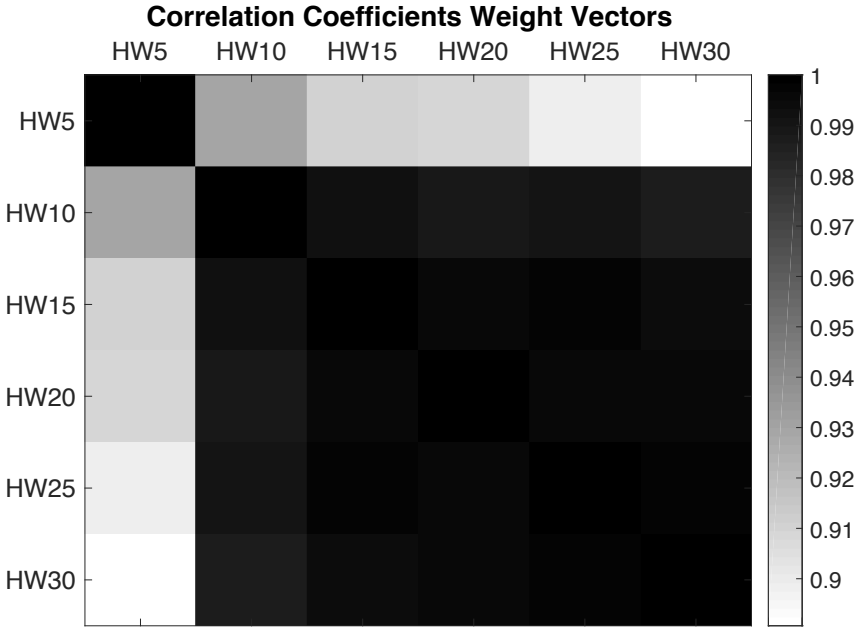


Figure 4-12: Correlation Coefficient Plot Watts Profile Hump (HW) Over Whole Set of Vehicle Velocities (E12)

Table 4-12: Outcome Evaluation and Analysis Table Watts Profile Hump (HW) Over Whole Set of Vehicle Velocities (E12)

| **Evaluation and Analysis** | **Value/Score** |
|---|---|
| MSE signal converged? | yes |
| MSE reduction satisfying? | yes, > -22db |
| subjective acceleration mitigation | 3 |
| maximum acceleration reduction | from ~7.3 $m/s^2$ to ~0.16 $m/s^2$, ~98 % reduction |
| subjective weight vector correlation | 3 |
| correlation coefficients | high, > 0.89 |
| FIR filter model adequate? | 3 |
| overall algorithm performance satisfying? | yes |
| correlation exists? | yes |

#### 4.4.1.4 Uneven Roads

All three uneven road profiles show approximately the same outcomes. However, uneven road A requires the most action from the active suspension system and has the highest uncontrolled acceleration, therefore it is shown below and is representative of the outcomes from the other two profiles. Figure 4-13 through Figure 4-15, and Table 4-13 present the data set, analysis, and evaluation of the uneven Road A over the whole set of vehicle velocities (E13).

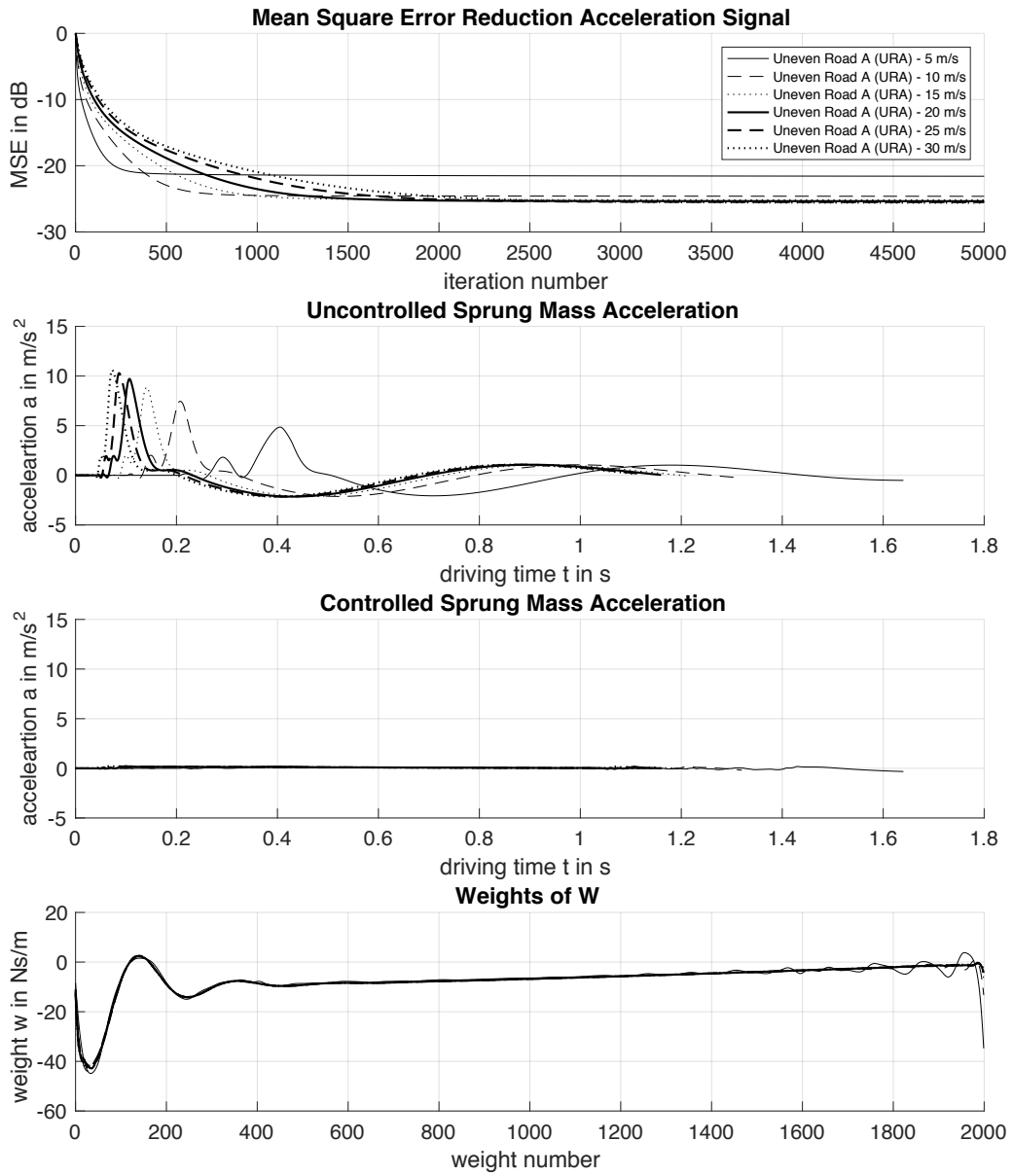


Figure 4-13: Overview Plot Uneven Road A (URA) Over Whole Set of Vehicle Velocities (E13)

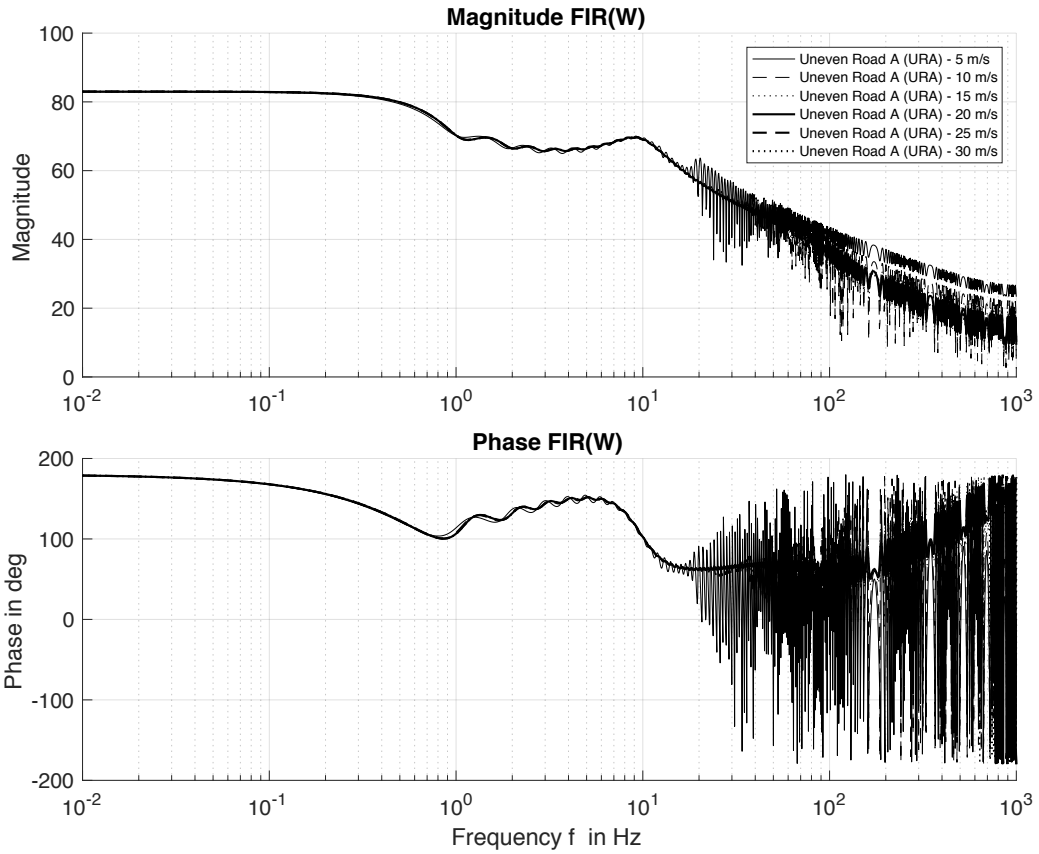


Figure 4-14: FIR Filter Plot Uneven Road A (URA) Over Whole Set of Vehicle Velocities (E13)

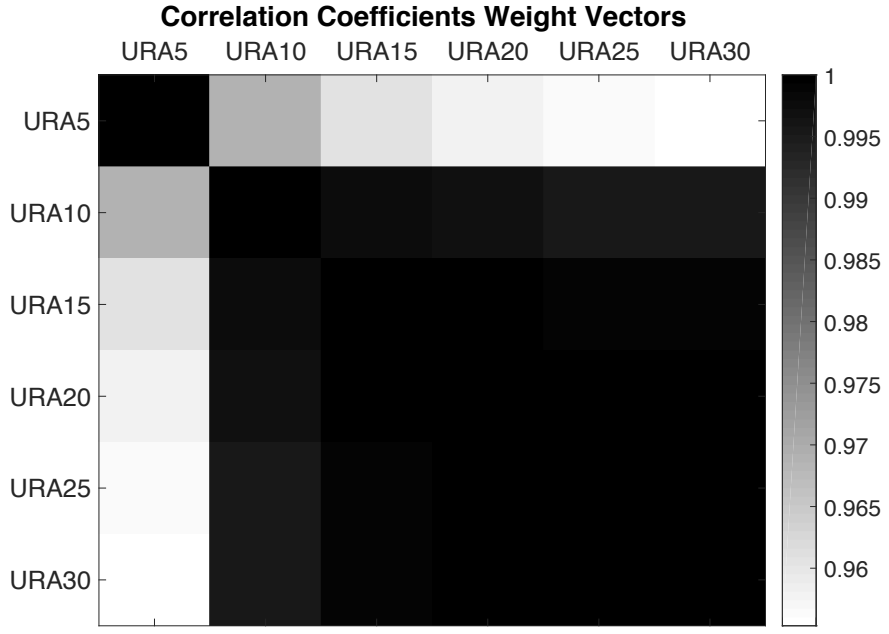


Figure 4-15: Correlation Coefficient Plot Uneven Road A (URA) Over Whole Set of Vehicle Velocities (E13)

Table 4-13: Outcome Evaluation and Analysis Table Uneven Road A (URA) Over Whole Set of Vehicle Velocities (E13)

| **Evaluation and Analysis** | **Value/Score** |
|---|---|
| MSE signal converged? | yes |
| MSE reduction satisfying? | yes, > -22db |
| subjective acceleration mitigation | 3 |
| maximum acceleration reduction | from ~10.6 $m/s^2$ to ~0.23 $m/s^2$, ~98 % reduction |
| subjective weight vector correlation | 3 |
| correlation coefficients | high, > 0.955 |
| FIR filter model adequate? | 3 |
| overall algorithm performance satisfying? | yes |
| correlation exists? | yes |

### 4.4.2 Analysis and Evaluation of Data Sets for a Given Vehicle Velocities Over Whole Set of Road Profiles

Chapter 4.4.1 showed that most data sets have a high internal correlation for their weights in the *w* values and their FIR filter representation. Comparing the different subchapters, it can be seen that most weight vectors/FIR filters look similar. Therefore, this chapter is presenting only two vehicle velocities (15 m/s and 30 m/s) over the whole set of profiles, i.e. E42 and E45.

#### 4.4.2.1 15 m/s

Figure 4-16 through Figure 4-18 and the text passage afterwards present the data set, analysis, and evaluation of a vehicle velocity of 15 m/s over all profiles (E42).

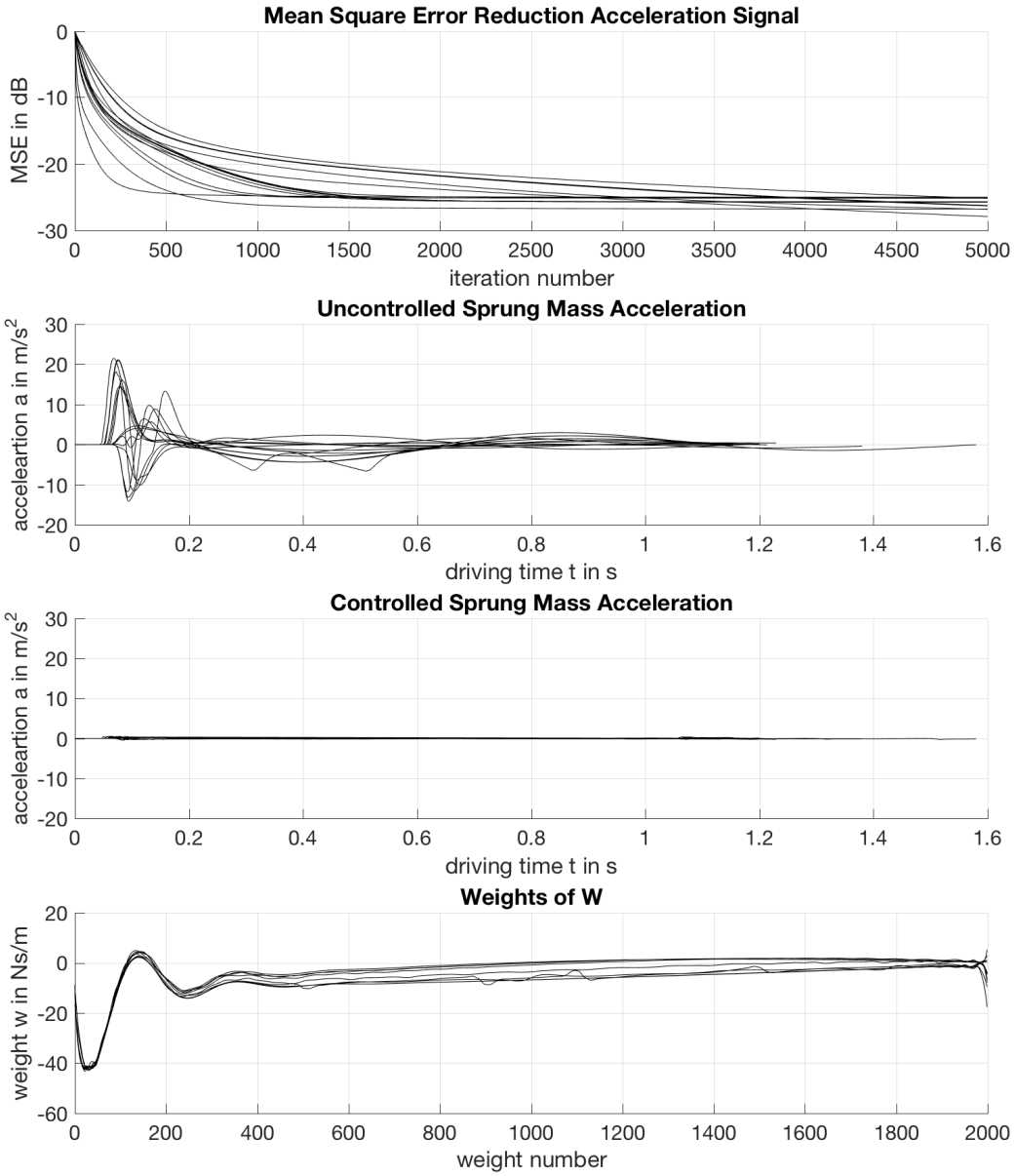


Figure 4-16: Overview Plot Vehicle Velocity 15 m/s Over Whole Set of Road Profiles (E42)

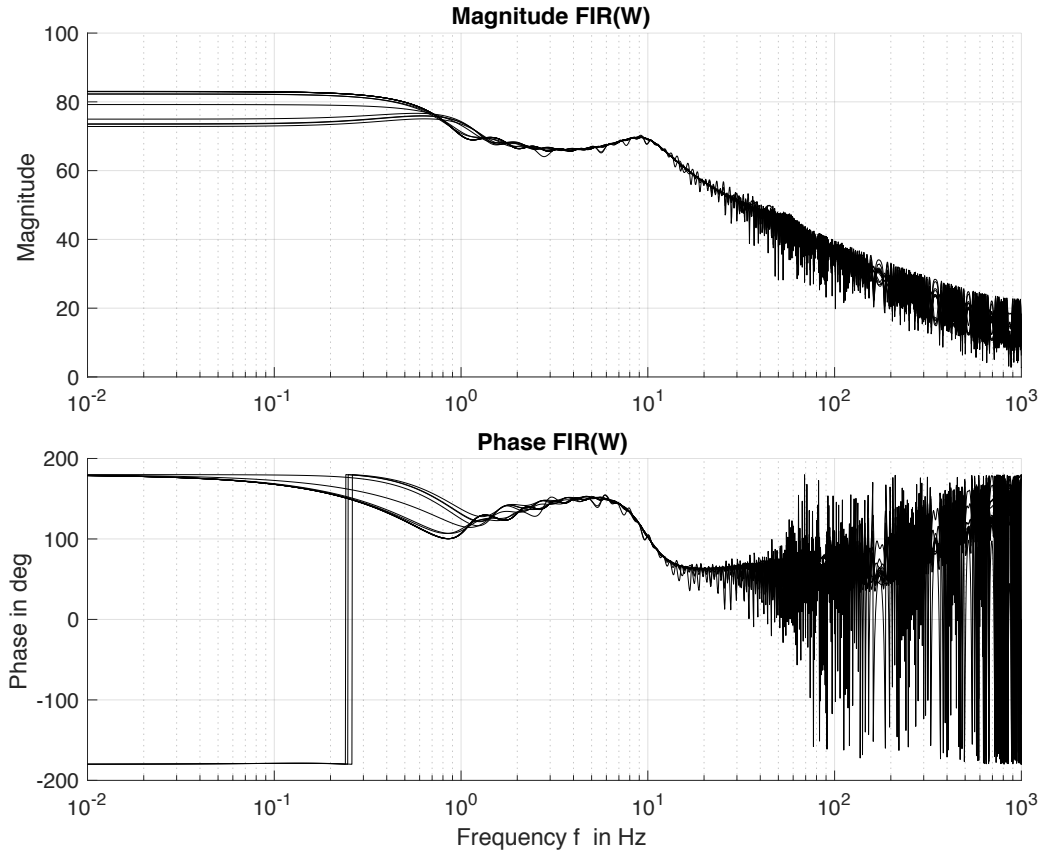


Figure 4-17: FIR Filter Plot Vehicle Velocity 15 m/s Over Whole Set of Road Profiles (E42)

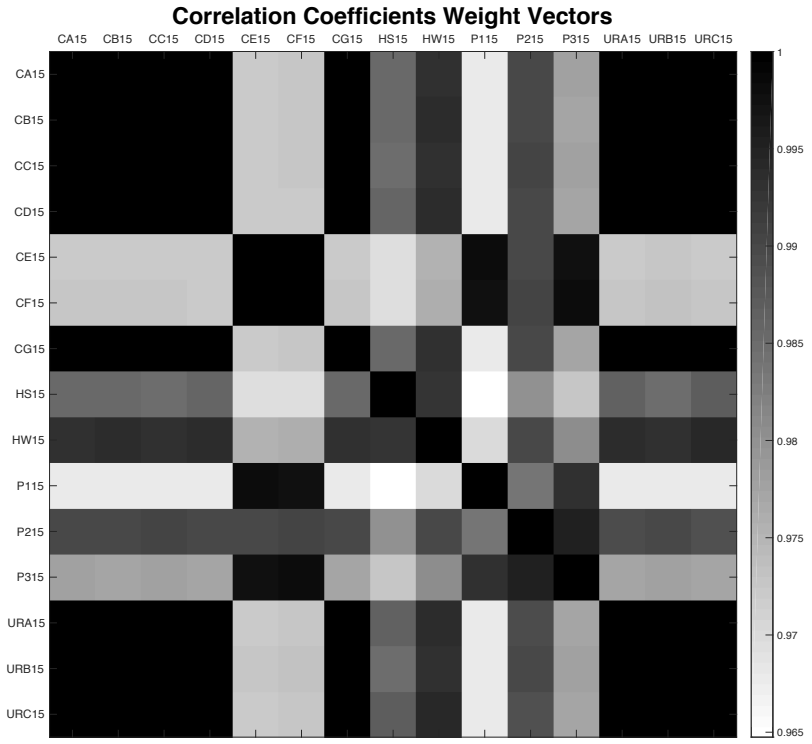


Figure 4-18: Correlation Coefficient Plot Vehicle Velocity 15 m/s Over Whole Set of Road Profiles (E42)

Each data set contained in the plots above has already been evaluated during chapter 4.4.1. Since all data sets have been proven to perform well concerning MSE and acceleration mitigation, these data sets do not have to be analyzed and evaluated again for their MSE signal and mitigation performance.

The more interesting and important part is the level of correlation between the different profiles. Both the weight vector plot in the overview plot as well as the Bode Diagram in the FIR Filter Plot show well-correlating signals. While the correlation in the weight plot is very high, the filter model does show some signals with deviation, especially in the low frequency range. However, the overall correlation is satisfying.

The Correlation Coefficients Plot states the same. As can be seen the correlation coefficients are very high, starting at around 0.965. The plot also shows the earlier explained subcategories in the road profiles very well. Edged and override curb profiles, as well as the uneven road profiles show internally high correlation because the road profiles are very similar.

#### 4.4.2.2 30 m/s

Figure 4-19 through Figure 4-21 and the text passage afterwards present the data set, analysis, and evaluation of a vehicle velocity of 30 m/s over all profiles (E45).

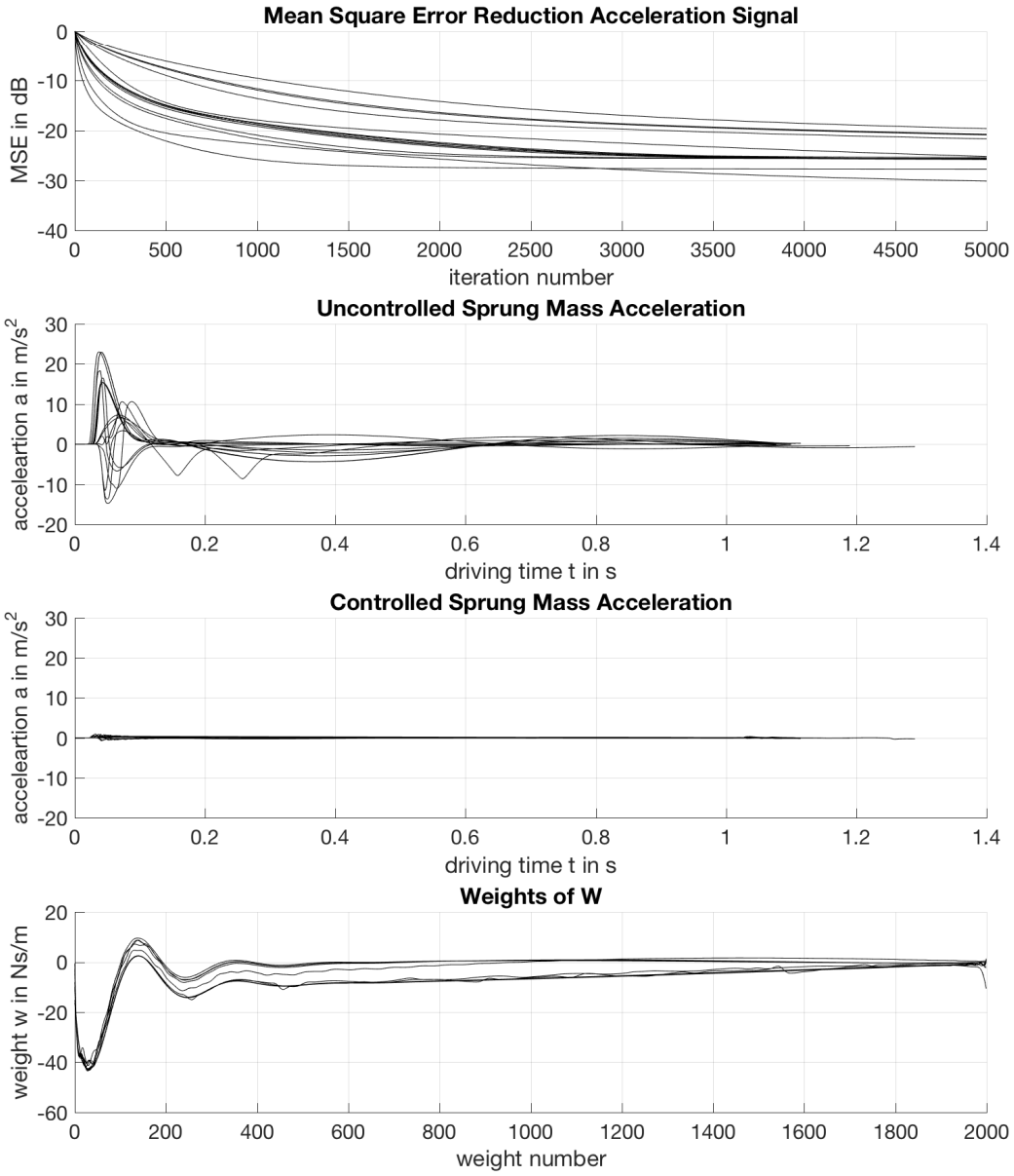


Figure 4-19: Overview Plot Vehicle Velocity 30 m/s Over Whole Set of Road Profiles (E45)

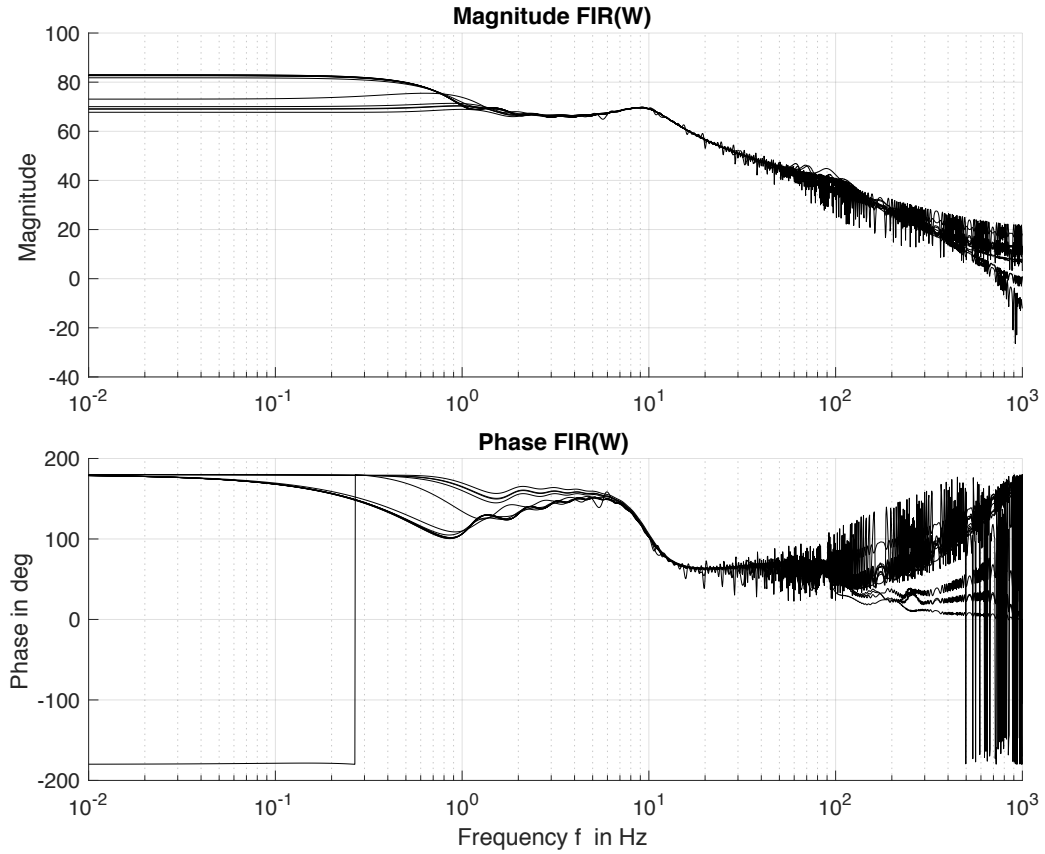


Figure 4-20: FIR Filter Plot Vehicle Velocity 30 m/s Over Whole Set of Road Profiles (E45)

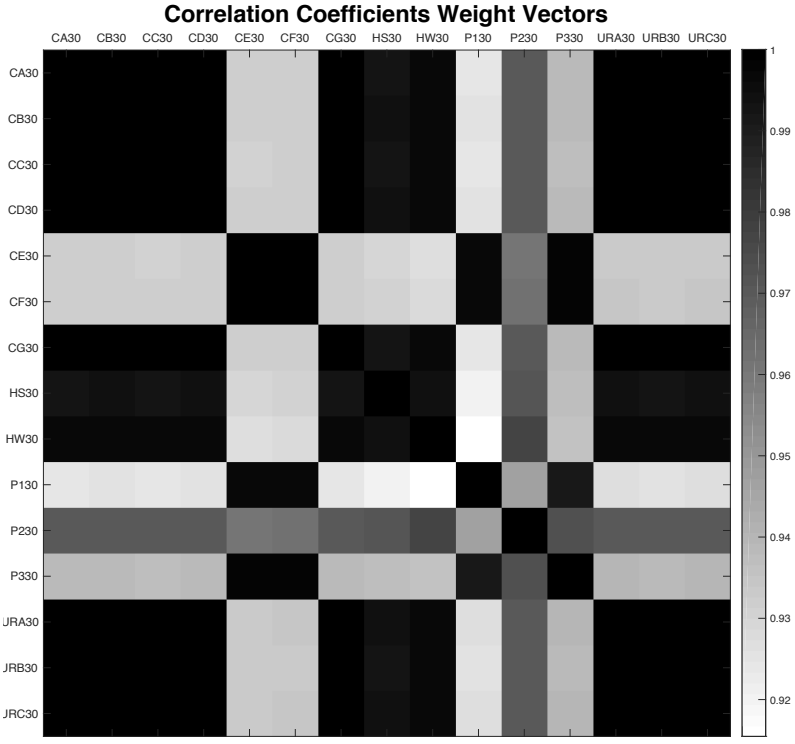


Figure 4-21: Correlation Coefficient Plot Vehicle Velocity 30 m/s Over Whole Set of Road Profiles (E45)

MSE and acceleration mitigation do not have to be evaluated again. Both the weight vector plot in the overview plot as well as the Bode Diagram in the FIR Filter Plot show well-correlated signals even though the correlation seems to be less than the one shown for 15 m/s. However, the overall correlation is satisfying.

The Correlation Coefficients Plot states the same result. As can be seen the correlations coefficients are very high, starting at around 0.915, which is less than 0.965 at 15 m/s. The plot also again shows the cluster representing each subcategory.

The lower correlation coefficients are most likely due to the higher vehicle velocity (30 m/s vs. 15 m/s). As Rao mentioned, the vehicle velocity is a very critical factor that does influence the system performance and the action required from the active suspension system.[167]

### 4.4.3 Summary and Conclusions of Overall Analysis and Evaluation of Data Sets

Chapter 4.4.1 and 4.4.2 proved the iFX-LMS algorithm performs well and finds solutions which mitigates the road excitations well. In addition, it shows a very high correlation in the weight signals of the given data. These results indicate that a universal filter model can be found in order to process the road profile input and generate a force profile signal. Recalling from chapter 2.2 outcome ❺ has occurred, which is very useful for future steps.

## 4.5 Universal Filter Model

Supported by outcomes of the evaluation and analysis process, the next step according to the introduced research methodology[168] is to derive a universal filter model. Ideally this model is as close as possible to the FIR Filter model of each data set and is able to use the road profile velocity input to generate a force profile input. This force profile should let the system behave and perform as well as the offline iFX-LMS solution. Depending on the accuracy of the filter model, the results could be slightly better or worse than the offline solution. However, it still needs to satisfy the mitigation expectations.

### 4.5.1 Empirical Universal Filter Model for W (EUFW)

The generated FIR Filter models proved to perform well and mitigate the road profiles. For each road profile a slightly different FIR Filter was generated by using the according weight vector *W*. In order to generate one empirical universal filter model which holds for all given road profiles, two different approaches are possible. First, by using a numerical tool like Matlab, and second by a manual filter analysis.

Before using Matlab, the weight vectors should be averaged in order to produce a more accurate signal. Afterwards a numerical tool like Matlab's built-in invfreqz function can be used. The built-in

[167] Cf. Rao, A. M.: A Structured Approach to Defining Active Suspension Requirements, 2016, p. 57.

[168] See chapter 2.2 Data Generation and Evaluation.

function called invfeqz is designed to "Identify discrete-time filter parameters from frequency response data"[169]. The function requires the FIR filter as an input and an estimation of the order of the numerator and denominator of the searched transfer-function.[170] Finally, a set of numerator and denominator values is provided which can be used to generate a transfer-function that represents the filter model.

The second approach requires good skills in reading and analyzing Bode Diagrams. From the given Bode Diagram of the FIR filter's zeros and poles for a new transfer-function representation can be estimated. These can be used afterwards in order to manually calculate the transfer-function representation of the filter.

Both approaches are not trivial and require a lot of skills in system identification. The current FIR filter has a numerator order of 4999 and a denominator order of 1, which is due to the FIR design. Even though both approaches can be carried out and will most likely lead to a reasonable solution, both are heavily time intensive. Considering the theoretical approach introduced in the next chapter, it is not reasonable to spend this amount of time.[171]

### 4.5.2 Theoretical Universal Filter Model for W (TUFW)

As mentioned above, an empirical universal filter model can be generated and used for a real-time application. At this point the research could be continued by designing the controller using an EUFW. However, since the outcome of the evaluation and analysis process was better than from what was expected, it is worthwhile to spend some more time considering and researching why this happened.

Earlier expectations considered a correlation between a given road profile over different vehicle velocities or between a given vehicle velocity over different road profiles to be likely. The better case, i.e. when both situations show correlation was not considered to be very likely. The process of examining the reason for this behavior is a rather chaotic and iterative process.

One of the first thoughts was that the found universal filter model is only valid for the specific vehicle and suspension set up. For example: Considering a change in the vehicle mass requires a change in the force profile as well. A higher mass needs a scaled-up version of the force profile, while a lower mass needs less force. However, using the above determined universal filter model and the same road profile input will always produce the same force profile. This means the vehicle mass has to have some kind of influence on the filter in order to produce a scaled-up or scaled-down version of the force profile. The same argument can be made for changing spring, shock absorber, or tire parameters.

The next determination was that the iFX-LMS algorithm converges to the same solution every time. As was shown in the chapters above all weights in the $W$ vector, or the shape of the FIR filter, correlate and look very similar. This finally means that if the algorithm's influence on the solution can be

169 Mathworks: Documentation invfeqz, 2017.

170 Cf. Mathworks: Documentation invfeqz, 2017.

171 See chapter 4.5.2 Theoretical Universal Filter Model for W (TUFW).

determined and a fixed version of it can be implemented into the system, then no iteration or adjustment processes are needed anymore. Figure 4-22 shows the block diagram of the overall system considering a non-active iFX-LMS algorithm and a fixed weight vector *W*.

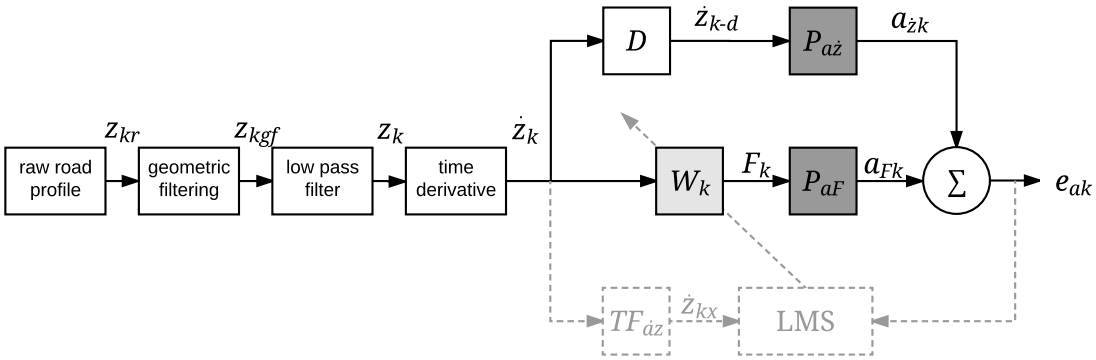


Figure 4-22: Block Diagram Quarter Car Model with Active Suspension System and Non-Active iFX-LMS Algorithm

The system equation for the controlled sprung mass acceleration, i.e. error signal, is as follows:

$$a = e = a_{\dot{z}k} + a_{Fk} = \dot{Z}_k D P_{a\dot{z}} + \dot{Z}_k W_k P_{aF} \qquad (4\text{-}1)$$

Here, *a* represents the controlled sprung mass acceleration. This is equal to the error signal $e_{ak}$, and is the sum from the sprung mass acceleration caused by the road profile excitation $a_{\dot{z}k}$ and the force generator excitation $a_{Fk}$. Considering a non-active iFX-LMS algorithm, meaning the weight vector/filter is constant and time independent with

$$W = W_k \qquad (4\text{-}2)$$

and taking the research and algorithm objective into account, a mitigated vertical vehicle acceleration

$$a = e_{ak} = 0 \qquad (4\text{-}3)$$

the final equation for *W* can be derived:

$$W = -\frac{D\, P_{a\dot{z}}}{P_{aF}} \qquad (4\text{-}4)$$

The plant models *P* can be replaced by using the system's transfer-functions derived in chapter 3.1:

$$W = -\frac{D\,TF_{a\dot{z}}}{P_{FG}TF_{aF}} \qquad (4\text{-}5)$$

In this equation $D$ is the delay due to the look ahead preview of the road surface scanner, and $P_{FG}$ is the transfer-function of the force generator/actuation system. The delay is a factor which will finally not change the general solution, it will only cause a shift in time. Also, as stated in earlier chapters the force generation is considered to work ideally for now. This means:

$$D = 1 \qquad (4\text{-}6)$$

$$P_{FG} = 1 \qquad (4\text{-}7)$$

Using all given information and assumptions, the following analytical equation can be found for *W*:

$$W = -\frac{TF_{a\dot{z}}}{TF_{aF}} \qquad (4\text{-}8)$$

Plugging ( 3-15 ) and ( 3-16 ) into ( 4-8 ), the following minimal realization of the system equation is calculated:

$$W = -\frac{(d_s d_t)s^2 + (d_s k_t + d_t k_s)s + (k_s k_t)}{(m_u)s^3 + (d_t)s^2 + (k_t)s} \qquad (4\text{-}9)$$

Using all known vehicle parameters from chapter 3.1:

$$W = -\frac{(5.511 \cdot 10^4)s^2 + (6.397 \cdot 10^6)s + (7.875 \cdot 10^7)}{s^3 + (36.74)s^2 + (3750)s} \qquad (4\text{-}10)$$

Figure 4-23 compares the TUFW (using ( 4-10 )) to the EUFW (curb A at 5 m/s).

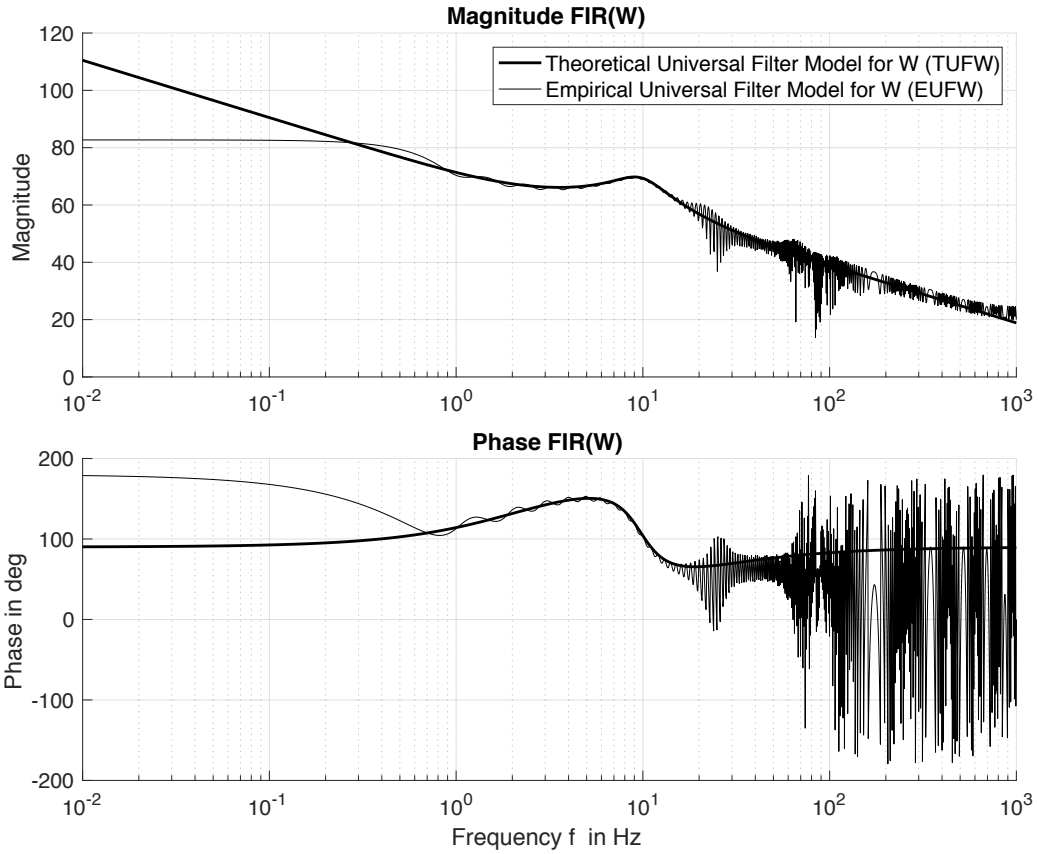


Figure 4-23: Filter Plot Theoretical vs. Empirical Universal Filter Model for W

As can be seen the theoretical filter is very similar to the empirical one. The differences/slopes in the low and high frequency range are due to two factors. First, the road profiles do not contain a lot of frequencies in this range, causing the algorithm to be inaccurate there. Secondly, the theoretical filter adjusts the system to be exactly zero over the whole time. This would cause issues in a real-time application while driving down- or up-hill. While driving downhill the system using the theoretical filter would try to generate more and more force in order to expand the gap between chassis and wheel to keep the vehicle on the same height level, which is of course not possible. Driving uphill the opposite would happen. Both cases are physically not realizable, since the gap can only expand and contract in a specific range due to hard stops, material, and component limits. This issue will be addressed in the controller design section of this research.

Concluding from the outcomes of this chapter, the finding of a theoretical and universal solution for replacing the filter model of W in a real-time application is very useful for further steps. First of all, this simplifies and reduces the complexity for the controller design process, because the same model can be used for all road profiles over all vehicle velocities. Secondly, the found solution is not an approximated or estimated solution but the ideal and analytical solution, meaning it most likely will perform even better than the iFX-LMS algorithm. Finally, having the option to calculate the filter instead of using empirical approximations will reduce the effort for a later real-time application. It

means that neither the simulation study using an iFX-LMS algorithm nor a real car need to drive several thousand times above one of the defined road profiles.

Expanding the area of interest, the ideal solution will most likely also work for disturbances other than the single events which are used and considered in this research project. The ideal solution will also work for long distance and low frequency profiles. However, it needs for be tuned of this application purpose because of the issues mentioned above.

# 5 Controller Design

Based on the outcomes of the data generation, evaluation, and analysis process the controller can be designed. The task description already listed and suggested several design options[172], which is why the first section below covers all available controller design options and outlines their advantages and disadvantages.[173] The following section then states the design choice made and determines the design objectives.[174] Next the control law is derived and tuned.[175] In preparation for the controller performance evaluation,[176] where the derived control law is applied to the whole set of road profiles, key controller evaluation parameters are derived and explained.[177]

First, some background information about this chapter and design process is given for clarification:

- This chapter designs a controller with the objective of mitigating the road excitation as best as possible, based on the assumptions, simplifications, and system design used by the iFX-LMS algorithm.[178] The next chapter will then adjust the derived control law in order to perform well in a real-time application in a real-world environment.[179]
- The following chapter will also introduce a novel approach by deriving a state-space realization which is able to take a displacement instead of velocity input.[180] Even though this will be implemented in the final controller design, this chapter does still consider a vertical velocity input. This way the ideal controller performance can be compared to the performance of the iFX-LMS algorithm, which is used as the base of the overall control law.

## 5.1 Controller Design Options

The correlation between all examined road profiles over the whole set of vehicle velocities and the found theoretical filter model is beneficial for the controller design process. Initially, it was expected to find only a few correlations depending on either the road profile or vehicle velocity. Therefore, it was intended for the initial controller design[181] to start with an open-loop non-adaptive gain scheduled controller which, depending on its performance, could then either be replaced or merged with a closed-loop adaptive controller. This approach would also require the implementation of a realistic force generator/actuation system model since a feedback signal is needed. These options and their

172 See Task Description in the introduction part of this Master's Thesis.

173 See chapter 5.1 Controller Design Options.

174 See chapter 5.2 Controller Design Choice and Design Objectives.

175 See chapter 5.3 Controller Design and Tuning.

176 See chapter 5.5 Controller Performance Evaluation.

177 See chapter 5.4 Controller Evaluation Parameters.

178 See chapter 3 Application Set Up and chapter 4 Data Generation and Evaluation.

179 See chapter 6 Real-Time Implementation.

180 See chapter 6.1.2 Road Displacement Input and Novel State Space Realization of the Quarter Car.

181 See Task Description in the introduction part of this Master's Thesis.

advantages and disadvantages are explained in more detail throughout this chapter. Due to the found correlations and TEFW, other simpler design options are explained as well.

### 5.1.1 Open-Loop Controller Design

A controller using an open-loop design does require preview information about the road profiles ahead of the vehicle and needs to preprocess them accordingly, as was already explained and done in the iFX-LMS algorithm. Otherwise the controller does not require any additional sensing hardware or software. Because this type of controller does not take any kind of feedback signal into account, it is necessary to know or estimate all possible vehicle excitations. Open-loop designed controllers generally have the advantage of being stable, quick, and compared to closed-loop controllers less expensive. Three open-loop design options are outlined below.

#### 5.1.1.1 Open-Loop Adaptive Controller Design

The iFX-LMS algorithm used in chapter 4 is mainly designed for offline processing. The used algorithm was tuned in order to produce a highly accurate solution, mostly by ignoring required processing time and resources. However, it is possible to tune and use an adjusted version of the algorithm for a real-time application. In order to do so, the input signal in a real-time application using an iFX-LMS algorithm must be divided and processed in segments, which would basically still be some sort of offline processing.

Advantages:

Chapter 4 already proved the iFX-LMS algorithm to be valid and showed it performed well. Due to the time spent tuning the algorithm in chapter 4, gathered experience can be used to tune the algorithm again for a time and resources-saving application. Using only this open-loop design without any additional feedback does not require the implementation of a realistic plant model of the force generator/actuation system, which also means the controller can be used regardless of the chosen hardware and its system behavior.

Disadvantages:

LMS filtering per se is not designed for a use in this kind of real-time application, especially the lengthy iterative algorithm. Segmenting the signal, adjusting each initial conditions, and a long distance scanning system, in order to give the LMS algorithm enough time to converge, makes the overall controlling process rather more complicated than necessary. Also, custom designed hardware in order to quickly run the LMS algorithm would be required.

Conclusion:

Overall this option is rather complex and expensive, and does not take advantage of the earlier found correlations and the TUFW. This option is only listed and discussed because of the previous work and for reasons of completeness.

#### 5.1.1.2 Open-Loop Non-Adaptive Gain Scheduled Controller Design

Using an open-loop non-adaptive gain scheduled control law is one of the recommended options from the task description.[182] It was suggested because of the expectation that each road profile or vehicle velocity needs a slightly different set of weights/filter model. Therefore, a mechanism which identifies either the appropriate road profile or vehicle velocity, and changes the weights/filter model accordingly would be necessary. The found weights/filter model from chapter 4 could have been used as the data base.

Advantages:

Implementing a linear combiner or filter model in a real-time application is a simple and less expensive option. Also, the needed processing time would be fairly quick and the required power low, even an analog implementation is possible. Chapter 4 proved the weight vectors and filter models to perform and mitigate the excitation due to the road profiles very well. The same performance would hold in a real-time application using the set of generated weights/filter models.

Disadvantages:

An additional road profile detection system would be necessary which also changes the controller behavior depending on the detected situation. This option would be more expensive, can mostly only be done digitally, and needs additional processing time.

Conclusion:

Having a theoretical universal filter model which works for all road profiles for all vehicle velocities makes this option superfluous. Instead of scanning the road, identifying the situation, and loading a set of weights/filter model, the theoretical universal filter model can just as well be used.[183] Using this filter model will be more accurate, meaning it will generate a better force profile and mitigate the disturbance better.

Besides that, this option would be a very great fit for the system if the correlation would not be valid over all road profiles and vehicle velocities simultaneously. It also does not require any adjustments due to the plant behavior of the force generator/actuation system.

[182] See Task Description in the introduction part of this Master's Thesis.

[183] See chapter 5.1.1.3 Optimal Force Control.

#### 5.1.1.3 Optimal Force Control

As the name indicates, this controller design references the found TUFW which generates the optimal force profile. This option is only available due to the fact that a theoretical and analytical correct solution was found and can be used instead of an approximated or manually designed filter model from the outcomes of the iFX-LMS algorithm. The design represents a more accurate and easier to implement version of the open-loop non-adaptive gain-scheduled design.

Advantages:

The theoretical filter model will generate a very accurate force profile and can mitigate the excitation very well because it was derived analytically for this purpose. The accuracy is only dependent on the quality of the input signals and known vehicle parameters. The filter model is implemented in a real-time application using either an analog or digital design. The given road profiles do not need to be identified or categorized, meaning it can directly feed into the preprocessor.

In addition, the filter is not only valid for the given road profiles, it basically holds for any given road profile, since it uses the optimal solution. As with the other open-loop systems designs, this controller design does not require any information of the plant behavior or the force generator/actuation system because feedback signals are not taken into account.

Disadvantages:

Additional tuning is necessary due to physical limitations in the low frequency range of the road signals.

Conclusion:

Having a theoretical universal filter model for $W$ which holds for all road profiles over every vehicle velocity makes this control law unique compared to the other designs and the preferred option due to its advantages.

*Additional note:* This design is a more accurate extension of the open-loop non-adaptive gain scheduled controller design, which was the anticipated preferred option from the initial task description.[184]

[184] See Task Description in the introduction part of this Master's Thesis.

### 5.1.2 Closed-Loop Controller Design

A closed–loop design was suggested as well in case an open-loop controller design is not accurate enough or needs additional support in form of a feedback signal. However, an open-loop controller design was and is the preferred option of this research project. Some closed-loop design options are covered in this section, because it was part of the initial task description.[185] However, with the found TUFW there is in reality no need for a closed-loop controller. Future research might consider adding a closed-loop control law in order to mitigate unexpected excitations from outside influences.

Generally, closed-loop controlling has some advantages compared to open-loop controlling, however, these are accompanied by several disadvantages and the high price of the required hardware and software.

**Advantages:**

A closed-loop controller design does not need any kind of preview information and controls any kind of excitation signal, either coming from the road or from the vehicle itself, by using measured feedback signals. Compared to open-loop, closed-loop does not need all the environmental information since it measures the system parameters on its own. The advantage of this is that also unexpected excitations can be handled and mitigated.

**Disadvantages:**

Because a closed-loop controller works with feedback signals, it requires more hardware in form of sensors which measure the system's states, making the system more expensive. The design process of such a controller can be very challenging and time intensive, often a trial and error approach is included in the overall tuning process. In addition, a closed-loop controller requires a realistic model of the force generator/actuation system plant while an open-loop controller does not. This also means that for each new system design the controller has to be tuned again.

All these listed disadvantages are on top of the general disadvantages of closed-loop controller designs: high price, need of additional hardware and software, risk of unstable behavior and longer processing time.

[185] See Task Description in the introduction part of this Master's Thesis.

#### 5.1.2.1 Closed-Loop Adaptive Controller Design

In the setup application an open-loop version of the LMS algorithm was implemented and used. Adaptive systems and the LMS algorithm can also be used in a closed-loop design. Therefore, such a design can be implemented in a real-time application as it was explained in chapter 5.1.1.1.

#### 5.1.2.2 Closed-Loop Merged Controller Design

Merging an open-loop and closed-loop controller design is an option in order to take advantage of the positive characteristics of both designs. For example, the open-loop optimal force controller can be merged with a closed-loop control law that takes care of all unknown excitation signals from the environment. In this way both the road excitation and all other unexpected excitations can be mitigated from both control laws simultaneously. However, this design requires much more research and experience in the performance of the open-loop optimal force controller behavior. Also, it requires a realistic force generator/actuation system model.

## 5.2 Controller Design Choice and Design Objectives

Chapter 5.1 discussed some of the possible controller design options and also covered each option's advantages and disadvantages. As it was already pointed out throughout the chapter, Optimal Force Control appears to be the most appropriate design choice considering the discoveries in chapter 4. Because of its design and implementation simplicity, Optimal Force Control is chosen and used in the further steps of this research project.

The design objective for the Optimal Force Controller design is the same as was given for the iFX-LMS algorithm: Mitigation excitation from the road profile in order to keep vertical vehicle acceleration as close as possible to a flat zero line. During the first design iteration the performance of the developed control law is also compared with the performance of the iFX-LMS approach. This way the control law is not only evaluated due to its performance, it will also be clear whether the control law behaves better or worse than the iFX-LMS algorithm.

## 5.3 Controller Design and Tuning

Figure 5-1 shows the block diagram of the overall quarter car model with an active suspension system, including the controller *C* and the force generator/actuation system *FG* of the active suspension system, which still has an ideal behavior of 1.

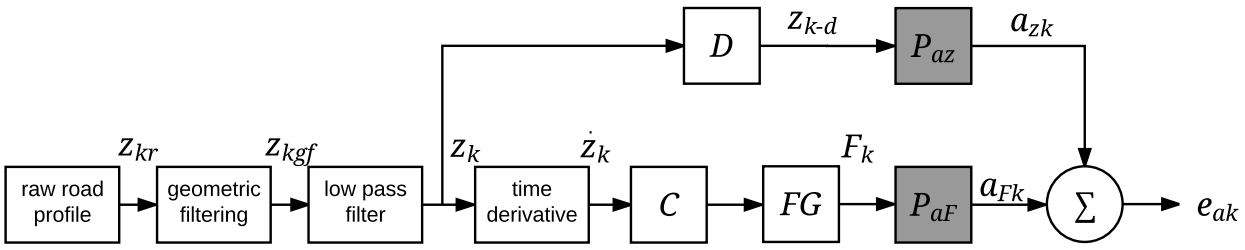


Figure 5-1: Block Diagram Quarter Car Model with Active Suspension System and Controller

Comparing this block diagram to earlier versions of itself which included either an active or non-active iFX-LMS algorithm, the control law for the controller *C* can be determined from the theoretical universal filter model of *W* derived in chapter 4.5.2.

Recalling from that chapter the general equation and its numerical realization for the used vehicle are:

$$W = -\frac{(d_s d_t)s^2 + (d_s k_t + d_t k_s)s + (k_s k_t)}{(m_u)s^3 + (d_t)s^2 + (k_t)s} \qquad (5\text{-}1)$$

$$W = -\frac{(5.511 \cdot 10^4)s^2 + (6.397 \cdot 10^6)s + (7.875 \cdot 10^7)}{s^3 + (36.74)s^2 + (3750)s} \qquad (5\text{-}2)$$

Figure 5-2 shows the pole-zero map of this controller setup. As can be seen in the figure, and indicated from the system equation, the controller *C* using *W* has two real and negative zeroes and three poles, one at zero and a pair of complex conjugate poles in the left half plane. Therefore, the system is stable.

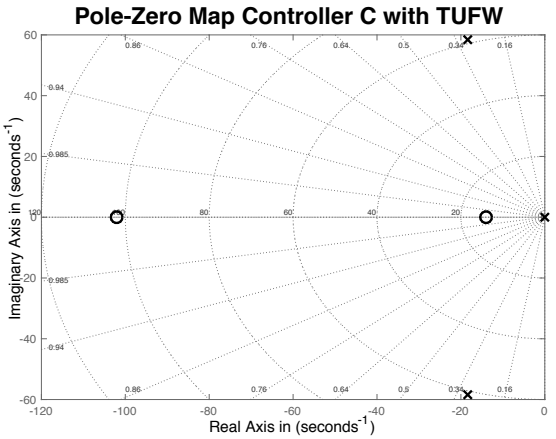


Figure 5-2: Pole-Zero Map Controller *C* with TUFW

In the upper path in Figure 5-1 the plant model which is used to process the vertical velocity profile in order to calculate the uncontrolled sprung mass acceleration now uses road profile signal with displacement instead. This change is made because it is not necessary to use a velocity input anymore since the iFX-LMS algorithm is not used. This representation displays the situation as it is in the real world. It does not influence the controller performance.

For the current setup the controller does not require any further tuning. In chapter 4.5.2 the theoretical filter $W$ was analytically derived in order to reduce the effective acceleration error to a flat zero line. While the delay and force generator/actuation system are still held ideally at 1, the performance of the controller only depends on the accuracy and quality of its input signal. Since it is an open-loop design and no feedback is required from the controller, no realistic plant model of the force generator/auction system is required in order to tune the controller.

## 5.4 Controller Evaluation Parameters

The iFX-LMS algorithm was tuned in order to generate a force profile which causes an inverse acceleration signal of the uncontrolled acceleration due to the road excitation. This way the iFX-LMS approach mitigated the road excitation. Design of the Optimal Force Controller has the same objective. The extracted force profile should be as close as possible to the ideal solution, which is also very close to the solution from the iFX-LMS algorithm. The accuracy of the Optimal Force Controller approach does not only depend on its design, it also depends on the accuracy of the input signal, meaning discretization of the road profile, preprocessing, and sample frequency.

To evaluate the controller's general performance and to compare it to the iFX-LMS algorithm, four evaluation parameters are determined and further explained.

### 5.4.1 Force Profile

The shape of the generated force profile should be similar to the one generated from the iFX-LMS algorithm. Both signals are compared and their correlation is evaluated. It must be noted that small deviations in the shape do not necessarily mean worse behavior of the controller. Since the controller uses an analytical solution it is possible for it to generate a better fitting solution.

While in addition to a visual comparison the correlation coefficient could also be calculated and checked, it seems reasonable enough to simply compare the shape for both signals visually, since a theoretical solution is used.

Also the maximum required force from the force generator/actuation system is determined during the evaluation process. It gives a first glance on the specification and requirements for a possible hardware design.

### 5.4.2 Uncontrolled vs. Controlled Acceleration

A deviation in the force signal would cause the vehicle to mitigate road disturbances differently, either better or worse. In order to make sure the Optimal Force Control law does perform well, the controlled acceleration signal of the sprung mass is compared to the uncontrolled acceleration. The controlled acceleration signal should be as close as possible to zero, however, due to discretization and digital sampling small deviations can exist and are acceptable.

### 5.4.3 Maximum Vertical Sprung Mass Acceleration

Vertical sprung mass acceleration was used throughout this research as an indicator of the mitigation performance. Even though this is still valid for this evaluation, one key parameter is the maximum vertical acceleration of the sprung mass. Since this parameter has a large impact on the behavior of the vehicle operator and its ability to steer the vehicle, the reduction of the maximum vertical sprung mass acceleration is considered as a performance parameter as well.

In addition, "Grenzwertliste 2015" from the German statutory accident insurance rates any vertical acceleration above 0.45 $m/s^2$ as potentially harmful and any vertical acceleration above 0.8 $m/s^2$ as highly potentially harmful to the health of the human body, i.e. the vehicle operator[186]. Therefore, it is evaluated whether or not the controlled sprung mass acceleration violates these limits. However, it must be kept in mind that the maximum vertical acceleration is mainly determined from the road excitation. If the road profile is too sharp and abrupt, the controller will most likely not be able to fully mitigate the excitation and reduce the maximum vertical acceleration underneath both mentioned limits.

### 5.4.4 Energy Reduction

Using the Parseval's Theorem the total energy of a signal can be calculated.[187] In order to give an estimation about how well the controller works, the amount of energy reduction in the controlled vehicle acceleration signal is compared to the uncontrolled signal. The higher the energy reduction, the better the controller, and the lighter the total impact of the road disturbance on the vehicle operator.

Until now there was no estimation made about the signal energy. It is also not known how high the energy reduction will be or what value is expected for a properly working system. From the results shown in chapter 3 a reduction above 90% seems reasonable for a proper system design.

The calculated value has an informative character and should provide an impression of the controller's performance.

[186] Cf. ot. DGUV Deutsche Gesetzliche Unfallversicherung: Grenzwertliste 2015, 2015, pp. 152-160.

[187] Cf. ot. Hochschule Karlsruhe Technik und Wirtschaft: Systemtheorie Online – Parsevalsche Gleichung, 2017.

## 5.5 Controller Performance Evaluation

The evaluation process is performed for all road profiles as well over the whole set of vehicle velocities according to the same operational test plan. All evaluation parameters show the controller performed well, and similar performance is seen throughout, therefore only a subset is shown in this chapter.

In order to present the results in a clean and easily readable way, a table for each presented data set is created. An example table is shown in Table 5-1. Additional comments are only provided if the data sets show anomalies.

Table 5-1: Example Controller Evaluation Table

| **Evaluation Parameter** | **Value/Score** | | | | |
|---|---|---|---|---|---|
| General shape of force profile | score 1-3, comment | | | | |
| Force profile correlation | score 1-3, comment | | | | |
| Mitigation performance | score 1-3, comment | | | | |
| | uncontrolled | controlled | con. reduction | iFX-LMS | iFX reduction |
| Maximum force requirement | | *F1* N | | *F2* N | |
| Maximum vertical acceleration | *a* $m/s^2$ | *b* $m/s^2$ | *b/a* % | *c* $m/s^2$ | *c/a* % |
| Holds acceleration limit? | | | | | |
| Energy of Acceleration Signal | *x* $m^2/s^4$ | *y* $m^2/s^4$ | *y/x* % | *z* $m^2/s^4$ | *z/x* % |
| Overall controller performance | score 1-3, comment | | | | |

### 5.5.1 Curbs

Figure 5-3 through Figure 5-5 and Table 5-2 through Table 5-4 evaluate the controller performance for three curb profiles using the designed controller C.

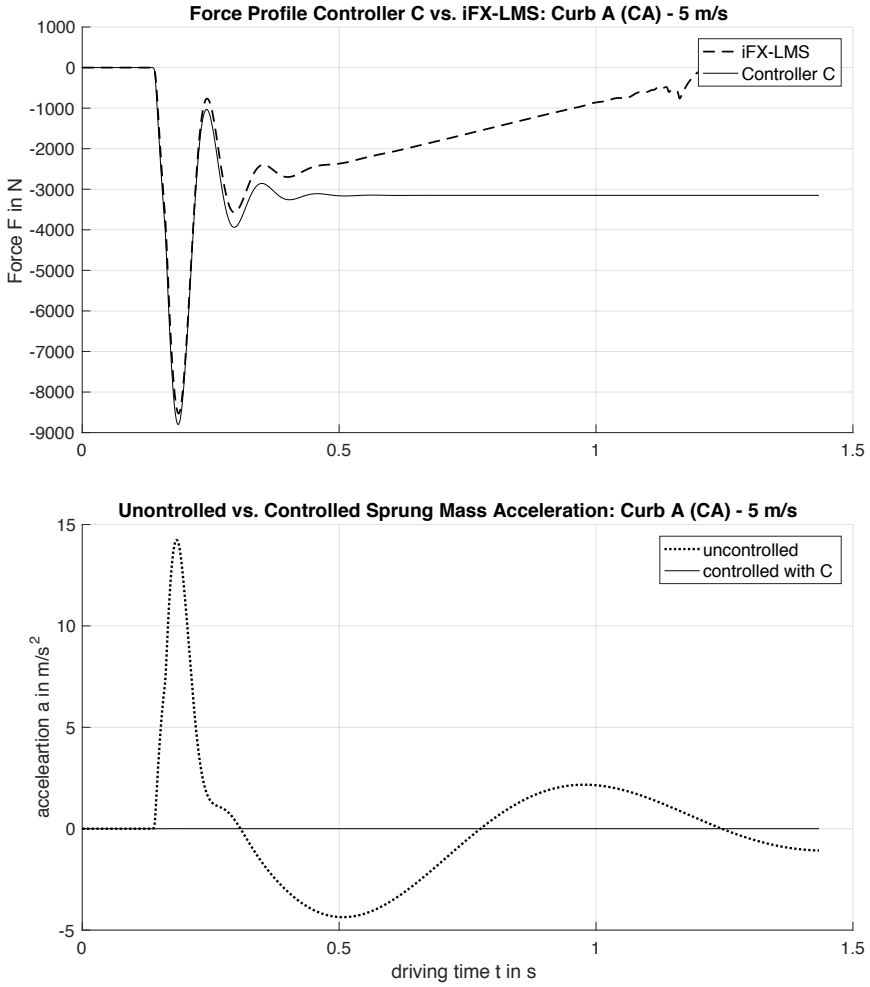


Figure 5-3: Controller Evaluation Plot Curb A (CA) at 5 m/s (#1)

Table 5-2: Controller Evaluation Table Curb A (CA) at 5 m/s (#1)

| **Evaluation Parameter** | **Value/Score** | | | | |
|---|---|---|---|---|---|
| General shape of force profile | 2, deviation at the end due to road offset at profile end | | | | |
| Force profile correlation | 2.5, deviation at the end due to road offset at profile end | | | | |
| Mitigation performance | 3 | | | | |
| | uncontrolled | controlled | con. reduction | iFX-LMS | iFX reduction |
| Maximum force requirement | | 8.8 kN | | 8.53 kN | |
| Maximum vertical acceleration | 14.2 $m/s^2$ | 0.0018 $m/s^2$ | 99.99 % | 0.5339 $m/s^2$ | 96.25 % |
| Holds acceleration limit? | | yes | | no >0.45 $m/s^2$ | |
| Energy of Acceleration Signal | $2.77 \cdot 10^4$ $m^2/s^4$ | $7.4 \cdot 10^{-4}$ $m^2/s^4$ | 99.99 % | 180.5 $m^2/s^4$ | 99.35 % |
| Overall controller performance | 2.5 | | | | |

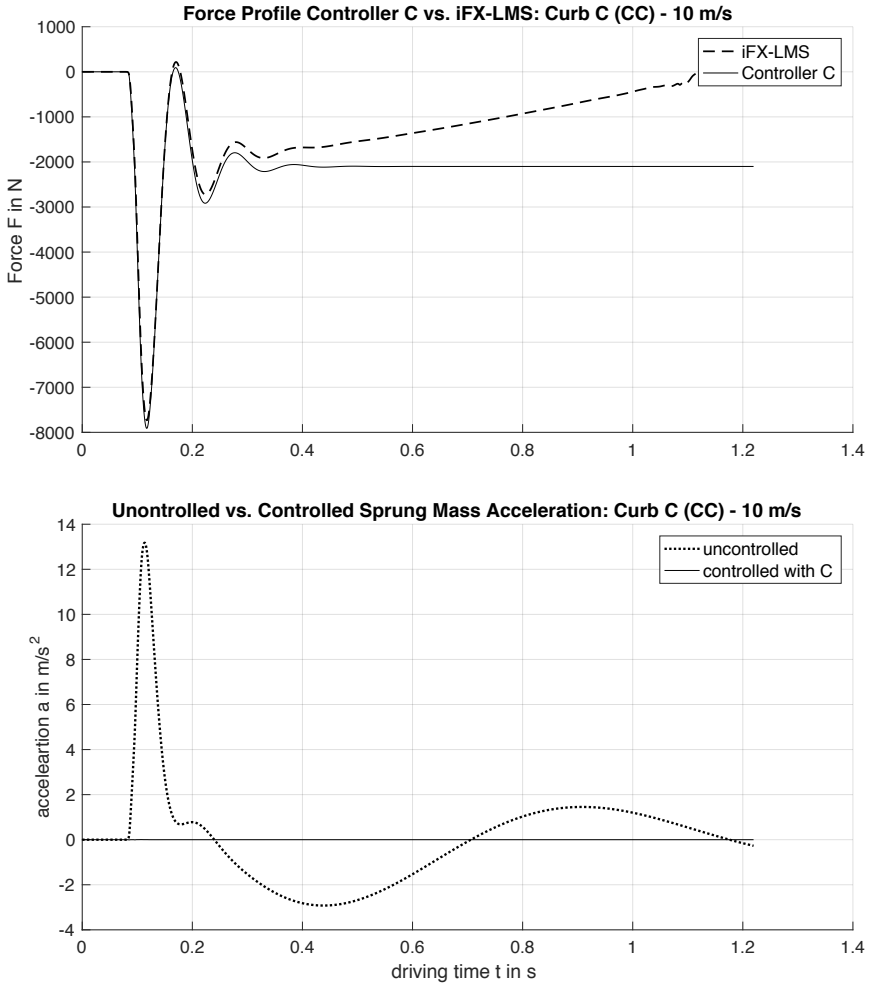


Figure 5-4: Controller Evaluation Plot Curb C (CC) at 10 m/s (#14)

Table 5-3: Controller Evaluation Table Curb C (CC) at 10 m/s (#14)

| **Evaluation Parameter** | **Value/Score** | | | | |
|---|---|---|---|---|---|
| General shape of force profile | 2, deviation at the end due to road offset at profile end | | | | |
| Force profile correlation | 2.5, deviation at the end due to road offset at profile end | | | | |
| Mitigation performance | 3 | | | | |
| | uncontrolled | controlled | con. reduction | iFX-LMS | iFX reduction |
| Maximum force requirement | | 7.91 kN | | 7.73 kN | |
| Maximum vertical acceleration | 13.18 $m/s^2$ | 0.0043 $m/s^2$ | 99.97 % | 0.2842 $m/s^2$ | 97.84 % |
| Holds acceleration limit? | | yes | | yes | |
| Energy of Acceleration Signal | $1.45 \cdot 10^4$ $m^2/s^4$ | $8 \cdot 10^{-4}$ $m^2/s^4$ | 99.99 % | 42.76 $m^2/s^4$ | 99.71 % |
| Overall controller performance | 2.5 | | | | |

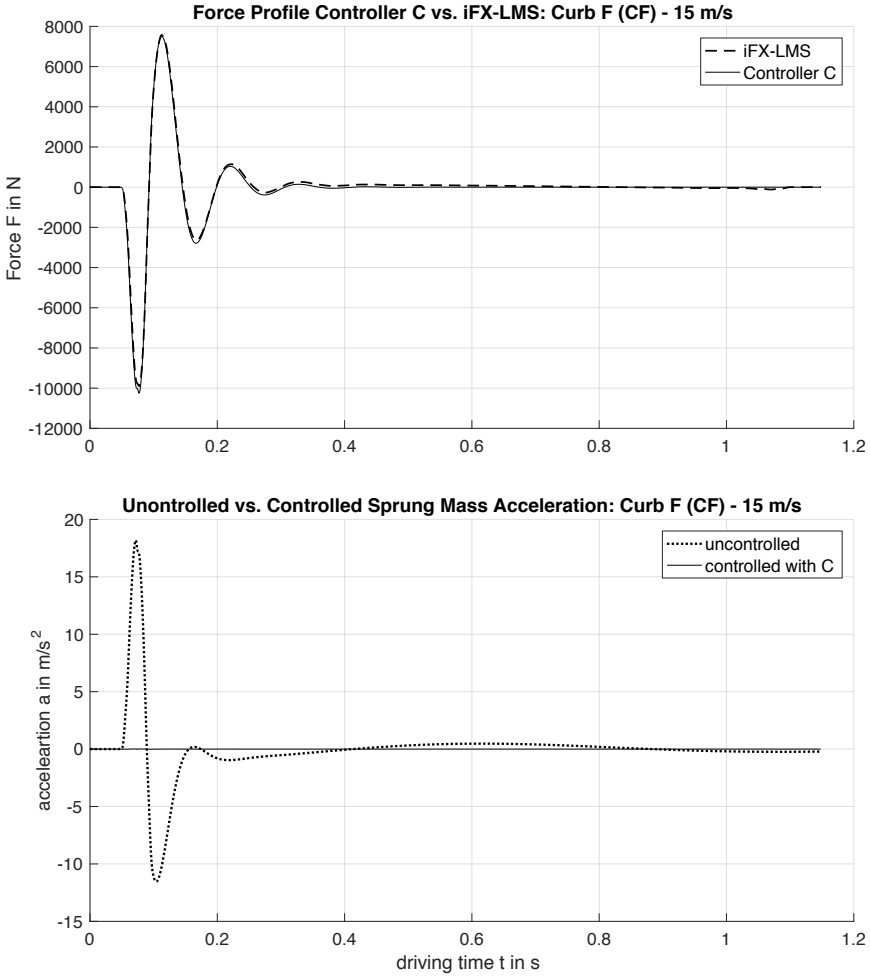


Figure 5-5: Controller Evaluation Plot Curb F (CF) at 15 m/s (#33)

Table 5-4: Controller Evaluation Table Curb F (CF) at 15 m/s (#33)

| **Evaluation Parameter** | **Value/Score** | | | | |
|---|---|---|---|---|---|
| General shape of force profile | 3 | | | | |
| Force profile correlation | 3 | | | | |
| Mitigation performance | 3 | | | | |
| | uncontrolled | controlled | con. reduction | iFX-LMS | iFX reduction |
| Maximum force requirement | | 10.25 kN | | 9.9 kN | |
| Maximum vertical acceleration | 18.19 $m/s^2$ | 0.0189 $m/s^2$ | 99.90 % | 0.5326 $m/s^2$ | 97.07 % |
| Holds acceleration limit? | | yes | | no >0.45 $m/s^2$ | |
| Energy of Acceleration Signal | $1.85 \cdot 10^4$ $m^2/s^4$ | 0.011 $m^2/s^4$ | 99.99 % | 43.28 $m^2/s^4$ | 99.77 % |
| Overall controller performance | 3 | | | | |

### 5.5.2 Pothole

Figure 5-6 and Table 5-5 evaluate the controller performance for pothole 2 at a vehicle velocity of 20 m/s using the designed controller C.

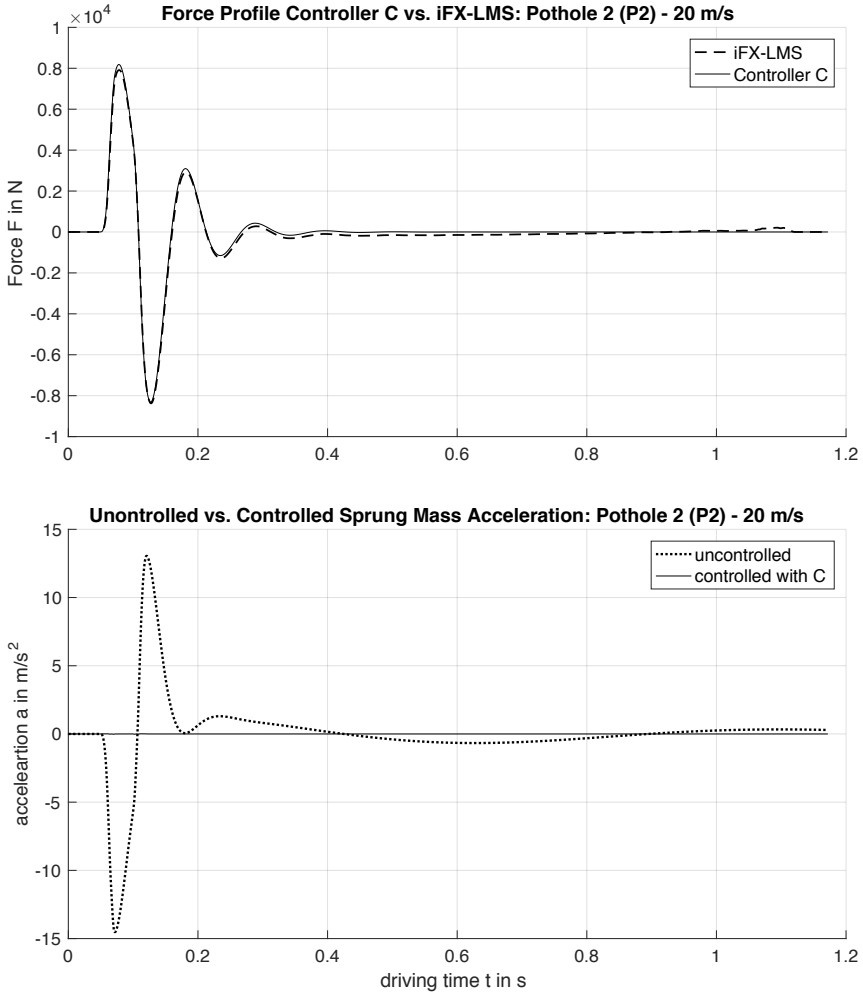


Figure 5-6: Controller Evaluation Plot Pothole 2 (P2) at 20 m/s (#52)

Table 5-5: Controller Evaluation Table Pothole 2 (P2) at 20 m/s (#52)

| **Evaluation Parameter** | **Value/Score** | | | | |
|---|---|---|---|---|---|
| General shape of force profile | 3 | | | | |
| Force profile correlation | 3 | | | | |
| Mitigation performance | 3 | | | | |
| | uncontrolled | controlled | con. reduction | iFX-LMS | iFX reduction |
| Maximum force requirement | | 8.31 kN | | 8.37 kN | |
| Maximum vertical acceleration | 13. 05 $m/s^2$ | 0.0123 $m/s^2$ | 99.91 % | 0.1576 $m/s^2$ | 98.79 % |
| Holds acceleration limit? | | yes | | yes | |
| Energy of Acceleration Signal | $1.86 \cdot 10^4$ $m^2/s^4$ | 0.0064 $m^2/s^4$ | 99.9 % | 0.1576 $m^2/s^4$ | 98.76 % |
| Overall controller performance | 3 | | | | |

### 5.5.3 Speed Hump

Figure 5-7and Table 5-6 evaluate the controller performance for the Watts Profile Hump at a vehicle velocity of 25 m/s using the designed controller C.

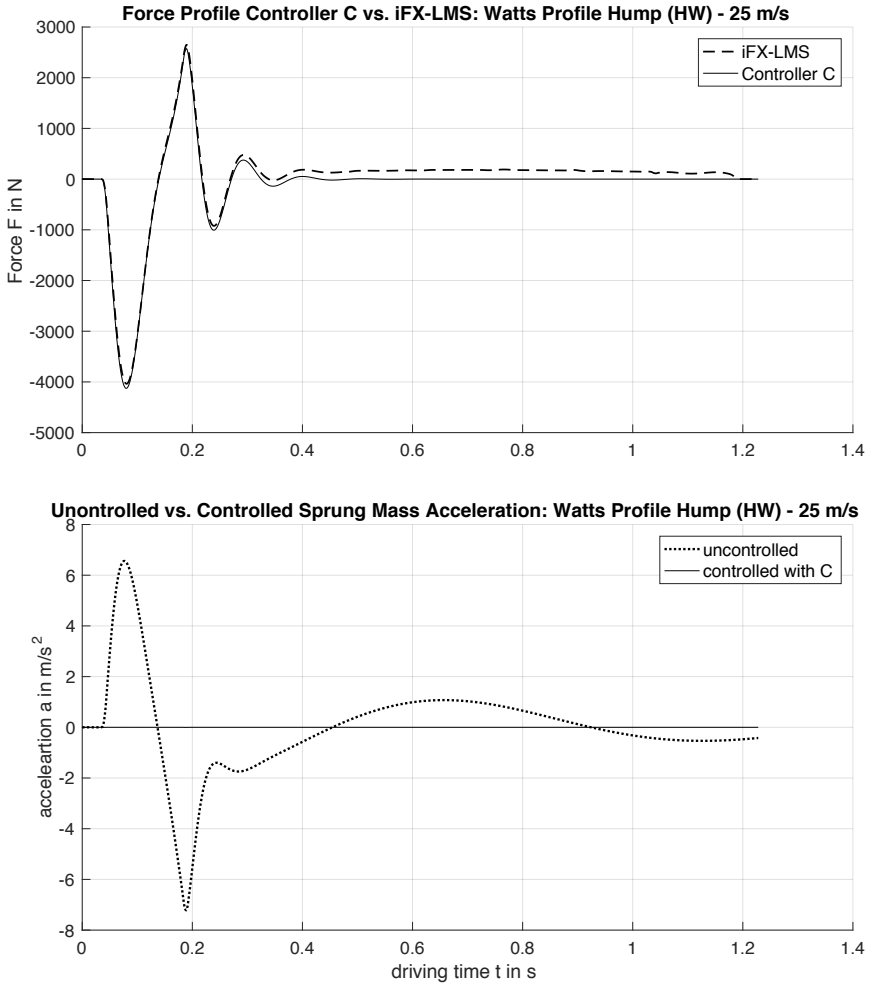


Figure 5-7: Controller Evaluation Plot Watts Profile Hump (HW) at 25 m/s (#71)

Table 5-6: Controller Evaluation Table Watts Profile Hump (HW) at 25 m/s (#71)

| **Evaluation Parameter** | **Value/Score** | | | | |
|---|---|---|---|---|---|
| General shape of force profile | 3 | | | | |
| Force profile correlation | 3 | | | | |
| Mitigation performance | 3 | | | | |
| | uncontrolled | controlled | con. reduction | iFX-LMS | iFX reduction |
| Maximum force requirement | | 4.13 kN | | 4.04 kN | |
| Maximum vertical acceleration | 6.56 $m/s^2$ | 0.0006 $m/s^2$ | 99.99 % | 0.1463 $m/s^2$ | 97.77 % |
| Holds acceleration limit? | | yes | | yes | |
| Energy of Acceleration Signal | $8.7 \cdot 10^3$ $m^2/s^4$ | $2.1 \cdot 10^{-4}$ $m^2/s^4$ | 99.99 % | 9.5 $m^2/s^4$ | 99.89 % |
| Overall controller performance | 3 | | | | |

### 5.5.4 Uneven Road

Figure 5-8 and Table 5-7 evaluate the controller performance for the uneven road Profile A at a vehicle velocity of 30 m/s using the designed controller C.

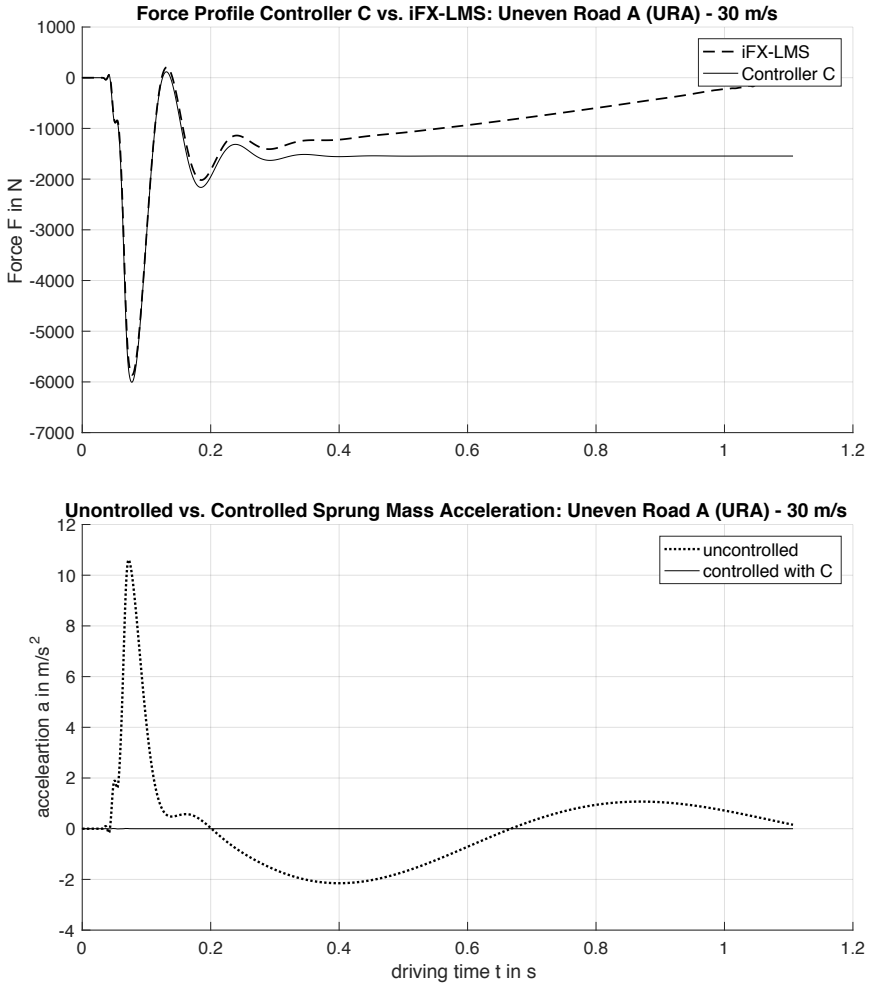


Figure 5-8: Controller Evaluation Plot Uneven Road A (URA) at 30 m/s (#78)

Table 5-7: Controller Evaluation Table Uneven Road A (URA) at 30 m/s (#78)

| **Evaluation Parameter** | **Value/Score** | | | | |
|---|---|---|---|---|---|
| General shape of force profile | 2, deviation at the end due to road offset at profile end | | | | |
| Force profile correlation | 2.5, deviation at the end due to road offset at profile end | | | | |
| Mitigation performance | 3 | | | | |
| | uncontrolled | controlled | con. reduction | iFX-LMS | iFX reduction |
| Maximum force requirement | | 6 kN | | 5.86 kN | |
| Maximum vertical acceleration | 10.6 $m/s^2$ | 0.0098 $m/s^2$ | 99.91 % | 0.2326 $m/s^2$ | 97.81 % |
| Holds acceleration limit? | | yes | | yes | |
| Energy of Acceleration Signal | $8.2 \cdot 10^3$ $m^2/s^4$ | 0.0022 $m^2/s^4$ | 99.99 % | 22.7 $m^2/s^4$ | 99.72 % |
| Overall controller performance | 3 | | | | |

### 5.5.5 Conclusion

As can be seen in these six sample evaluations the controller performs well. While the iFX-LMS algorithm violated the given maximum acceleration limit twice, the control law did not violate it a single time. In general the control law performed better than the iFX-LMS algorithm.

It stands out that in three of these six examples the controller generated a force profile which is quite different from the iFX-LMS algorithm at the end of the driving time. This is due to the earlier explained low frequency offset. Since the controller uses the analytical and theoretical solution it forces the sprung mass acceleration to be zero the whole time, even when driving up- or downhill. This issue will be addressed in the next chapter.

The controller performs very well, as was expected. The control law will not be changed and needs no additional adjustment in this chapter. Therefore, it is ready to be adjusted in the next chapter in order to work in a real-time and real-world application.

# 6 Real-Time Implementation

Throughout this Master's Thesis a control law was designed in order to mitigate the impact of single event disturbances by reducing the sprung mass's (vehicle chassis) vertical acceleration. Therefore, most of the surrounding components (hardware and software) were ignored and assumed to work ideally by simplifying their behavior. However, the research objective is to develop a controller that works in a real-time environment. In order to address this objective, this chapter outlines and talks about the surrounding components and adjusts the control law according to their real-time behavior.

First, road surfaces are discussed.[188] Here the required hardware for road surface scans is introduced[189] and afterwards the control law is adjusted accordingly. Additionally, a novel state space realization of the quarter car model is derived and introduced.[190] Next, the characteristics of sampled road data are discussed.[191] These characteristics require road preprocessing, as was shown in chapter 3.3, which is why the implementation of a real-time preprocessor is outlined.[192] However, the control law still needs to be adjusted in order to handle low frequency road profile characteristics.[193] Lastly, this chapter discusses the force generator/actuation system.[194] Here, system requirements[195] and an appropriate sub control strategy are outlined.[196] In the end, the impacts of the adjustments are shown by comparing the ideal version of the control law with the adjusted one.[197]

## 6.1 Road Surface

### 6.1.1 Road Surface Scanner

The chosen Optimal Force Controller design works, as was explained, like an open-loop controller. Therefore, it requires preview information about the road surface in front of the vehicle in order to generate an appropriate force profile which mitigates the upcoming road excitation. Thus, a road surface scanner is needed. While the scanning system per se is not part of this research project, some of the key specifications required to aid a properly working controller are outlined.

Resolution and accuracy in depth and width of the scanning system directly influence the overall mitigation performance of the active suspension system. This is due to the fact that the force profile is directly extracted from the road profile, meaning a poorly scanned road profile signal will lead to a poor force signal, impacting the mitigation performance. Further research is required to specify

188 See chapter 6.1 Road .

189 See chapter 6.1.1 Road Surface Scanner.

190 See chapter 6.1.2 Road Displacement Input and Novel State Space Realization of the Quarter Car.

191 See chapter 6.2 Road Characteristics.

192 See chapter 6.2.1 Real-Time Road Preprocessor.

193 See chapter 6.2.2 Low Frequency Signals.

194 See chapter 6.3 Force Generator/Actuation System.

195 See chapter 6.3.1 Force Generator System Requirements.

196 See chapter 6.3.2 Force Generator Control Strategy.

197 See chapter 6.4 Controller Design.

numeric values for the resolution and accuracy of the scanning system by also including the interlink with resolution requirements for the geometric filter. However, even with a poor road profile signal the system will still work with restricted performance.

A more critical design requirement of the scanning system is the total length of the preview distance. Taking the vehicle velocity into consideration, this distance will set the minimum time delay between a point on the road when it was first seen and when it actually reaches the vehicle. In order to provide enough time for the road preprocessor, controller, and force generator/actuation system to react properly to the road disturbance the distance needs to be scanned far enough ahead of the vehicle. If the preview distance is too short the applied force to the suspension system will occur too late because the vehicle will pass the disturbance point in the road before the suspension system can react. The minimum length of required preview information depends on the vehicle speed and processing time of the other components. While the controller, which can be implemented in analog, will mostly likely be very fast in extracting a force profile, the road preprocessor might need the most time to perform all required steps.

However, a properly working real-time road surface scanning system is estimated to be very likely designable and manufacturable. A lot of research in road surface scanning was conducted in the past and especially lately, due to a lot of interest in autonomous driving systems which also need information about their surrounding and the road surface. Scanning systems using cameras ("Road Surface Scan" from Mercedes Benz uses stereo cameras[198]), laser based systems[199], and systems based on LIDAR[200] have all proven to be valid. Especially due to developments in autonomous driving vehicle, an increasing number of detecting and scanning systems are being implemented into vehicles, which then possibly could be used some day to scan the road surface and deliver the needed information.

### 6.1.2 Road Displacement Input and Novel State Space Realization of the Quarter Car

In chapter 3.1 a quarter car model was derived in order to represent the behavior of a passenger vehicle and to be used for the filtered-X version of the LMS algorithm. As was explained, tire damping is a factor not to be neglected, even though it causes problems and difficulties when deriving a state-space realization of the quarter car model. Because of that, previous research at PERL VT determined to use and input vertical velocities instead of vertical displacement signals into an iFX-LMS algorithm. The same procedure was continued during this research project in order to stay consistent for the overall research project and to compare results. Therefore, the designed control law requires a vertical velocity signal as well.

However, a road scanning system or data coming from different sensors in the vehicle will most likely deliver a map/signal corresponding to vertical displacement. Taking the first order time derivative by

198 Cf. ot. Mercedes-Benz Techcenter: Magic Body Control, 2017.

199 See Lopes, G., Ribeiro, A. F., Sillero, N., Gonçalves-Seco, L., Silva, C., Franch, M., and Trigueiros, P.: High Resolution Trichromatic Road Surface Scanning with a Line Scan Camera and Light Emitting Diode Lighting for Road-Kill Detection, 2016.

200 Cf. Fernández, C., Gavilán, M., Llorca, D. F., Parra, I., Quintero, R., Lorente, A. G., Vlacic, Lj., and Sotelo, M. A.: Free Space and Speed Humps Detection using Lidar and Vision for Urban Autonomous Navigation, 2012.

using either an analog filter or a digital converter is one way to handle this difference, but it might not be the best way since these operations can cause inaccuracies.

Therefore, an alternative method is shown, which addresses this issue and also derives a novel state space realization which represents the same quarter car model but requires only a displacement input.

Figure 6-1 shows the same block diagram as Figure 5-1 but without the time derivative block and with a control law *C**, an adjusted version of the original control law *C*.

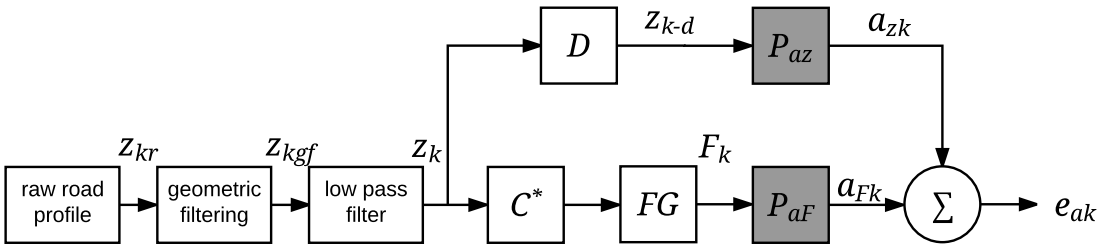


Figure 6-1: Block Diagram Quarter Car Model with Active Suspension System and Controller without Time Derivative

Carrying out the same derivation steps as shown in chapter 4.5.2, the total vertical acceleration of the sprung mass is given by:

$$a = \varepsilon_{ak} = a_{zk} + a_{Fk} = Z_k D P_{az} + Z_k W_k^* P_{aF} \qquad (6\text{-}1)$$

Compared to ( 4-1 ) the vertical velocity input $\dot{Z}_k$ is replaced with vertical displacement $Z_k$ and the plant model of the quarter car $P_{a\dot{z}}$ is replaced with $P_{az}$. Instead of deriving an equation for the weight vector $W_k$, an equation for its adjusted version $W_k^*$ is derived. Therefore, the same steps as earlier are carried out and lead to:

$$W^* = -\frac{TF_{az}}{TF_{aF}} = -\frac{(d_s d_t)s^2 + (d_s k_t + d_t k_s)s + (k_s k_t)}{(m_u)s^2 + (d_t)s + (k_t)} \qquad (6\text{-}2)$$

$$W^* = -\frac{(5.511 \cdot 10^4)s^2 + (6.397 \cdot 10^6)s + (7.875 \cdot 10^7)}{s^2 + (36.74)s + (3750)} \qquad (6\text{-}3)$$

Compared to the original control law *C* which uses *W*, the controller $C^*$ used $W^*$ which only differs in the order of the denominator meaning:

$$W^* = Ws \qquad (6\text{-}4)$$

By using $C^*$ instead of $C$, the first order time derivative element is superfluous, which simplifies the preprocessing, making the overall system less expensive and increasing accuracy.

These steps could only be carried out due to the transfer-functions derived in chapter 3.1. Being able to derive transfer-functions using displacement input, but having a state-space realization of the system which requires velocity, makes one wonder if there is a way after all to generate a state-space realization using only displacement input.

In order to derive such a realization, it is clear that the system matrix A of the system must be identical, since it determines the systems characteristics which cannot change. Dropping the fifth state, replacing the velocity input $\dot{z}$ with displacement input $z$, and replacing all other elements with variable $b$, the following state-space realization results:

Input-Equation:

$$\begin{bmatrix} \dot{z}_s \\ \ddot{z}_s \\ \dot{z}_u \\ \ddot{z}_u \end{bmatrix} = \begin{bmatrix} 0 & 1 & 0 & 0 \\ -\frac{k_s}{m_s} & -\frac{d_s}{m_s} & \frac{k_s}{m_s} & \frac{d_s}{m_s} \\ 0 & 0 & 0 & 1 \\ \frac{k_s}{m_u} & \frac{d_s}{m_u} & -\frac{(k_s+k_t)}{m_u} & -\frac{(d_s+d_t)}{m_u} \end{bmatrix} \begin{bmatrix} z_s \\ \dot{z}_s \\ z_u \\ \dot{z}_u \end{bmatrix} + \begin{bmatrix} b_{11} & b_{12} \\ b_{21} & b_{22} \\ b_{31} & b_{32} \\ b_{41} & b_{42} \end{bmatrix} \begin{bmatrix} z \\ F \end{bmatrix} \tag{6-5}$$

Output-Equation:

$$[\ddot{z}_s] = \begin{bmatrix} -\frac{k_s}{m_s} & -\frac{d_s}{m_s} & \frac{k_s}{m_s} & \frac{d_s}{m_s} & 0 \end{bmatrix} \begin{bmatrix} z_s \\ \dot{z}_s \\ z_u \\ \dot{z}_u \\ z \end{bmatrix} + [b_{21} \quad b_{22}] \begin{bmatrix} z \\ F \end{bmatrix} \tag{6-6}$$

Afterwards the transfer-function of this state-space realization is calculated using the following equation, where $A$ is the system matrix, $B$ the input matrix, $C$ the output matrix, and $D$ the feed-through matrix:

$$TF = C(sI - A)^{-1}B + D \tag{6-7}$$

This two-element vector transfer-function, can be separated and its parametric form looks like:

(6-8)

$$\frac{\ddot{z}_s}{z} = \frac{(b_{11}m_sm_u)s^4 + (-b_{11}(m_uk_s) + b_{21}m_s(d_s+d_t) + b_{31}(m_uk_s) + b_{41}(m_ud_s))s^3 + (-b_{11}(k_sd_t) + b_{21}m_s(k_s+k_t) + b_{31}(k_sd_t - k_td_s) + b_{41}(m_uk_s))s^2 + (-b_{11}(k_sk_t))s}{(m_sm_u)s^4 + (m_s(d_s+d_t) + m_ud_s)s^3 + (m_s(k_s+k_t) + m_uk_s + d_sd_t)s^2 + (d_sk_t + d_tk_s)s + (k_sk_t)}$$

(6-9)

$$\frac{\ddot{z}_s}{F} = \frac{(b_{12}m_sm_u)s^4 + (-b_{12}(m_uk_s) + b_{22}m_s(d_s+d_t) + b_{32}(m_uk_s) + b_{42}(m_ud_s))s^3 + (-b_{12}(k_sd_t) + b_{22}m_s(k_s+k_t) + b_{32}(k_sd_t - k_td_s) + b_{42}(m_uk_s))s^2 + (-b_{12}(k_sk_t))s}{(m_sm_u)s^4 + (m_s(d_s+d_t) + m_ud_s)s^3 + (m_s(k_s+k_t) + m_uk_s + d_sd_t)s^2 + (d_sk_t + d_tk_s)s + (k_sk_t)}$$

Chapter 3.1 has already derived $\frac{\ddot{z}_s}{z}$ and $\frac{\ddot{z}_s}{F}$ in ( 3-15 ) and ( 3-16 ). This means the unknown variables *b* in ( 6-8 ) and ( 6-9 ) can be calculated using these two equations. The final state-space realization then has the following form:

Input-Equation:

$$\begin{bmatrix} \dot{z}_s \\ \ddot{z}_s \\ \dot{z}_u \\ \ddot{z}_u \end{bmatrix} = \begin{bmatrix} 0 & 1 & 0 & 0 \\ -\frac{k_s}{m_s} & -\frac{d_s}{m_s} & \frac{k_s}{m_s} & \frac{d_s}{m_s} \\ 0 & 0 & 0 & 1 \\ \frac{k_s}{m_u} & \frac{d_s}{m_u} & -\frac{(k_s+k_t)}{m_u} & -\frac{(d_s+d_t)}{m_u} \end{bmatrix} \begin{bmatrix} z_s \\ \dot{z}_s \\ z_u \\ \dot{z}_u \end{bmatrix} + \begin{bmatrix} 0 & 0 \\ \frac{d_s d_t}{m_s m_u} & \frac{1}{m_s} \\ \frac{d_t}{m_u} & 0 \\ \frac{m_u k_t - d_s d_t - d_t^2}{m_u^2} & -\frac{1}{m_u} \end{bmatrix} \begin{bmatrix} z \\ F \end{bmatrix} \qquad ( 6\text{-}10 )$$

Output-Equation:

$$[\ddot{z}_s] = \begin{bmatrix} -\frac{k_s}{m_s} & -\frac{d_s}{m_s} & \frac{k_s}{m_s} & \frac{d_s}{m_s} & 0 \end{bmatrix} \begin{bmatrix} z_s \\ \dot{z}_s \\ z_u \\ \dot{z}_u \end{bmatrix} + \begin{bmatrix} \frac{d_s d_t}{m_s m_u} & \frac{1}{m_s} \end{bmatrix} \begin{bmatrix} z \\ F \end{bmatrix} \qquad ( 6\text{-}11 )$$

This state-space realization represents the same system as the initial state space-realization, but uses a displacement input instead. Even though this new realization does not need to be implemented in the controller design process, it represents a new and novel way to model a quarter car system including tire damping. The author did not find any system representations like this before in the literature. However, it must be noted that this way of deriving a state-space realization must not work for any kind of system. In addition to do that, the calculation was simpler due to the fact that the sought-after output is given by one of the states. If this is not the case more unknown variables *c* and *d* must be implemented, which requires more known equations to solve for the unknown variables.

In the appendix a Matlab script is shown carrying out the above shown derivation process. It can also be used for further derivations like this.[201]

## 6.2 Road Characteristics

### 6.2.1 Real-Time Road Preprocessor

Chapter 3.3 outlined the overall preprocessing steps including geometrical filtering, low pass filtering, and the first order time derivation. With the use of $W^*$ the time derivate step is not needed anymore. The need for the low pass filtering element depends on the width resolution of the road scanning system, i.e. its sample frequency. However, low pass filtering is an easy to implement step which can be done using analog or digital filters, both with fairly quick processing time.

[201] See Appendix.

The most time expensive preprocessing step is the geometrical filtering. It will most likely dominate the time needed for the overall signal processing time from road detection until the tracking signal reaches the force generator/actuation system. This also means that look ahead preview distance and the design of the preprocessing unit must be coordinated. Most likely a highly simultaneously working hardware or software element must be designed in order to reach a satisfying processing time.

### 6.2.2 Low Frequency Signals

As chapter 5.5 has already pointed out, implementing the TUFW in the controller $C$ or $C^*$ causes the force profile to have an offset at the end if the road profile includes a step or a lot of low frequency signals. This is due to the fact that the TUFW forces the sprung mass to always stay at the same height, which is obviously not acceptable for a practical real-time implementation. To address this issue further, research on the road scanning system and the behavior of a full car model is needed. Something that is also not taken into account in this research is that the road profile input is measured always relative to the car. In theory, this means an uncontrolled vehicle will scan an equally shaped disturbance profile in front of the vehicle while driving over one. This is due to the fact that the road scanning system is mounted on and moves with the vehicle.

While more research on this problem is needed, one simple and easy to implement way to fix this issue is to add a high-pass filter in front of the controller $C^*$. Now low frequency signals, i.e. step profiles, reach the controller and it will not try to mitigate them. Instead of an additional high-pass filter in front of the controller $C^*$, it is also valid and simpler to replace the low pass filter in the preprocessor with a band-pass filter. Chapter 6.4 shows the impact of a high pass filter on the force profiles offset and the total mitigation performance.

## 6.3 Force Generator/Actuation System

### 6.3.1 Force Generator System Requirements

As it was outlined in the introduction, several different hardware designs and approaches can be found to make an active suspension system feasible, powerful, and energy efficient. The literature also outlines the difficulties and challenges in designing such a system, which is why the hardware design is not part of this research project. However, the discoveries made and the controller designed can be used as a tool to further determine product specifications for such a system.

None of the control strategies found in the literature approached an optimal force control solution, meaning the optimal force profile for a given road profile might never have been calculated or examined before. However, using the TUFW, the optimal force profile can be extracted and afterwards examined in order to determine further or more accurate hardware specifications for every given road profile.

For example, some of them are:

- maximum force requirements
- required reaction speed/velocity
- total ideal power needed for mitigation purposes.

Table 6-1 shows as an example of all maximum forces requirements for the used road profiles in this research project using the controller $C^*$.

Table 6-1: Table of Maximum Force Requirements

| Velocity / Profile | 5 m/s | 10 m/s | 15 m/s | 20 m/s | 25 m/s | 30 m/s |
|---|---|---|---|---|---|---|
| **CA** | 8.8 kN | 11.7 kN | 12.5 kN | 12.8 kN | 12.9 kN | 13.9 kN |
| **CB** | 8.4 kN | 11.5 kN | 12.4 kN | 12.7 kN | 12.9 kN | 12.9 kN |
| **CC** | 6.0 kN | 7.9 kN | 8.4 kN | 8.5 kN | 8.6 kN | 8.6 kN |
| **CD** | 7.9 kN | 11.2 kN | 12.3 kN | 12.7 kN | 12.8 kN | 12.9 kN |
| **CE** | 6.7 kN | 8.8 kN | 9.2 kN | 9.1 kN | 8.4 kN | 8.5 kN |
| **CF** | 7.5 kN | 9.9 kN | 10.3 kN | 10.1 kN | 9.9 kN | 9.6 kN |
| **CG** | 5.9 kN | 7.8 kN | 8.4 kN | 8.5 kN | 8.6 kN | 8.6 kN |
| **P1** | 5.1 kN | 6.4 kN | 6.5 kN | 6.2 kN | 6 kN | 5.6 kN |
| **P2** | 5.7 kN | 7.6 kN | 8.1 kN | 8.3 kN | 8.3 kN | 8.3 kN |
| **P3** | 5.4 kN | 7.2 kN | 7.5 kN | 7.6 kN | 7.5 kN | 7.3 kN |
| **HS** | 1.6 kN | 1.8 kN | 2.5 kN | 3.2 kN | 3.7 kN | 4.1 kN |
| **HW** | 1.6 kN | 2.1 kN | 2.9 kN | 3.6 kN | 4.1 kN | 4.6 kN |
| **URA** | 3.6 kN | 4.5 kN | 5.2 kN | 5.6 kN | 5.9 kN | 6.0 kN |
| **URB** | 2.3 kN | 3.1 kN | 3.4 kN | 3.6 kN | 3.8 kN | 3.9 kN |
| **URC** | 3.3 kN | 4.6 kN | 5.1 kN | 5.9 kN | 6.3 kN | 6.5 kN |

The total maximum over all road profiles and vehicle velocities is 13.9 kN for Curb A at 30 m/s. Figure 6-2 visualizes Table 6-1. Most profiles require more force with increasing vehicle velocity. However, it is interesting to see that some profiles require less force after a specific peak velocity was reached, in this example Curb E, Curb F, Pothole 1, Pothole 2, and Pothole 3.

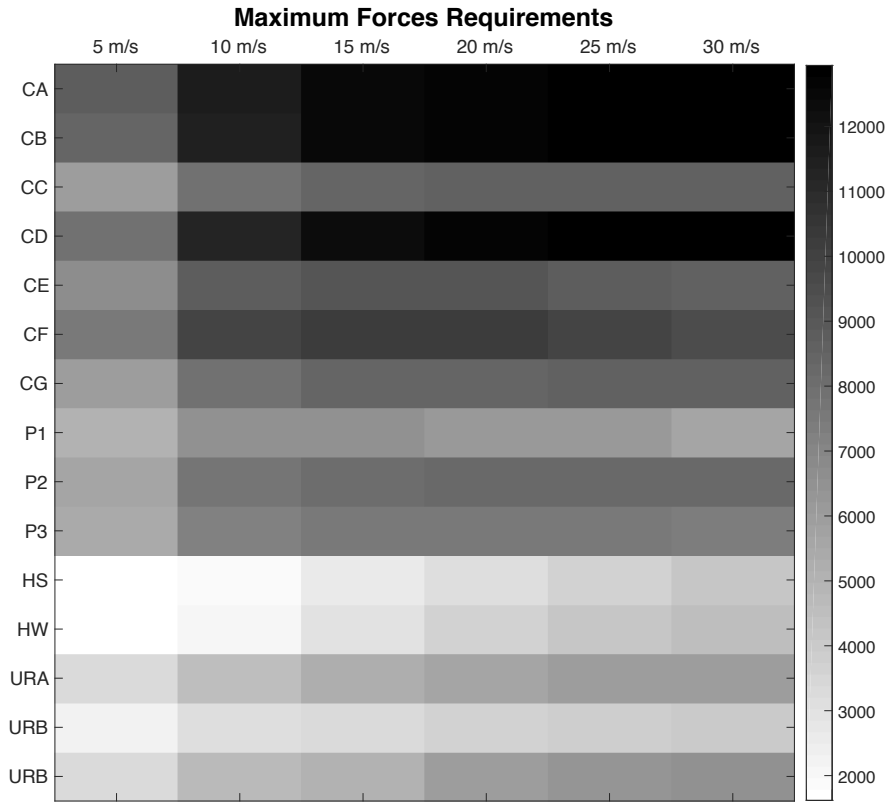


Figure 6-2: Image Plot Maximum Force Requirements in N

### 6.3.2 Force Generator Control Strategy

The controller $C^*$ can be used with any kind of hardware (force generator/actuation system) implemented in the active suspension system. This is due to its open-loop design which does not require or take any feedback signal into account. However, this causes the need for a second, inner controller which makes sure the force generator/actuation system tracks the optimal force profile generated from $C^*$. Figure 6-3 shows the full block diagram, including a force generator controller *FGC*.

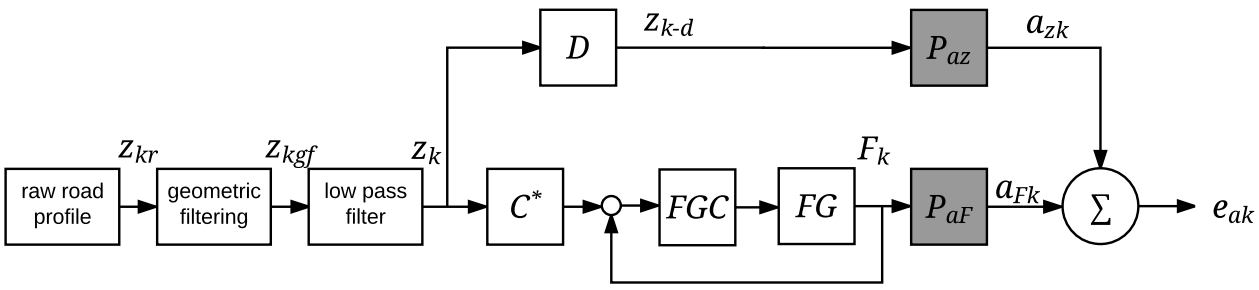


Figure 6-3: Block Diagram Quarter Car Model with Active Suspension System, Controller $C^*$, Force Generator *FG*, and Force Generator Controller *FGC*

This inner Force Generator Controller *FGC* must be designed according to the chosen system design and its system behavior/characteristics. While an electromagnetic hardware design probably won't require too much work on the controller generation and tuning process, a pneumatic design with its high nonlinearities will probably require more work and control effort.

Regarding the implementation of a realistic force generator/actuation system or real-time, real-world application, the controller $C^*$ will always generate the ideal force profile as a tracking signal for the force generator and its controller *FGC*. The final system performance, then, mostly depends on the following questions, which need to be answered during the hardware design process:

- Is the force generator/actuation system capable of holding the maximum force requirement?
- Does the *FGC* make the force generator/actuation system track the optimal force profile well enough?
- Is the vehicle able to provide enough power to the force generator/actuation system?

These and other questions are not part of this research, but the results and discoveries from this research are a suitable tool in order to design a system which meets and satisfies the requirements in order to mitigate the disturbances.

## 6.4 Controller Designs Comparison

Figure 6-4 and Figure 6-5 compare the controller performance of $C$ vs. $C^*$, i.e. the comparison of the controller using vertical velocity to vertical displacement input. As examples, Curb A at 15 m/s and Pothole 2 at 30 m/s are shown, since both profiles are quite rough on the suspension. As can be seen both times, the controller $C^*$ works better. This is due to the fact that taking the first order derivative causes small inaccuracies, which are an influence on the mitigation performance.

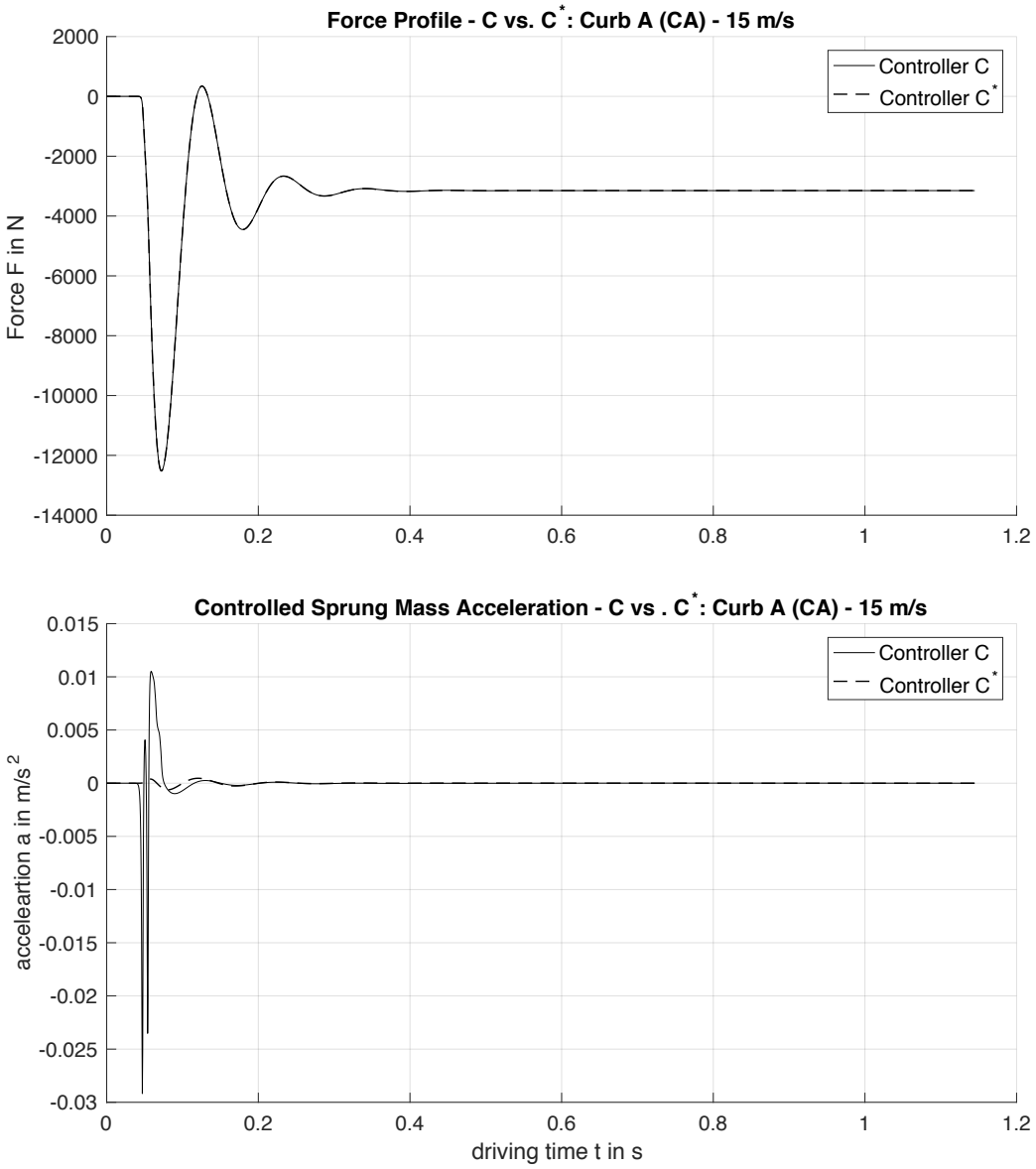


Figure 6-4: Comparison $C$ vs. $C^*$ for Curb A (CA) at 15 m/s

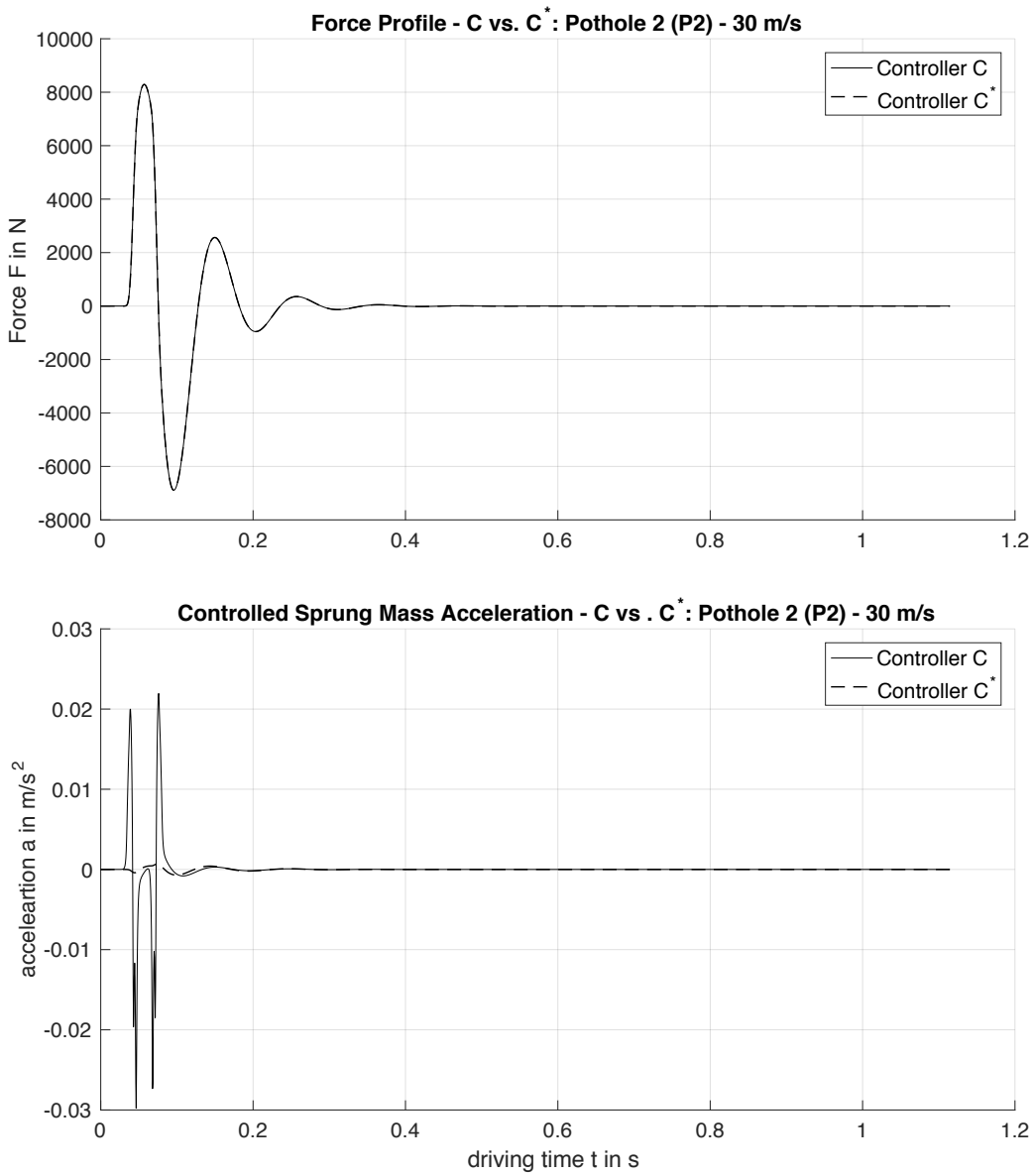


Figure 6-5: Comparison $C$ vs. $C^*$ for Pothole 2 (P2) at 30 m/s

Next Figure 6-6 through Figure 6-8 compare all developed control laws, iFX-LMS, controller $C$, controller $C^*$, and controller $C^*$ including a high pass filter.

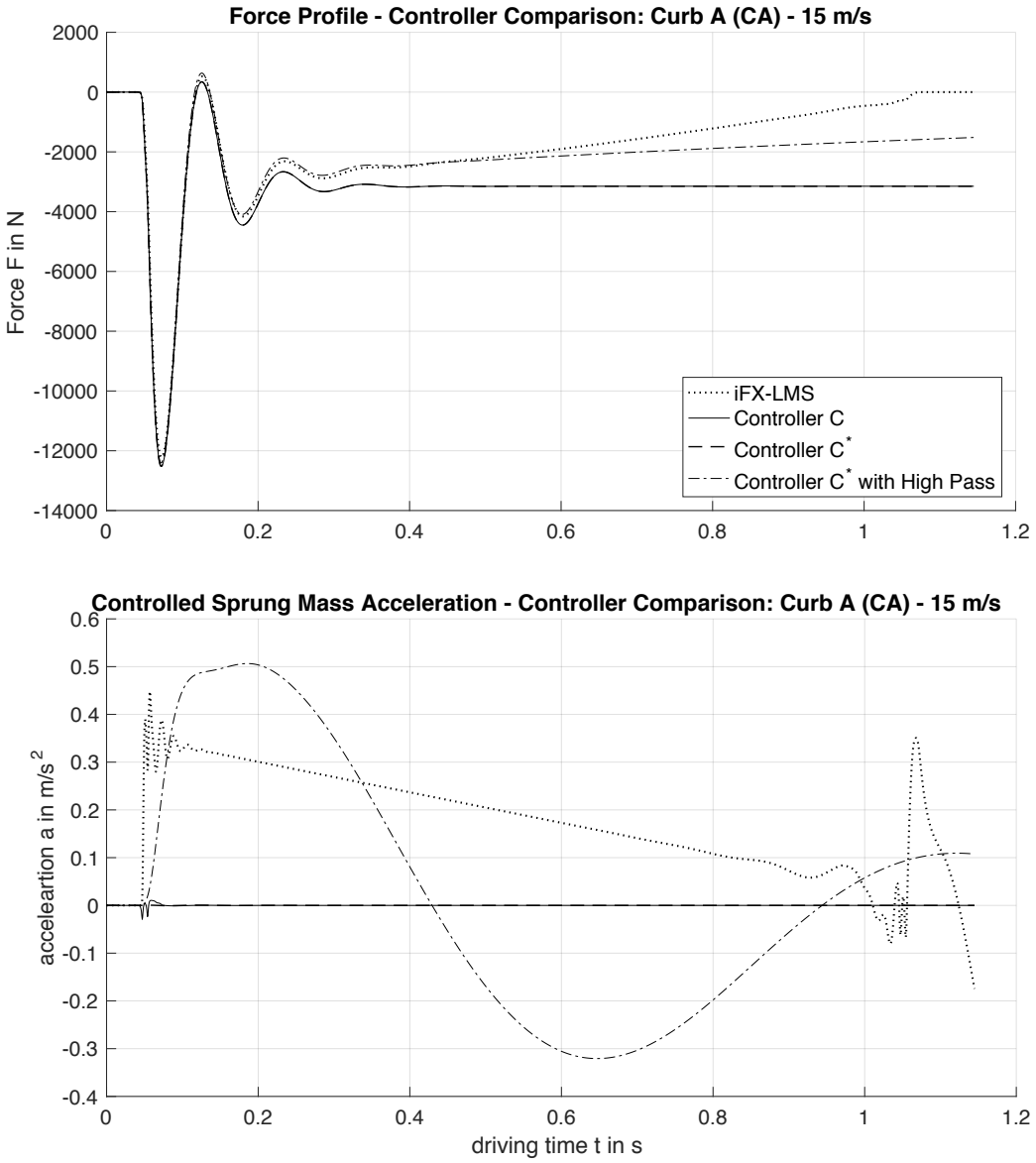


Figure 6-6: Control Law Comparison Curb A (CA) at 15 m/s

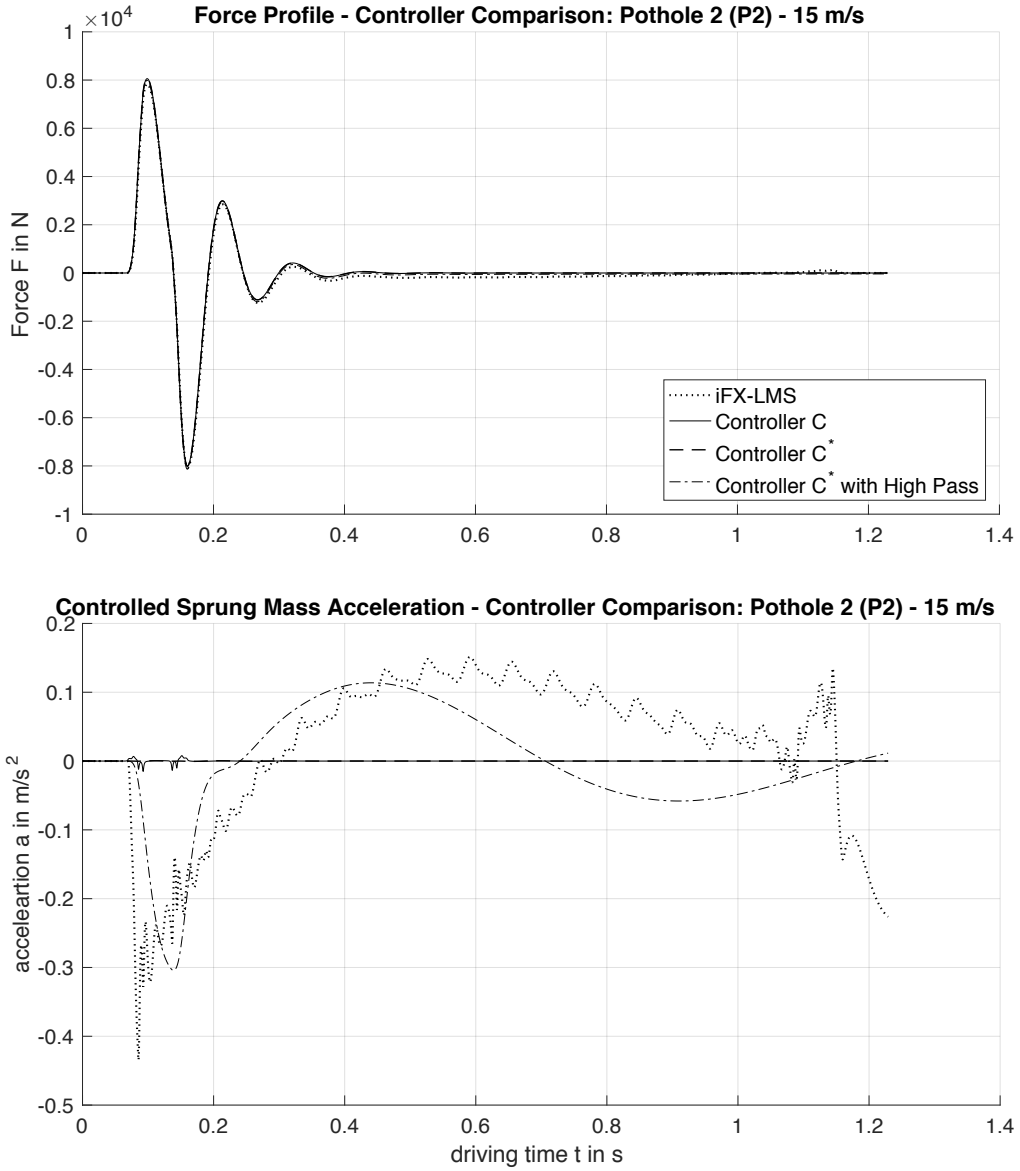

Figure 6-7: Control Law Comparison Pothole 2 (P2) at 15 m/s

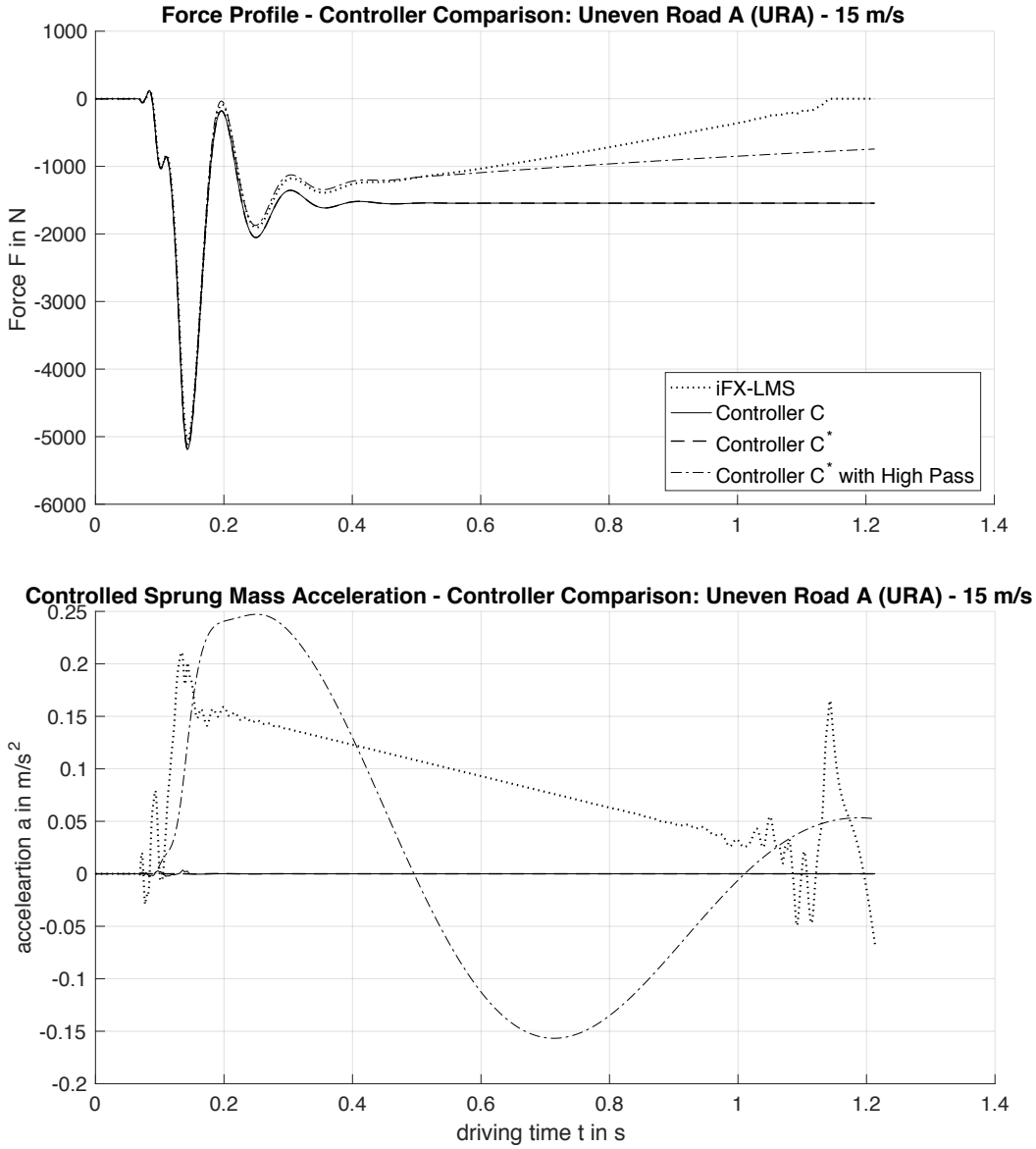

Figure 6-8: Control Law Comparison Uneven Road A (URA) at 15 m/s

The high pass filter used above is in the form of:

$$HP = \frac{s}{s + 2\pi f} \qquad (6\text{-}12)$$

The above shown examples are using $f = 0.1$, which was determined to be a good fit for the system. As can be seen the force offset at the end goes slowly down, but at the same time the controlled sprung mass acceleration goes up. Using a high break frequency will cause the offset to disappear quicker, however, the controlled sprung mass acceleration becomes worse. Therefore 0.1 Hz was determined to be a good fit. Figure 6-7 shows that the filter also influences the non-offset affected profiles. As mentioned before, more research on the overall problem needs to be done in future work.

# 7 Conclusion

## 7.1 Summary and Contributions

In the beginning of this Master's Thesis the current state of the art of active suspension systems, the Army's need for new approaches in this area, previous research at PERL VT, as well as the objective for this research project were described. It was concluded that none of the control approaches for active suspension system implemented so far tried to mitigate single event disturbances, which is the Army's main objective. Also, the approach for generating and using ideal force profiles from previous research was determined to be promising and is the base for this research project.

In preparation for the research presented above, a four-section methodology was developed and laid out, which led to the following four chapters and proved itself to be very convenient and helpful.

The first of these four-sections developed an application that extracts ideal force profiles from single event disturbance signals in order to mitigate their impact to the vehicle. The application uses a quarter car model with a partially loaded active suspension system, a set of predefined road profiles, a road profile preprocessor, and an adaptive algorithm. The preprocessing included geometric filtering using a Tandem-Cam Model, while the adaptive processor used an iterative version of the Filtered-X Last-Mean-Square algorithm. The tuned application performed and mitigated the excitation signals very well throughout the entire research project.

Next, several data sets with varying road profiles and vehicle velocities were generated, processed, and evaluated according to a developed operational test plan using the setup application. The evaluation and analysis discovered high correlations in the generated and adjusted adaptive system, which led to an empirical and theoretical universal filter model. These universal models can replace the adaptive system and can be used to generate ideal force profiles in real-time.

After balancing out all possible controller design options, an open-loop control law, called Optimal Force Control, was designed and tested on each road profile for all considered vehicle velocities. The performance evaluation proved the controller can successfully mitigate vehicle excitations even better than the adaptive system designed before.

Therefore, the last section reiterated through all assumptions and simplifications made throughout the research and adjusted the control law accordingly to be used in a practical real-time application. In addition, a novel approach was made in deriving a new state-space realization of a quarter car model with tire damping.

The real-time controller design using an Optimal Force Control approach proved to perform very well over all road profiles and considered vehicle velocities. It also proved to be generally feasible for commercial vehicles, to satisfy the Army's needs, and has the potential to handle other excitations besides single event disturbances. However, more work needs to be done before the overall research project can be finished, which is a great opportunity for further student research projects.

## 7.2 Future Work

As it was already outlined, especially in chapter 6, more research is needed before such a system can be implemented in a commercial vehicle. Most of the work concerns the supporting components which provide information and signals to the controller designed in this Master's Thesis.

Even though the use of a high-pass filter reduced the impact of step and low-frequency profiles, more research needs to be conducted concerning the overall road scanning system. It is of special importance to include here the effects of the absolute and relative movements of the vehicle compared to the road.

Extending this research, the controller needs to be tested and adjusted using a full car model instead of the used quarter car model. Also, a consideration of non-linear spring and shock absorber behavior might be necessary.

As explained, some of the assumed and used hardware needs to be designed first, for example the road preprocessing unit and the force generator/actuation system. The developed tools can be used in order to determine accurate design specifications for these components. Depending on the chosen hardware, the force generator/actuation system also requires an appropriate tracking controller in order to follow the generated force profiles.

# Appendix

## Appendix 1: Army Solicitation



SBIR·STTR America's Seed Fund™ POWERED BY SBA

# High Capability Off-Road Active Suspension System

NOTE: The Solicitations and topics listed on this site are copies from the various SBIR agency solicitations and are not necessarily the latest and most up-to-date. For this reason, you should use the agency link listed below which will take you directly to the appropriate agency server where you can read the official version of this solicitation and download the appropriate forms and rules.

The official link for this solicitation is: http://www.acq.osd.mil/osbp/sbir/solicitations/index.shtml

| | | | |
|---|---|---|---|
| **Agency:** | Department of Defense | **Release Date:** | November 20, 2013 |
| **Branch:** | Army | **Open Date:** | November 20, 2013 |
| **Program / Phase / Year:** | SBIR / Phase I / 2014 | **Application Due Date:** | January 22, 2014 |
| **Solicitation:** | 2014.1 | **Close Date:** | January 22, 2014 |
| **Topic Number:** | A14-061 | | |

Description:

OBJECTIVE: A high capability active suspension that maximizes soft soil mobility and mitigates road breakaway rollovers on 10-37 ton wheeled vehicles. i.e. Joint Light Tactical Vehicle (JLTV) and Mine Resistant Ambush Protected (MRAP) Vehicles. DESCRIPTION: The Army is looking for opportunities to enhance soft soil (mud and sand) mobility and reduce vehicle rollovers caused by road breakaways using advanced suspension technologies. The suspension technology would be designed and developed for use on JLTV and MRAP vehicle platforms with the intent of maximizing the vehicles soft soil performance and reducing the severity of road break away rollovers. There has been significant work in the past on advanced suspension technologies that improve ride and handling

stability of various vehicles, but no work in the area of suspension control algorithms that can walk a vehicle out of an immobilized condition in soft soil or prevent a rollover when the road breaks away under a heavy vehicle. These are the two largest mobility issues for MRAPs and have a high likelihood to be an issue for JLTV especially since it is intended to operate in much softer soils than MRAP. This suspension system will require the ability to rapidly respond to unexpected events, and control the vehicle"s movement throughout its entire suspension"s travel range. Control algorithms will need to be developed that can detect a rollover event and properly mitigate it while at speeds of up to 65 mph without causing a loss of control of the vehicle. Additionally, control algorithms will need to be developed to determine when a vehicle is stuck in mud or sand, and generate enough load transfer, from side to side, to get the vehicle unstuck. The Army is looking for innovative ideas in the area related to mobility, and more specifically suspension systems, to improve Soldier performance in the field when they encounter unexpected mission or life threatening events. The final product of this effort would be to build and test a prototype system to determine and demonstrate the systems ultimate level of capability. PHASE I: In phase I, the Contractor would propose a technological solution that would enhance soft soil (mud and sand) mobility and reduce vehicle rollovers caused by road breakaways using an advanced suspension technology, develop a model that demonstrates the functionality and performance improvements that can be expected with the technology, and then write a final report that summarizes the effort and the expected benefits should the system be built and developed for the MRAP Family of Vehicles or the JLTV. The report will include a summary of the data generated, the benefits of the system, the concerns related to integration onto the vehicle, an estimate of the expected durability of the proposed system, and any commercial applications of the system. PHASE II: In Phase II, the Contractor would generate detailed designs of the parts modeled in Phase I. The contractor would fabricate the parts and install them in an MRAP or JLTV. Once the parts are installed the contractor would conduct a proof of principle (PoP) test to demonstrate the performance improvements. Finally the contractor would write a technical report detailing the results of the test, the potential of manufacturability of the components, and the cost of the integration and parts should the system go into production. PHASE III: In Phase III, the Contractor shall develop detailed manufacturing and instillation plans for use on the MRAP All Terrain Vehicle (M-ATV), the MaxxPro Plus, and the JLTV vehicle (still to be determined). The Contractor shall also determine the potential use of this product on agricultural and mining vehicles.

## Appendix 2: Matlab Script for Calculation new State-Space Realizations

# Description

This script can be used as an example in order to determine new stata-space relaizations of a known system. It is necessary that a transfer-function representation of the searched system is available. Also several iterations might be necessary, while an existance of a solution is not guaranteed.

The shown example is for a quarter car model using a partial loaded active suspension system including tire damping.

Author: Christopher Kappes, Dr. Steve C. Southward Virginia Tech - Performance Engineering Research Laboratory Durham Hall, 1145 Perry Street, Blacksburg (VA) 24061, USA email: ckappes@vt.edu
2017-03-30; Last revision: 2017-04-26

```
% ------------- BEGIN CODE --------------

syms s ms mu ks kt ds dt b11 b12 b21 b22 b31 b32 b41 b42

% system matrix A
A = [     0,      1,             0,             0; ...
     -ks/ms, -ds/ms,         ks/ms,         ds/ms; ...
          0,      0,             0,             1; ...
      ks/mu,  ds/mu, -(ks + kt)/mu, -(ds + dt)/mu]; ...


% input matrix B (variable)
B = [b11, b12; ...
     b21, b22; ...
     b31, b32; ...
     b41, b42];

% output matrix C
C = [-ks/ms, -ds/ms, ks/ms, ds/ms];

% feedthrough matrix D (variable)
D = [b21 b22];

% calculating variable tranfer-function representation
sI_A     = s*eye(4) - A;
inv_sI_A = inv(sI_A);
H        = simplify(C*inv_sI_A*B + D);

% storing numerators and denominatores
HZ = H(1);
HF = H(2);

[NZ, DZ] = numden(HZ);
[NF, DF] = numden(HF);

NZ = simplify(collect(NZ, s))
DZ = simplify(collect(DZ, s))
NF = simplify(collect(NF, s))
DF = simplify(collect(DF, s))
```

```
n1 = coeffs(NZ, s);
n2 = coeffs(NF, s);

% solving for bxx
S = solve( n1(4) ==         (ds*dt), ...
           n1(3) == (ks*dt + ds*kt), ...
           n1(2) ==         (ks*kt), ...
           n1(1) ==             (0), ...
           n2(4) ==            (mu), ...
           n2(3) ==            (dt), ...
           n2(2) ==            (kt), ...
           n2(1) ==             (0), ...
           b11, b12, b21, b22, b31, b32, b41, b42);

% extracting and storing solutions
b11 = S.b11;
b12 = S.b12;
b21 = S.b21;
b22 = S.b22;
b31 = S.b31;
b32 = S.b32;
b41 = S.b41;
b42 = S.b42;

% show new state-space system
disp('------------------------');
disp('new SS');
A
B = subs(B)
C
D = subs(D)
disp('------------------------');

% calculate new transfer-function realization
H = simplify(C*inv_sI_A*B + D);

HZ = H(1);
HF = H(2);

[NZ, DZ] = numden(HZ);
[NF, DF] = numden(HF);

% compare to real numerator
NZ = simplify(collect(NZ,s))
disp('s^2*(ks + ds*s)*(kt + dt*s) <- real Numerator')
DZ = simplify(collect(DZ,s));
NF = simplify(collect(NF,s))
disp('s^2*(mu*s^2 + dt*s + kt) <- real ')
DF = simplify(collect(DF,s));

% ------------- END CODE --------------


NZ =
```

```
b21*ms*mu*s^4 + (b21*ds*ms + b21*dt*ms + b41*ds*mu - b11*ks*mu +
 b31*ks*mu)*s^3 + (b31*dt*ks - b31*ds*kt - b11*dt*ks + b21*ks*ms +
 b21*kt*ms + b41*ks*mu)*s^2 - b11*ks*kt*s


DZ =

ms*mu*s^4 + (ds*ms + dt*ms + ds*mu)*s^3 + (ds*dt + ks*ms + kt*ms +
 ks*mu)*s^2 + (ds*kt + dt*ks)*s + ks*kt


NF =

b22*ms*mu*s^4 + (b22*ds*ms + b22*dt*ms + b42*ds*mu - b12*ks*mu +
 b32*ks*mu)*s^3 + (b32*dt*ks - b32*ds*kt - b12*dt*ks + b22*ks*ms +
 b22*kt*ms + b42*ks*mu)*s^2 - b12*ks*kt*s


DF =

ms*mu*s^4 + (ds*ms + dt*ms + ds*mu)*s^3 + (ds*dt + ks*ms + kt*ms +
 ks*mu)*s^2 + (ds*kt + dt*ks)*s + ks*kt

------------------------
new SS

A =

[      0,      1,             0,             0]
[ -ks/ms, -ds/ms,          ks/ms,          ds/ms]
[      0,      0,             0,             1]
[  ks/mu,  ds/mu, -(ks + kt)/mu, -(ds + dt)/mu]


B =

[                             0,     0]
[              (ds*dt)/(ms*mu),  1/ms]
[                        dt/mu,     0]
[ -(dt^2 + ds*dt - kt*mu)/mu^2, -1/mu]


C =

[ -ks/ms, -ds/ms, ks/ms, ds/ms]


D =

[ (ds*dt)/(ms*mu), 1/ms]

------------------------
```

```
NZ =

s^2*(ks + ds*s)*(kt + dt*s)

s^2*(ks + ds*s)*(kt + dt*s) <- real Numerator

NF =

s^2*(mu*s^2 + dt*s + kt)

s^2*(mu*s^2 + dt*s + kt) <- real
```

*Published with MATLAB® R2016a*

## References


Ab. Talib, M. H. and Mat Darus, I. Z.: [Self-Tuning PID Controller for Active Suspension System with Hydraulic Actuator, 2013], IEEE Symposium on Computers & Informatics, 2013, pp. 86-91

Aboud, W. S., Haris, S. M., and Yaacob,Y.: [Advances in the control of mechatronic suspension systems, 2014], Journal of Zhejiang University-SCIENCE C (Computers & Electronics), 2014 15(10): 848-860, 2014, pp. 849-860

Audi Technology Portal: [adaptive air suspension, 2017], Audi Technology Portal, https://www.audi-technology-portal.de/de/fahrwerk/fahrwerksregelsysteme/adaptive-air-suspension, 2017, access date: 2017-04-04

Auto Motor und Sport: [Aktives Fahrwerk von Bose, 2004], auto-motor-und-sport.de, http://www.auto-motor-und-sport.de/news/aktives-fahrwerk-von-bose-672534.html, 2004, access data: 2017-07-02

Automobile Club Southern California: [Pothole Damage Costs Drivers $3 Billion Annually Nationwide, 2016], Automobile Club Southern California, http://news.aaa-calif.com/news/pothole-damage-costs-drivers-3-billion-annually-nationwide, 2016, access date: 2017-02-01

BMW Techniklexikon: [Adaptive Drive, 2017], BMW Techniklexikon , http://www.bmw.com/com/de/insights/technology/technology_guide/articles/adaptive_drive.html, 2017, access date: 2017-04-04

Changizi, N. and Rouhani, M.: [Comparing PID and Fuzzy Logic Control a Quarter Car Suspension System, 2011], The Journal of Mathematics and Computer Science, Vol. 2 No. 3, 2011, pp. 559-564

Dash, K. D.: [Bad roads killed over 10k people in 2015; 3,416 deaths due to potholes, 2016], The Times of India, http://timesofindia.indiatimes.com/india/Bad-roads-killed-over-10k-people-in-2015-3416-deaths-due-to-potholes/articleshow/53482615.cms, 2016, access date: 2017-02-02

DGUV Deutsche Gesetzliche Unfallversicherung: [Grenzwertliste 2015, 2015], Grenzwertliste 2015, IFA Report 4/2015, Sicherheit und Gesundheitsschutz am Arbeitsplatz, 2015

Dyer, E.: [3 Technologies That Are Making Car Suspensions Smarter Than Ever, 2017], Popular Mechanics, http://www.popularmechanics.com/cars/technology/a14665/why-car-suspensions-are-better-than-ever/, 2017, access date 2017-04-04

Fernández, C., Gavilán, M., Llorca, D. F., Parra, I., Quintero, R., Lorente, A. G., Vlacic, Lj., and Sotelo, M. A.: [Free Space and Speed Humps Detection using Lidar and Vision for Urban Autonomous Navigation, 2012], 2012 Intelligent Vehicles Symposium, Alcalá de Henares Spain, 2012-06-03/07, 2012

Fischer, D. and Isermann, R.: [Mechatronic semi-active and active vehicle suspensions, 2003], Control Engineering Practice 12 (2004), Science Direct, 2003, pp. 1353-1367

Ghazaly, N. M. and Moaaz, A. O.: [The Future Development and Analysis of Vehicle Active Suspension Systems, 2014], IOSR Journal of Mechanical and Civil Engineering (IOSR-JMCE), Vol. 11, Issue 5 Ver. V (Sep-Oct. 2014), 2014, pp. 19-25

Golovanov, A.: [BMW 5 Series (5th generation) icon, 2017], Noun Project, https://thenounproject.com/icon/543818/, 2017, access date and bought on 2017-04-03

Hać, A.: [Optimum Linear Preview Control of Active Vehicle Suspension, 1992], Vehicle System Dynamics, 21 (1992), pp. 167-195

Hegde, S., Mekali, H. V., and Varaprasad, G: [Pothole Detection and Inter Vehicular Communication, 2014], 2014 IEEE International Conference on Vehicular Electronics and Safety (ICVES), Hyderabad India, 2014-12-16/17, 2014

Hochschule Karlsruhe Technik und Wirtschaft: Systemtheorie Online: [Parsevalsche Gleichung, 2017], Systemtheorie Online , http://www.eit.hs-karlsruhe.de/mesysto/nc/teil-a-zeitkontinuierliche-signale-und-systeme/spektrum-eines-signals/rechenregeln-der-fourier-transformation/parsevalsche-gleichung.html?sword_list%5B%5D=parse, 2017 access date: 2017-04-18

Houben, L. W. L.: [Run flat tires versus conventional tires, 2006], DCT, Vol. 2006.112, Technische Universiteit Eindhoven, 2006

Hrovat, D.: [Survey of Advanced Suspension Developments and Related Optimal Control Applications, 1997], Automatica, Vol.33, No. 10, 1997, pp. 1781–1817

Ikenaga, S., Lewis, F. L., and Davis, L.: [Active Suspension Control of Ground Vehicle based on a Full-Vehicle Model, 2000], Proceedings of the American Control Conference, Chicago (IL) USA, 2000-06, 2000

Kappes, Christopher: [ME 5964 – Advanced Design Project, 2016], Report ME 5964 – Advanced Design Project, Spring Semester 2016 Virginia Tech, 2016

Lopes, G., Ribeiro, A. F., Sillero, N., Gonçalves-Seco, L., Silva, C., Franch, M., and Trigueiros, P.: [High Resolution Trichromatic Road Surface Scanning with a Line Scan Camera and Light Emitting Diode Lighting for Road-Kill Detection, 2016], Sensors 2016, 16, 558, 2016

Maher, D. and Young, P.: [An insight into linear quarter car model accuracy, 2011], Vehicle System Dynamics, Vol. 49, No. 3, 2011-03, 2011, pp. 463-480

Mathworks: [Documentation invfeqz, 2017], https://www.mathworks.com/help/signal/ref/invfreqz.html, 2017, access date 2017-04-17

Mercedes-Benz Techcenter: [Magic Body Control, 2017], Mercedes-Benz Techcenter, http://m.mercedes-benz.de/techcenter/magic_body_control/detail.html, 2017, access date: 2017-04-04

Military.com: [Cougar 6x6 MRAP, 2017], Military.com, http://www.military.com/equipment/cougar-6x6-mrap, 2017, access date: 2017-04-03

Military.com: [Joint Light Tactical Vehicle (JLTV), 2017], Military.com, http://www.military.com/equipment/joint-light-tactical-vehicle-jltv, 2017, access date: 2017-04-03

Mitschke, M. and Wallentowitz, H.: [Dynamik der Kraftfahrzeuge, 2014], Dynamik der Kraftfahrzeuge, 5th Edition, Springer, 2014

Pacejka, H.: [Dynamic Tire Response to Short Road Unevennesses, 2012], Tire and Vehicle Dynamics, Chapter 10, Elsevier Ltd., 2012

Parkhill, M., Sooklall, R., and Bahar, G.: [Updated Guidelines for the Design and Application of Speed Humps, 2007], CITE 2007 Conference, Toronto (ON) Canada, 2007

Plaxico, C. A., Ray, M. H., Orengo, F., Tiso, P., McGee, H., Council, F., and Eccles, K.: [Recommended Guidelines for Curb and Curb–Barrier Installations, 2005], National Cooperative Highway Research Program – Report 537, 2005

Rao, A. M.: [A Structured Approach to Defining Active Suspension Requirements, 2016], A Structured Approach to Defining Active Suspension Requirements, Virginia Polytechnic Institute and State University, 2016

Robinson, H.: [National Definition Of Pothole Called For, 2016], Road Surface Treatments Association (RSTA), 2016, access date: 2017-04-10

Rudny, D. F. and Sallmann, D. W.: [Analysis of Accidents Involving Alleged Road Surface Defects (i.e., Shoulder Drop-offs, Loose Gravel, Bumps and Potholes), 1996], SAE Technical Paper Series, International Congress & Exposition, Detroit (MI) USA, 1996-02-26/29, 1996

SBIR STTR: [High Capability Off-Road Active Suspension System, 2013], SBIR STTR, America's Seed Fund, Powered by SBA, https://www.sbir.gov/sbirsearch/detail/561551, 2013, access date: 2017-01-30, pp. 1-2

Schmeitz, A. J. C.: [A Semi-Empirical Three-Dimensional Model of the Pneumatic Tire Rolling over Arbitrarily Uneven Road Sur-faces, 2004], A Semi-Empirical Three-Dimensional Model of the Pneumatic Tire Rolling over Arbitrarily Uneven Road Sur-faces, Teschnische Universiteit Delft, 2004

Sharp, R. S. and Crolla, D. A.: [Road Vehicle Suspension System Design - a review, 1987], Vehicle System Dynamics, 16 (1987), 1987, pp. 167-192

Thompson, A. G.: [An Active Suspension with Optimal Linear State Feedback, 2007], Vehicle System Dynamics, Vol. 5 (1976), 20007, pp. 187-203.

Tseng, H. E. and Hrovat, D.: [State of the art survey: active and semi-active suspension control, 2015], Vehicle System Dynamics, Vol. 53, No. 7, 2015, pp. 1034-1062.

Türkay, S. and Akçay, H.: [Influence of tire damping on the ride performance potential of quarter-car active suspensions, 2008], Proceedings of the 47th IEEE Conference on Decision and Control, Cancun Mexico, 2008-12-09/11, 2008, pp. 4390-4395

Uncini, A.: [Fundamentals of Adaptive Signal Processing, 2015], Fundamentals of Adaptive Signal Processing, Springer, 2015

US Army Research, Development, and Engineering Command (RDECOM): [ARMY 14.1 Small Business Innovation Research (SBIR) Proposal Submission Instructions, 2013], Office of the UnderSecretary of Defense for Acquisition, Technology and Logistics, www.acq.osd.mil/osbp/sbir/solicitations/sbir20141/army141.pdf, 2013, access date: 2017-01-27, pp. 94-95

Weber, P. A., and Braaksma, J. P.: [Towards a North American Geometric Design Standard for Speed Humps, 2000], Institute of Transportation Engineers - ITE Journal, 2000, pp. 30-34

Widrow, B., and Stearns, S. D.: [Adaptive Signal Processing, 1985], Adaptive Signal Processing, Prentice-Hall, Inc., 1985

Wikipedia: [Nyquist–Shannon sampling theorem, 2017], Nyquist–Shannon sampling theorem, https://en.wikipedia.org/wiki/Nyquist–Shannon_sampling_theorem, 2017, access date: 2017-04-14.

Zaloshnja, E. and Miller, T. R.: [Cost of Crashes Related to Road Conditions, United States, 2006, 2009], 53rd AAAM Annual Conference Annals of Advances in Automotive Medicine, 2009-10-5/7, 2009